Serotonin-dependent Modulation of Working Memory and Decision Activity in Primate Prefrontal Cortex

Dissertation

zur Erlangung des Grades eines

Doktors der Naturwissenschaften

Der Mathematisch-Naturwissenschaftlichen Fakultät und
Medizinischen Fakultät
der Eberhard-Karls-Universität Tübingen

vorgelegt von

Anna M. Stein

aus Aachen, Deutschland

März 2020

Tag der mündlichen Prüfung: .....21 Oktober 2020.....

Stellv. Dekan der Math.-Nat. Fakultät: Prof. Dr. József Fortágh
Dekan der Medizinischen Fakultät: Prof. Dr. Bernd Pichler

1. Berichterstatter: Prof. Dr. / PD Dr. / Dr. ….....Andreas Nieder.....

2. Berichterstatter: Prof. Dr. / PD Dr. / Dr. .....Steffen Hage.....

Prüfungskommission: Prof. Dr. / PD Dr. / Dr .....Ziad Hafed.....

Prof. Dr. / PD Dr. / Dr. .....Steffen Hage.....

Prof. Dr. / PD Dr. / Dr. .....Uwe Ilg…….....….

Prof. Dr. / PD Dr. / Dr.....Andreas Nieder.....…

Erklärung / Declaration:

Ich erkläre hiermit, dass ich die zur Promotion eingereichte Arbeit mit dem Titel:

„Serotonin-dependent Modulation of Working Memory and Decision Activity in Primate Prefrontal Cortex”

selbstständig verfasst, nur die angegebenen Quellen und Hilfsmittel benutzt und wörtlich oder inhaltlich übernommene Stellen als solche gekennzeichnet habe. Ich versichere an Eides statt, dass diese Angaben wahr sind und dass ich nichts verschwiegen habe. Mir ist bekannt, dass die falsche Abgabe einer Versicherung an Eides statt mit Freiheitsstrafe bis zu drei Jahren oder einer Geldstrafe bestraft wird.

I hereby declare that I have produced the work entitled

“Serotonin-dependent Modulation of Working Memory and Decision Activity in Primate Prefrontal Cortex”

, submitted for the award of a doctorate, on my own (without external help), have used only the sources and aids indicated and have marked passages included from other works, whether verbatim or in content, as such. I swear upon oath that these statements are true and that I have not concealed anything. I am aware that making a false declaration under oath is punishable by a term of imprisonment of up to three years or by a fine.

Tübingen, den …….. ……..…….

Datum / Date Unterschrift / Signature

Untuk ibuku tercinta

Abstract

The serotonergic system is one of the oldest and most widespread neuromodulator systems in the animal kingdom. In mammals, serotonin is synthesized in the raphe nuclei in the brain stem, from where serotonergic neurons project to almost all areas of the brain. Especially the prefrontal areas receive rich input from the anterior located raphe nuclei. With its many different receptor types, the serotonin system is suited to fulfill various functions throughout the brain. One of serotonins best known functions is its role in the emotional and motivational behavior in humans and its connection to the pathology of mood disorders. Treatment with serotonin reuptake inhibitors and other drugs targeting the serotonin system often show positive effects not only on the emotional state of the patients but also improve different cognitive functions in cases of accompanying cognitive impairments. There is further evidence that serotonin modulates individual aspects of cognition, such as working memory and decision-making. Most studies made use of systemic application or depletion of serotonin or its derivates, eliciting behavioral effects. This, however, leaves the question unanswered how serotonin modulates working memory and decision-related single cell activity; therefore, we recorded neurons in the dorsolateral prefrontal cortex in two awake monkeys performing a numerical same-different decision task. Simultaneously to the extracellular recordings we used Iontophoresis to apply minute amounts of serotonin and a serotonin 2A receptor antagonist in proximity of the recorded cells. We report, that serotonin decreased numerosity tuning during the first stimulus presentation by suppressing neuronal firing for the preferred stimulus whereas blockage of serotonin 2A receptor blockage increased working memory, reducing neuronal activity for not preferred stimuli. Further, we find that sensory information is reduced by blockage of serotonin 2A receptors, while information about the decision is increased by serotonin itself. The results suggest that different serotonin receptor types contribute differently to cognitive and sensory processes in prefrontal cortex and highlight the importance of further research to tackle mental illnesses with accompanying cognitive impairment.

Content

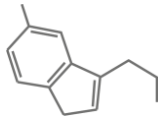

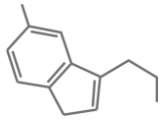

1 Introduction

Serotonin (5-Hydroxytrypthamin, or 5-HT) is a monoamine neurotransmitter, with a manifold of different functions. It can be found in all eukaryotic domains: protists (Csaba, 1993), plants (Garattini and Valzelli, 1965; Saxena et al., 1966; Smith, 1971; Azmitia, 1999), funghi (Azmitia, 1999) and animals. The latter pertains all invertebrates arguably above the phylum cnidaria (Anctil, 1989), for example annelids (Welsh and Moorhead, 1960; Kerkut et al., 1967; Marsden and Kerkut, 1969), molluscs (Welsh and Moorhead, 1960; Kerkut and Cottrell, 1963; Gerschenfeld and Stefani, 1965) and insects (Dewhurst et al., 1972; French et al., 2014). Also, all investigated vertebrates produce and utilize serotonin. This includes birds (Paczoska-Eliasiewicz and Rzasa, 1983), fish (reviewed by Lillesaar, 2011), reptiles (Quay and Wilhoft, 1964) and mammals (Twarog and Page, 1953). The broad distribution of 5-HT in the phylogenetic tree implies the evolutionary old age of the neurotransmitter. A molecular evolution analysis proved that the primordial G-protein coupled 5-HT receptor (see **Section 1.3**) evolved more than 700 – 800 million years ago (Peroutka and Howell, 1994), which makes the serotonergic system older than the dopaminergic, muscarine and adrenergic systems.

In mammals, around 95 % of all 5-HT is present in the intestines. The substance is synthesized either by the intestinal enterochromaffin cells (Erspamer, 1953, 1966; Vialli, 1966) or serotonergic neurons in the myenteric plexus (Gershon et al., 1965; Wade et al., 1994), which innervate the gut muscles. The enterochromaffin cells produce a greater proportion of the intestinal 5-HT, which overflows to the gastrointestinal lumen (Grønstad et al., 1985; Wingren and Ahlman, 1988) and blood (Rand and Reid, 1951; Morrissey et al., 1977; Tamir et al., 1985).

The 5-HT of the central nervous system (CNS) is synthesized in the raphe nuclei (Dahlström and Fuxe, 1964), a group of nuclei in the brain stem (for more detailed information see **Section 1.4.1**). A micro dialysis study in freely moving rats showed that the extracellular 5-HT concentration was similar in all (six) analyzed brain areas, except for the raphe nuclei (RN) and the prefrontal cortex (PFC), where concentrations were approximately 40 % higher (Adell et al., 1991).

In mammals, 5-HT is involved in a host of different functions like neurodevelopment (Moiseiwitsch and Lauder, 1995; Choi et al., 1997; reviewed by Azmitia, 2001),

cardiovascular functions (Villalón and Centurión, 2007), sexual behavior (Marson and McKenna, 1992; Normandin and Murphy, 2011), aggression (Cases et al., 1995; Mejia et al., 2002), sleep (Bradley and Hance, 1956; Urbain et al., 2006), pain (Messing and Lytle, 1977; Sommer, 2004; Viguier et al., 2013) regulating gastrointestinal functions (Gershon and Tack, 2007) and feeding regulations (Blundell, 1977; Simansky and Nicklous, 2002; Voigt and Fink, 2015). However, its involvement in autism and affective disorders made the monoamine most famous and attracted the attention of many neuroscientists, neurologists and psychologists.

The aim of this thesis was to investigate the modulatory effects of 5-HT in cognitive processing. Therefore, we will focus on cellular processes, anatomy and other information regarding the serotonergic system in the brain. For more information about serotonin's role in the rest of the animal and human body, we suggest work by Berger et al., 2009 and Tricklebank and Daly, 2019.

1.1 Serotonin- a brief look into history

Research into serotonin began in the 1930s when Vittorio Erspamer extracted a substance from enterochromaffin cells (EC) in the epithelium of the digestive tract, which caused intestinal tissue contraction. He called the substance enteramine (Negri, 2006). In 1948, Rapport and colleagues extracted and purified a vasoconstrictive amine in beef serum. They called it serotonin ('sero' from serum and 'tonin' from tonus). The chemical structure (and the chemical name) was identified in 1951 by Hamlin and Fischer. In 1952, it was shown that serotonin was identical with Erspamers substance (Feldberg and Toh, 1953). Shortly afterwards, 5-HT was found in the central nervous system of several mammals (Twarog and Page, 1953) with different concentrations depending on the area of the brain (Amin et al., 1954). This led to the idea of 5-HT as a neurotransmitter (Woolley and Shaw, 1954). Years before, in 1904, Ramon y Cajal used silver chromatin impregnation to stain several nuclei in the brain stem, now called raphe nuclei. Within one region, most likely the dorsomedial part of the dorsal raphe nucleus (DRN) (Cajal, 1999), he identified four different cell types, distinguishable due to their morphology. Their fibers were located in bundles, either ascending or descending dorsoventrally. At the time, Cajal knew little about the function of the raphe nuclei and the destination of their bundles. But in 1962, thanks to the newly refined

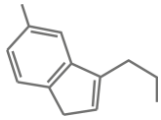

Falck-Hillarp method of histochemical fluorescence to visualize monoamines (Carlsson et al., 1962; Falck, 1964), a half-century old mystery could be solved. Dahlström and Fuxe (Dahlström and Fuxe, 1964, 1965; Fuxe, 1965) not only revealed the serotonergic nature of the raphe nuclei but also lay the foundation for the research of the most extensive and complex neurochemical projection system in the mammal brain. This research was continued over the next two decades, while methods became more and more specific for labeling neurochemical pathways (Kristensson and Olsson, 1971; Hökfelt and Ljungdahl, 1972; Hökfelt et al., 1973; Steinbusch et al., 1978). During this time, the serotonergic system gained a lot of interest because of its role in psychoses. This observation was made with synthesized psychedelic lysergic acid diethylamide (LSD) (Hofmann, 1996) which is structurally related to 5-HT. Further, it was shown that LSD attenuates or facilitates the effects of 5-HT in smooth muscles (Gaddum and Picarelli, 1957).

As mentioned above, 5-HT was proposed to be a neurotransmitter. Evidence for this was provided by several studies showing that 5-HT and enzymes necessary for its synthesis were present in the cerebral cortex (Bogdanski et al., 1957; Kuntzman et al., 1961), stored in vesicles in nerve endings (Michaelson and Whittaker, 1963; Maynert et al., 1964; Fuxe, 1965). The physiological role of 5-HT in the cerebral cortex was proved through iontophoretic studies in cats, which showed that administration of 5-HT inhibited cell firing (Krnjević and Phillis, 1963a, 1963b). However, these studies were conducted in anesthetized animals, and the effects of serotonin were probably confounded by the general effects of the narcotics. In 1967, Roberts and Straughan lay the foundation for modern electrophysiological research into the function of 5-HT. They investigated whether 5-HT had modulatory effects on cortical neurons in awake animals. They used micro iontophoresis to apply 5-HT into the post-sigmoid and suprasylvian gyri of cats in *encéphale isolé* preparations (Roberts and Straughan, 1967). They were able to elicit excitatory (25 %), inhibitory (31 %) as well as mixed (7%) effects on the spontaneous firing rate of recorded neurons upon 5-HT application. Additionally, they applied 5-HT antagonists like LSD 25, 2-brom LSD, 2'-(3-dimethylaminopropylthio) cinnamanilid and methysergide and their findings indicated another important aspect of the serotonergic system: the existence of at least two different receptor types. While all four antagonists reduced the excitatory effects of 5-HT, they failed to rescue the depression produced by 5-HT.

The next big step to investigate the serotonergic system was taken by Aghajanian and colleagues. They inserted microelectrodes into the rat dorsal raphe nucleus to record spontaneous extracellular firing of serotonergic cells after parenteral (either intraperitoneal or intravenous) injections of LSD (Aghajanian et al., 1968). They found that cells near or in the midline of the medial and dorsal raphe nuclei exhibited a slow, but very regular firing pattern. Upon systematic administration of LSD, serotonergic cells showed a complete inhibition.

In 1979, Peroutka and Snyder used radioligand binding to investigate binding sites of 5-HT receptors. They used three different ligands, assuming the maximum density of binding sites to be identical when all ligands bind to the same population of neurons. They provided the first proof for different 5-HT receptor types in the CNS of a mammal. During the 1980s and early 1990s, the identification and characterization of various 5-HT receptor types continued. Besides classical pharmacology, modern molecular analyses were used. Today, 14 different receptor types have been identified in the human brain (see **Section 1.3**).

1.2 Serotonin synthesis

5-HT is synthesized from the large and aromatic amino acid (AA) l-tryptophan. Tryptophan is the least frequent building block in proteins and, due to its hydrophobic nature, serves as an important folding signal in the structure of proteins (Aoyagi et al., 2001). For all monogastric animals and preweaning ruminants, tryptophan is an essential AA, as they are unable to synthesize the molecule in their bodies and need to take it up with their diet. Interestingly, many important molecules derive from tryptophan. This encompasses adenosine and thymidine, both nuclei acids and bases of the DNA, the hormone melatonin (Wurtman and Anton-Tay, 1969), coenzymes nicotinamide adenine dinucleotide (NAD) and NAD phosphate (NADP), important for electron transfer reactions in all living cells (Khan et al., 2006; Mattevi, 2006; Wang et al., 2006), Niacin (vitamin B3) (Ikeda et al., 1965) and the phytohormone class auxin (Stepanova et al., 2008; Tao et al., 2008) just to name a few. Further, tryptophan, due to the indole ring in its structure, is a frequent amino acid in the light absorbing molecules necessary for photosynthesis or other light-dependent processes (Angiolillo and Vanderkooi, 1996). Once digested, tryptophan is transported to the brain, either

free or bound in the plasma. However, only free l-tryptophan can cross the blood brain barrier.

Within the cells of the raphe nuclei, serotonin is synthesized from tryptophan by two enzymes (**Figure 1.1**). The first one, tryptophan hydroxylase (TPH, **Figure 1.1 A**), requires iron as cofactor. It catalyzes a tetrahydrobiopterin- and molecular oxygen-dependent reaction from tryptophan to 5-hydroxytryptophan (5-HTP). During this reaction a hydroxy group is added to the carbon 5. To activate, TPH needs to be phosphorylated by a calcium-activated protein kinase. The necessary calcium is provided by calcium influx during neuronal firing (Jacobs and Azmitia, 1992). There are two different genes for TPH in mammals, which encode two different but homologous enzymes, TPH1 and TPH2 (Walther and Bader, 2003). TPH1 is mainly expressed in the EC cells in the gut, whereas TPH2 is produced by serotonergic cells in the CNS. TPH is the rate-limiting factor in the serotonin synthesis. The second

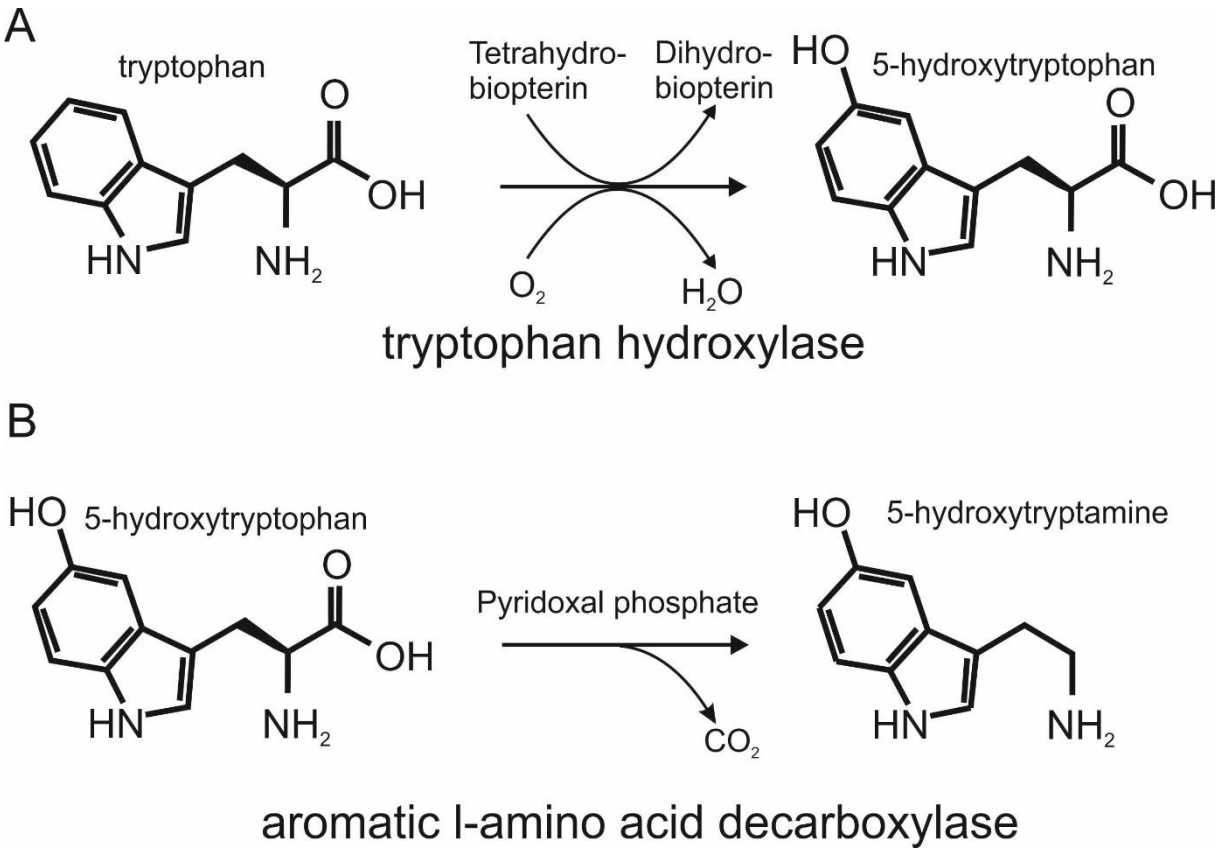

Figure 1.1: The enzymes, cofactors and respective reactions necessary for the synthesis of serotonin are shown. A) shows the action of the enzyme tryptophan hydroxylase, which catalyzes the hydroxylation of l-tryptophan to 5-hydroxytryptophan. This is the rate limiting step in the serotonin synthesis. B) shows the decarboxylation reaction from 5-hydroxytryptophan to serotonin, accelerated by the enzyme aromatic l-amino acid decarboxylase.

enzyme is called aromatic l-amino acid decarboxylase (AADC **Figure 1.1 B**) which requires pyridoxal phosphate as co-substrate to decarboxylate 5-HTP to 5-HT. Only 3 % of the absorbed tryptophan is used in 5-HT synthesis throughout the body (Praag and Lemus, 1986) and only approximately 1 % happens in the brain (Richard et al., 2009). The synthesis takes place in the axonal terminals where, upon activation, serotonin is released into the extracellular space. Serotonin release correlates with tryptophan levels (Schaechter and Wurtman, 1990). Serotonin degradation is facilitated by the enzyme monoamine oxidase (MAO).

1.3 Serotonin receptors

In 1988, Fargin and colleagues successfully cloned a 5-HT receptor for the first time in history (Fargin et al., 1988). During the process, they discovered a strong sequence resemblance to adrenergic receptors, which led them to assume that the 5-HT receptor they cloned was a G-protein coupled receptor (GPCR). GPCRs are integral membrane proteins with 7 α-transmembrane helices. They have a ligand binding site within the transmembrane helices (Römpler et al., 2007; Trzaskowski et al., 2012). On the intracellular site, GPCRs are coupled to a guanine nucleotide-binding protein or short

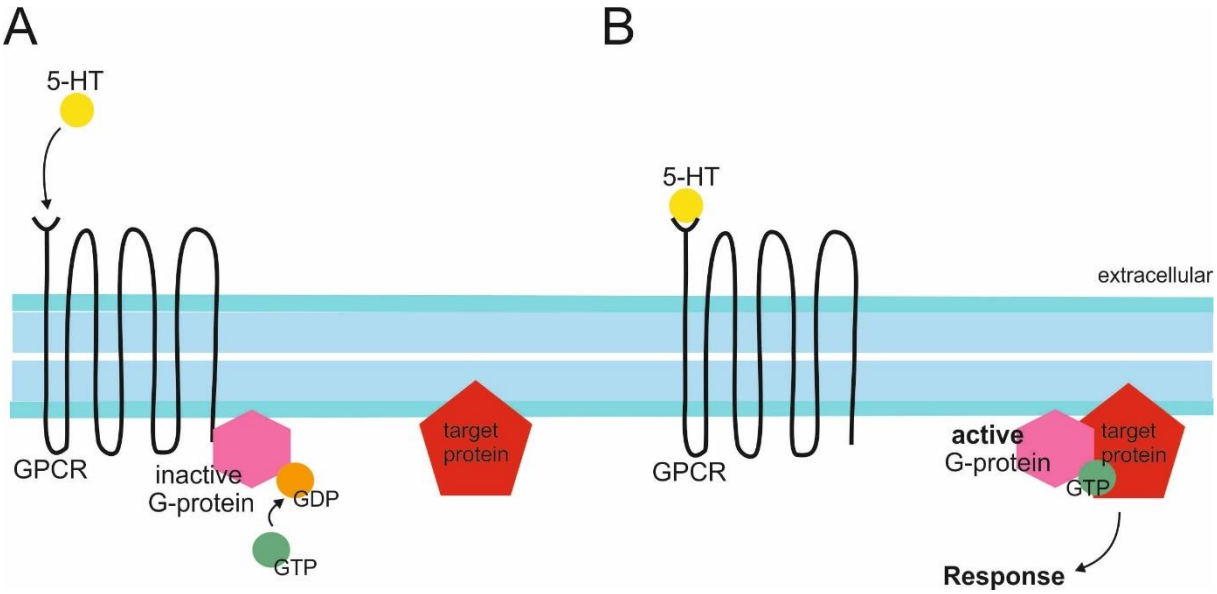

Figure 1.2: Schematic illustration of a G protein coupled serotonin receptor and the intracellular effect upon extracellular ligand binding. A) shows the inactive form of a GPCR with 7 α-transmembrane helices. The G protein is coupled to the GPCR and to a GDP molecule. The target protein is unaffected by the inactive G protein. B) shows the effect of extracellular ligand binding. The G protein is dissociated from the GPCR and coupled to a GTP molecule. In this conformation it binds to the target protein and regulates its activity.

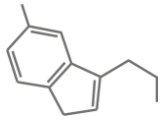

G protein. G proteins are heterotrimeric, they comprise of three subunits (α-, β-, and γ-subunit). The α-subunit possesses the ability to bind either guanin diphosphate (GDP) or the energy-rich guanine triphosphate (GTP). Upon GPCR activation an internal signal transduction pathway, a so-called second messenger system, is either activated or inactivated. **Figure 1.2 A** and **B** show a schematic of the mechanism. The ligand binding to the receptor leads to a conformational change of the GPCR, which in turn enables the α-subunit to exchange the bound GDP for a GTP molecule (**Figure 1.2 B**). The α-subunit then dissociates from the βγ-dimer. Depending on the G protein type, either the α-subunit and/or the βγ-dimer now binds to a target-protein, which subsequently alters its function. Mammals possess a diverse repertoire of genes, which encode G protein subunits (Syrovatkina et al., 2016), which results in a multitude of possible intracellular effects.

Today, 14 different 5-HT receptor types have been identified, most of which are class A (Rhodopsin-like) (Fredriksson et al., 2003) GPCRs. The only exception is the so called 5-HT3 receptor type, a ligand-gated ion channel. The receptor types are subdivided into 7 families (5-HT_1 – $5HT_7$), due to structural and genetic differences (**Table 1**). For example, they differ with regard to the coupled G protein.

Table 1: List of different 5-HT receptor families and subtypes

Receptor familiy	Receptor subtypes	Type
5-HT1	5-HT1A 5-HT1B 5-HT1C 5-HT1E 5-HT1F	GPCR
5-HT2	5-HT2A 5-HT2B 5-HT2C	
5-HT3		Ligand-gated
5-HT4		
5-HT5	5-HT5A 5-HT5B	GPCR
5-HT6		
5-HT7		

As mentioned briefly above, the serotonergic system, with its primordial receptor type, is one of the most ancient neurosignaling systems (Peroutka and Howell, 1994). The three major 5-HT GPCR families (5-HT_1, $5HT_2$ and 5-HT_7) are less than 25 % homologous, which indicates the genetic divergence took place around 600 – 700 million years ago (Römpler et al., 2007), even before the evolutionary split of invertebrates and vertebrates (Nichols, 2006). The evolutionary old age of the serotonergic system is also the explanation for the high number of serotonin receptor types (Peroutka and Howell, 1994) and the multitude of functions.

While all 5-HT receptor types have been implicated in important functions of the brain, the receptor types 5-HT1A and 5-HT2A are among the most studied due to their abundance in the cerebral cortex. 5-HT1A is often coupled to the $G_{i/o}$ protein in the cortex (Mannoury La Cour et al., 2006). Activation of this class of G-proteins leads to inhibition of the adenylyl cyclase (Albert et al., 1999; Liu et al., 1999), which decreases the concentration of cAMP (3',5'-cyclic adenosine monophosphate). cAMP, a very common intracellular signaling molecule, usually stimulates the protein kinase A (PKA). Additionally, it was shown that the βγ-dimer also activates G protein coupled rectifying potassium channels in the hippocampus (Andrade and Nicoll, 1987; Colino and Halliwell, 1988; Oleskevich, 1995) and DRN (Clarke et al., 1996). Thus, the cells hyperpolarize upon activation, regardless of whether the 5-HT1A is pre- or postsynaptically expressed, and exhibit reduced neuronal activity. 5-HT1A receptors are also expressed on the serotonergic neurons of the DRN and MRN. Here, they function as somatodendritic autoreceptors, downregulating the synthesis and release of 5-HT.

5-HT2A receptors are excitatory. The coupled $G_{q/11}$ α-subunit mainly activates the enzyme phospholipase C (PLC) (Golebiewska and Scarlata, 2008), which hydrolyzes the membrane phospholipid phosphatidylinositol 4,5-biphosphate (PIP_2) to diacyl glycerol (DAG) and inositol triphosphate (IP_3) (Sue Goo Rhee and Kang Duk Choi, 1992; Lee and Rhee, 1995; Essen et al., 1997). Both DAG and IP_3 act as second messenger. IP_3 elicit Ca^{2+} release from the endoplasmic reticulum (ER) by activation of IP_3 receptors in the ER membrane. Due to increased Ca^{2+} concentration, DAG then activates the protein kinase C (PKC) which in turn phosphorylates other effectors. Increased intracellular Ca^{2+} levels also lead to opening of voltage independent calcium

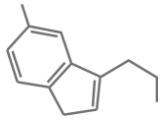

channels (Millan et al., 2008) which increases the excitability of a cell while Ca^{2+} influx elicits exocytosis of synaptic vesicles containing neurotransmitters in presynaptic terminals (Neher and Sakaba, 2008).

1.4 Serotonergic System Anatomy

1.4.1 Raphe nuclei and other brainstem areas

The cell bodies of CNS neurons with the ability to produce serotonin are located in the brain stem - more precisely, in the raphe nuclei, the median part of the reticular formation (Brodal, 1981). However, they are also found in the lateral reticular formation. The raphe nuclei flank the sagittal midline, where they lay distributed from the medulla oblongata to the rostral midbrain. The term ‘raphe’, a word from Greek origin, means seam or ridge and refers to the location close to the midline. There is disagreement in the literature about the number (7 or 8) and nomenclature of raphe nuclei. We decided to employ Törks description (Törk, 1990), which refers to 7 nuclei. **Table 2** lists serotonin containing structures in the midbrain.

Table 2: Brainstem nuclei and areas with respective clusters of serotonergic cells

5-HT Structure	B-cluster
Nucleus raphe pallidus	B1
Nucleus raphe obscurus	B2
Dosolateral nucleus raphe obscurus	B4
Nucleus raphe magnus	B3
Rostral ventrolateral medulla	B3
Lateral paragigantocellular reticular nucleus	B3
Caudal ventrolateral medulla	B1
Median raphe nucleus, caudal part	B5
Median raphe nucleus, rotral main part	B8
Dorsal raphe nucleus, caudal part	B6
Dorsal raphe nucleus principal, rostral part	B7
Caudal linear nucleus	B8
Nucleus pontis oralis	B8/B9
Supralemniscal region	B9

As it was revealed that the cytoarchitectonically identified raphe nuclei did not coincide entirely with clusters of serotonergic cells, Dahlström and Fuxe (Dahlström and Fuxe,

1964) introduced a serotonergic cell group nomenclature (see **Table 2**) during their histofluorescence studies of the rat brain. It starts with B1 for the most caudal located cluster and increases towards the rostral clusters (**Figure 1.3**). Most B-clusters correspond to the individual raphe nuclei, however, sometimes two B-clusters make up one raphe nucleus or one B-cluster extends the scale of one raphe nucleus. Serotonergic neurons are most often located in the raphe nuclei, however studies showed that there are serotonergic populations, which extend laterally into the medial and lateral reticular formation (Poitras and Parent, 1978; Steinbusch, 1981; Wiklund et al., 1981; Jacobs et al., 1984; Törk, 1990; VanderHorst and Ulfhake, 2006). Not all cells in the raphe nuclei synthesize serotonin and the percentages greatly vary from nucleus to nucleus. For example, in the DRN around 80% of all neurons are serotonergic, whereas in the Nucleus raphe pallidus only between 10 and 20 % of the cells produce 5-HT. Further, it is noteworthy that additional neurotransmitters were discovered in the raphe nuclei, like dopamine (Lindvall and Bjorklund, 1974), GABA (Belin et al., 1979) and glutamate (Kaneko et al., 1990).

The distribution and projections of raphe nuclei are similar in all mammals (**Figure 1.3**) (Schofield and Everitt, 1981). The raphe nuclei can be allocated into two groups (green and blue versus red nuclei in **Figure 1.3**), according to genetic and developmental differences (Ding et al., 2003). The rostral group (**Figure 1.3**, blue and green nuclei),

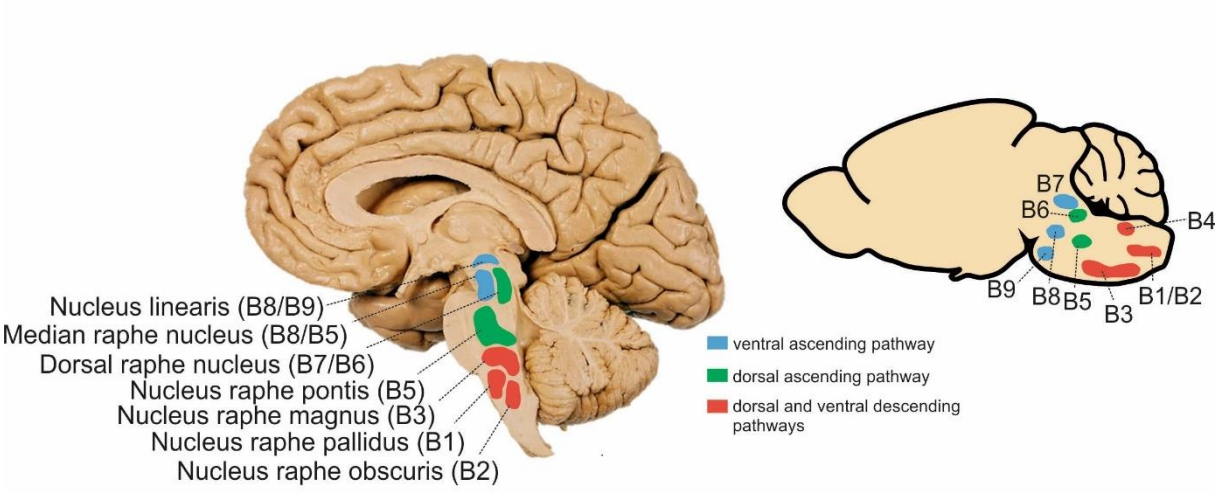

Figure 1.3: Distribution of serotonergic cell clusters in the brain stem of humans (left) and mice (right). Clusters are color coded according to projection pathway. The distribution and projection pathways are similar in all mammals

consisting of the nuclei in the midbrain and pons, nucleus linearis, nucleus centralis superior (also called median raphe nucleus MRN), DRN and nucleus raphe pontis,

projects to the forebrain. This group contains almost 85% of all serotonergic cells in the brain. The second group (**Figure 1.3**, red nuclei), the caudal group, comprises the nuclei in the medulla: the nucleus raphe magnus, nucleus raphe obscurus and the nucleus raphe pallidus. These cells project to the caudal brainstem and the spinal cord. The serotonergic cells are a morphologically and functional heterogeneous group (Steinbusch et al., 1981; Azmitia and Gannon, 1983). They have distinct cytoarchitectural, neurochemical and projection characteristics. Most serotonergic cells are multipolar, but closer to the midline the cells get smaller and exhibit dendrites along the sagittal plane. Lateral located cells tend to be the largest (Törk, 1990).

1.4.2 Serotonergic projections to the forebrain

The following will describe the projections from the serotonergic midbrain cells to cortical and subcortical areas, relevant to the present study. For more information regarding projections to lower brainstem areas and the spinal cord, we suggest work by Hornung (Hornung, 2003; Mai and Paxinos, 2011) and Törk (Törk, 1990).

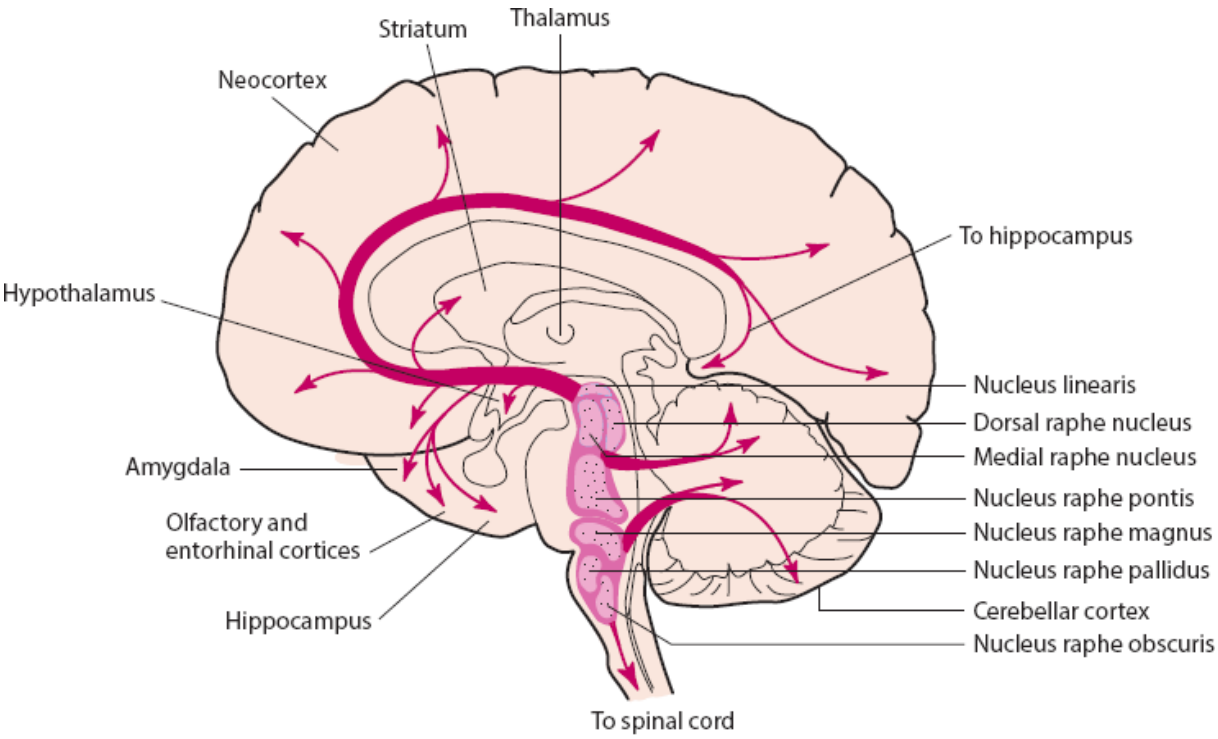

Figure 1.4: The serotonergic system and its projections. The raphe nuclei send out far reaching projection neurons to almost all areas of the brain. Especially the forebrain receives a rich serotonergic input originating in the dorsal raphe nucleus. Source Nestler, Hyman, Holtzman and Malenka: *Molecular Neuropharmacology: A Foundation for Clinical Neuroscience, 3rd Edition*

Figure 1.4 shows a rough schematic of the raphe projections. Almost all areas of the brain receive input from the serotonergic system. Two raphe nuclei play an important role in the innervation of the forebrain: the DRN and MRN. The (human) DRN, probably the most investigated raphe nucleus, can be divided into several subdivisions: dorsal (DRD), ventral (DRV), interfascicular (DRI), and ventro-lateral (DRVL) dorsal raphe nucleus (Baker et al., 1990). It contains approximately 235000 neurons, of which around 70-80% are serotonergic (Baker et al., 1991). The DRN extends from the periventricular gray matter of the rostral pons to the level of the nucleus *nervi oculomotorii*. There are four main cell types found in the DRN, which differ in morphology and neurochemical function. These cells are not confined to the midline but are well distributed also to the lateral parts. Additionally, they are topographically organized along the rostrocaudal axis in regard to their projections (Waterhouse et al., 1986; Abrams et al., 2004). Cells project to more rostral brain areas, if they are located more rostrally in the DRN and vice versa. The median raphe nucleus ranges from the level of the trigeminal motor nucleus to the caudal end of the decussation of the superior cerebellar peduncle.

The MRN is also divided into subdivisions, of which one, which extends dorsally into the nucleus pontis oralis (PnO), is particularly developed in primates (Hubbard and di Carlo, 1974; Schofield and Everitt, 1981; Schofield and Dixson, 1982; Felten and Sladek, 1983). The DRN and MRN receive their inputs mostly from the limbic system. The efferent projections are divided into two parallel pathways. The dorsal pathway runs parallel to medial longitudinal fasciculus. These fibers originate from the DRN and PnO (Azmitia and Gannon, 1983, 1986) (**Figure 1.3**, green nuclei). The ventral pathway, consisting out of axons of MRN and caudal DRN neurons **Figure 1.3**, blue nuclei), enters the VTA at the dorsal limit of the interpeduncular nucleus (Azmitia and Segal, 1978; Jacobs et al., 1978; de Olmos and Heimer, 1980; Fallon and Loughlin, 1982). Azmitia and Gannon showed in 1986 that the relative size of the dorsal pathway is larger in non-human primates due to their larger cortices and DRN projections (Azmitia and Gannon, 1986). The two pathways meet and mingle at the caudal end of the diencephalon and split into two: the first one passes through the internal capsule on its way to the lateral cerebral cortex (Kievit and Kuypers, 1975; Van Der Kooy and Kuypers, 1979; Steinbusch et al., 1980, 1981; Van der Kooy and Hattori, 1980; Porrino and Goldman-Rakic, 1982; Tigges et al., 1982; Waterhouse et al., 1986; Corvaja et al.,

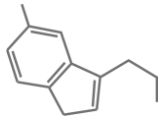

1993) whereas the second one ascends within the medial forebrain bundle, innervating the hypothalamus, basal forebrain, amygdala, medial cortex and hippocampus (Azmitia and Segal, 1978; Köhler and Steinbusch, 1982; Imai et al., 1986; Vertes and Martin, 1988; Datiche et al., 1995). Most projections end in the ipsilateral hemisphere (Miller et al., 1975) and the few contralateral projections terminate close to the midline (Köhler and Steinbusch, 1982; Waselus et al., 2006).

1.4.3 Serotonergic input to the lateral prefrontal cortex

It has been long known that the lateral prefrontal cortex (lPFC) receives rich serotonergic input (Fuxe, 1965). These studies were mostly conducted in rodents or other small mammals (Steinbusch, 1981; O'Hearn et al., 1988; Vertes and Martin, 1988). To investigate the non-human primate brain, Porrino and Goldman-Rakic used the retrograde axonal transport of the enzyme horseradish peroxidase (HRP) to determine the origin as well as the distribution of monoaminergic input to the lPFC (Porrino and Goldman-Rakic, 1982). They injected HRP into distinct areas of 12 monkeys' forebrains to trace back the fibers to their origin. Labeled somata were found in the DRN and the MRN, especially after HRP injections into the principal sulcus (Brodmann's area 46). Today, it is known that projection neurons from the DRN terminate in almost all areas of the forebrain (Berger et al., 1988), especially, the primary sensory areas (Morrison et al., 1982; Campbell et al., 1987). They possess rather small varicosities (Kosofsky and Molliver, 1987), which occur most often in layer IV (Takeuchi and Sano, 1984). Further, it was shown in an electron microscopic study that serotonergic fibers originating from the DNR do not form conventional synapses (Defelipe and Jones, 1988), but most likely using the intercellular communication mode of volume transmission (reviewed by Fuxe et al., 2013). The MRN cells projections overlap greatly with those of the DRN neurons. However, their varicosities are rather large (Kosofsky and Molliver, 1987) and abundant, especially in frontal and hippocampal areas. They form true chemical synapses (Smiley and Goldman-Rakic, 1996). In some areas of the non-human primate brain, including the PFC, the MRN projections terminate in clusters, forming so-called baskets, which surround certain population of interneurons (Hornung et al., 1990; Wilson and Molliver, 1991; Hornung and Celio, 1992; Smiley and Goldman-Rakic, 1996).

1.5 The lateral prefrontal cortex

Since the discovery of serotonin and other monoamines in the lPFC it has been suggested that these have modulatory effects on cognition. That is because the lPFC is a key structure for cognitive control (Fuster, 2001). It is one of three major divisions of the primate prefrontal cortex. The others being the orbitofrontal cortex (OFC), which is involved in reward-based decision-making and processing of emotions (Kringelbach, 2005; Rushworth et al., 2007; Rolls and Grabenhorst, 2008; Rolls, 2016), and the medial PFC, similarly strongly connected to the amygdala and also involved in emotion processing (Aggleton et al., 1980; Chiba et al., 2001; Ghashghaei and Barbas, 2002; Stefanacci and Amaral, 2002). The lPFC comprises of Brodmann areas 8, 9, 10, 45, 46 and 47 (Petrides and Pandya, 1994) and possesses a well-developed internal granular (IV) layer, which separates it from the rest of the frontal areas (v. Economo, 1929; Walker, 1940; Von Bonin and Bailey, 1947; Bailey and von Bonin, 1951; Akert, 1964). Due to distinct architectonic differentiations, the lPFC is further parcellated into two divisions, the ventrolateral (vlPFC) and dorsolateral part (dlPFC) (reviewed by Tanji and Hoshi, 2008). Histological studies suggest that the vlPFC receives, retrieves and integrates input from different sensory areas, whereas the dlPFC receives already integrated multimodal information sets, which can be integrated with one another (Carmichael and Price, 1994; Ongur and Price, 2000). This and the fact that the lPFC has many efferents to premotor areas makes the lPFC the ideal candidate for guiding top-down control.

In 1971, it was shown that the spiking activity of cells in the granular PFC (lPFC) corresponded to the process of working memory (Fuster and Alexander, 1971). In a delayed response task, cells increased their discharge rate during the delay phase. Since then the lPFC has been proven to be crucial for executing goal-directed behavior (reviewed by Miller, 2000). This includes three executive functions (Fuster, 2015): i) executive attention (with subcomponents working memory (Fuster, 1973; Goldman-Rakic, 1987; Quintana et al., 1988; Funahashi et al., 1989; Miller et al., 1996), top-down attention (Wilkins et al., 1987; Buschman and Miller, 2007) and inhibitory control (Iversen and Mishkin, 1970; Casey et al., 2001; Liddle et al., 2001)), ii) planning (reviewed by Tanji and Hoshi, 2001) and iii) decision-making (Kim and Shadlen, 1999; Hussar and Pasternak, 2012).

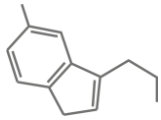

1.6 Serotonin receptors in the lPFC

5-HT receptors are densely expressed in the PFC of rodents (Araneda and Andrade, 1991; Amargós-Bosch et al., 2004; Santana et al., 2004; Puig and Gulledge, 2011), non-human primates (Jakab and Goldman-Rakic, 1998, 2000; De Almeida and Mengod, 2007, 2008) and humans (De Almeida and Mengod, 2007, 2008; Beliveau et al., 2017). The most common receptor types in the primate PFC are the 5-HT1A and 5-HT2A receptors (De Almeida and Mengod, 2007, 2008). Most pyramidal neurons express both receptor types (Araneda and Andrade, 1991; Amargós-Bosch et al., 2004; Santana et al., 2004; De Almeida and Mengod, 2007, 2008), despite their functionally distinct effects on prefrontal pyramidal cells. Activation of 5-HT1A, expressed mostly on the soma and the axon initial segments (Azmitia et al., 1996; DeFelipe et al., 2001; Cruz et al., 2004), generate inhibitory responses (Nicoll et al., 1986; Hamon et al., 1990; Béique et al., 2004) whereas the excitatory 5HT2A receptors are located at the apical dendrites (Jakab and Goldman-Rakic, 1998; Martín-Ruiz et al., 2001) and presumably amplify excitatory input (Araneda and Andrade, 1991; Marek and Aghajanian, 1999; Puig and Gulledge, 2011). In the rat PFC, two distinct populations of fast-spiking interneurons express one receptor type, 5-HT1A or 5-HT2A, respectively (Puig et al., 2010). These neurons are especially abundant in layer V. de Almeida and Mengod (2007, 2008) used double *in situ* hybridization to quantify the colocalization of 5-HT1A and 5-HT2A receptor mRNA with markers for glutamatergic as well as for parvalbumin and calbindin expressing GABAergic cells in the PFC of men and monkeys. They found that almost all (86 – 100 %) glutamatergic cells in layers III – V expressed 5-HT2A receptors, whereas 5-HT1A receptors are expressed by 80 % of the glutamatergic neurons in layer II – III and by half of the pyramidal and tiny stellate cells in layer VI. Both receptors are either absent or less abundant in excitatory cells of other layers. Percentages of GABAergic cells expressing either receptor type are irrefutably lower. In the monkey layers II – V, 13 – 31 % of the cells expressed 5-HT2A receptors. 5-HT1A receptors were expressed with similar percentages in layer II – III and VI (13 – 21 %), most of which cells were calbindin-expressing interneurons. The number of cells expressing 5-HT2A in layer VI was increased to 28 – 46 %. Interestingly, they found higher percentages of GABAergic neurons expressing 5-HT2A receptors in the Brodmann area 9 (46 – 69 % (45 – 63 %) parvalbumin-expressing and 61 – 75 % (61 – 87 %) calbindin-positive neurons in the monkey

(human)).They suggested that both receptor types are partly segregated in terms of their distribution in the cortical layers, suggesting a complementary layer coverage. Their data was compatible with previous findings (Lidow et al., 1989b, 1989a; Goldman-Rakic et al., 1990; Bigham and Lidow, 1995) and findings in rodents (Santana and Artigas, 2017).

1.7 Serotonin's role in cognition

Cognitive impairment is a prominent symptom of many mental disorders, like anxiety (reviewed by Paterniti et al., 1999), major depression (reviewed by Marazziti et al., 2010) and schizophrenia (reviewed by Green, 2006). It is well known, that 5-HT is involved in the pathophysiology and treatment of these diseases (Terry et al., 2008; Mück-Seler and Pivac, 2011; Rodríguez et al., 2012; Lin et al., 2014). Many studies have demonstrated that serotonin modulates different cognitive functions either directly or indirectly. Firstly, cognitive flexibility is positively correlated to 5-HT levels. Bari and colleagues (Bari et al., 2010) manipulated the central 5-HT levels in rats while the animals were performing a probabilistic reversal leaning task. They found that low levels of a selective serotonin reuptake inhibitor (SSRI) decreased cognitive flexibility while simultaneously increased the reaction towards negative stimuli. Higher levels of the same SSRI showed reversed effects. Consistently, 5-HT depletion in the PFC of marmosets inhibited cognitive flexibility (Clarke, 2004), however, the same group showed later that this impairment was restricted to changing stimulus-reward association and not to higher-order attentional set shifting (Clarke et al., 2005). This indicates that different populations of neurons exhibit distinct gradations towards the modulatory effect of 5-HT. Systemic administration of the highly selective 5-HT2A antagonist MDL100907 impaired reversal leaning in rats (Boulougouris et al., 2008), however, intra mPFC 5-HT2A antagonism failed to elicit significant modulation of reversal leaning (Boulougouris and Robbins, 2010). Further, these receptors seem to play a role in attentional set shifting, as 5-HT2A receptor gene polymorphism is connected to deteriorated performance in Wisconsin Card Sorting Test (WCST) (Üçok et al., 2007). Carli and colleagues (Carli et al., 2006) showed that stimulation of 5-HT1A receptors and blockage of 5-HT2A receptors in the medial PFC of rats abolished attentional capacity impairment, induced through blockage of glutamate NMDA

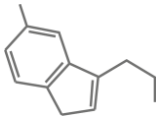

receptors, indicating an indirect effect on attentional functioning. Further, MDL100907 also decreased any negative effect on inhibitory response control, also induced through NMDA blockage. Pharmaceutical studies proved the involvement of the serotonin system in behavioral inhibition; however, the exact mechanisms remain elusive. This is also due to the fact that findings are contradicting. A recent study (Costa et al., 2016) in monkeys showed that systemic administration of SSRIs decreased impulsive responding. However, a study in humans (Scholes et al., 2007), investigating the effect of serotonin depletion on attentional flexibility and response inhibition towards distracting stimuli, found that a tryptophan-free diet improved performance in a Stroop task, increasing attentional control. This indicated the involvement of different serotonin receptors with different functional roles. Systemic administration of the 5-HT1A full agonist flesinoxan impaired working-memory performances in a delayed conditional discrimination task in rats (Herremans et al., 1995), while iontophoretic application of MDL100907 decreased spatial working memory during the execution of a oculomotor delayed response task in monkeys (Williams et al., 2002). However, another study in rats showed no effect on spatial working memory but on object memory after a tryptophan free diet (Lieben et al., 2004). Modulation effect differences may be due to individual or species-specific genetic/epigenetic variations or even distinct target receptor systems. However, it is important to note that the majority of research investigating serotonin's role in cognition was conducted with systemic administration of serotonergic agents. Thus, it remains unclear whether elicited effects were of direct or indirect nature.

1.8 Goal of this study

How does serotonin modulate different aspects of cognition? The majority of neurocognitive serotonin research tackles this question by systemically manipulating serotonin levels within the whole system. The findings derived from systemic application are valuable contributions to treat cognition deficiency symptoms in patients suffering from mental disorders. However, in order to understand the underlying mechanism, it is also important to study the effect of serotonin and the role of its receptors on a cellular level. In this doctoral thesis, we were interested in the general effects of serotonin onto visual working memory related single cell activity and

decision-making related single cell activity but also investigated the role of 5-HT2A receptors specifically. Therefore, we recorded the neuronal activity of cortical neurons in the dorsolateral prefrontal cortex of two awake rhesus monkeys while they performed a numerical same-versus-different decision task. Simultaneously with the extracellular recordings, we used iontophoresis to apply minute quantities of serotonergic agents (5-HT and MDL100907, see **Section 2.6**) in proximity of the recorded neurons. We then analyzed how serotonergic manipulations altered the response properties of single neurons alone and within neuronal circuits involved in cognitive processes necessary to solve the abstract decision task.

2 Experimental Procedures

2.1 Animals and Surgical Procedures

Two male rhesus monkeys (*Macaca mulatta*) were subjects in this study. Monkey E was 9 years old, whereas monkey Y was 7 years old. Both were housed in social groups, with climbing and foraging enrichments. Both had been extensively trained on the task (see **Section 2.3**), as training started prior to this study, involving the same task with iontophoretic application of dopaminergic agents. During training and experiments, both monkeys were under a controlled water protocol. They received their daily amount of water by completing trials in the experimental set-up. In accordance to the German animal protection law, they were provided with fruits and water *ad libidum* in regular intervals.

Both monkeys were implanted with a titanium head post, as well as a recording chamber centered over the principal sulcus of the lateral PFC anterior to the frontal eye fields. One monkey's chamber was implanted on the right hemisphere (monkey E) and one on the left hemisphere (monkey Y). All surgeries were conducted under general anesthesia using aseptic techniques. Before implantation structural magnetic resonance imaging was performed to locate anatomical landmarks. All experimental procedures were in accordance with the guidelines for animal experimentation approved by the authority, the Regierungspräsidium Tübingen, Germany.

2.2 Experimental set-up

Training and experiments were conducted in a darkened chamber (**Figure 2.1**, gray shaded area). Monkeys (**Figure 2.1**, brown box) sat in custom-made primate chairs, equipped with a metal response bar (**Figure 2.1**, second small green box) in the front of the monkey. Their heads were fixated, facing the front, by the means on an attachment, mounted on the primate chair. Animals were positioned 57 cm in front of a TFT screen (15 inch, 1024 x 768 pixel resolution, 60 kHz refresh rate, **Figure 2.1**, white screen), which was used to present the task (**Section 2.3**), inside the set-up chamber ('receiver' computer was used by the experimenter to monitor the presented task, **Figure 2.1**, yellow box) . Presentation of the stimuli was controlled by the software Cortex (NIMH, Bethesda, MD) on the 'server' computer (**Figure 2.1**, big green box). Eye-movements were tracked, using pupil position and corneal reflexes, with a camera

(**Figure 2.1**, small blue box) and infrared light (ISCAN, Woburn, MA). A software (ISCAN) on the ISCAN computer (**Figure 2.1**, blue big box) was used to do configuration and adjustment, when needed to secure seamless eye-tracking. Information about the monkeys' response and the position of its gaze was transmitted to the Cortex software. Rewards were delivered through a water pipe (**Figure 2.1**, small green box), which was attached to the chair in front of the monkeys' mouth. After a correct answer by the monkey a valve opened for alterable times. The amount of valve openings was controlled through the Cortex software. However, the experimenter could also change the amount of received reward manually though an adjustment of valve opening time.

For recording, a baseplate with specialized electrical microdrive towers (NAN Instruments) were mounted onto the recording chamber. The microdrives held and placed the recording electrodes in the recording chamber. A computer (**Figure 2.1**, big red box) which was connected to the NAN Electrode Drive (NAN Instruments, Nazareth; Israel, **Figure 2.1**, small red box) which in turn controlled the microdrives, was used to move the recording electrodes precisely up and down. The recording electrodes were connected to a head stage (**Figure 2.1**, dark grey box) which in turn was connected to a preamplifier (Plexon, Dallas, Texas, band-pass filter 100 Hz – 8 kHz, gain 1000, **Figure 2.1**, lower small orange box). Form here the signal was transmitted to the Plexon Multichannel Acquisition Processor (MAP box, 40 kHz sampling rate, **Figure 2.1**, upper small orange box). The MAP box also received behavioral information (in the form of 8-bit codes), which was synchronized to the neuronal data. The up to here analog signal was digitalized and send together with the 8-bit strobe codes to a 'recording' computer (**Figure 2.1**, big orange box), which visualized the digital signal into waveforms according to preadjusted settings (eg. threshold potential, which must be exceeded) and stored the data. Iontophoresis was implemented with an iontophoresis device (IontoD - npi, Tamm, Germany, light blue box, **Figure 2.1**), which was connected to the electrode inside the iontophoretic agent containing barrel. The device was used to manually set iontophoresis settings like iontophoresis condition and iontophoretic current strength. Information from ine iontophoresis device was also transmitted to the 'recording' computer. We used an oscilloscope (**Figure 2.1**, pink box) and loudspeakers (**Figure 2.1**, loudspeaker symbol), both connected to the MAP box, for visualization and audio monitoring,

respectively, of the analog neuronal signal. Further, one extra camera (**Figure 2.1**, small purple box) was used for visual monitoring (**Figure 2.1**, big purple box) of the monkey's behavior. Further, the signal was synchronized with information about the iontophoresis condition.

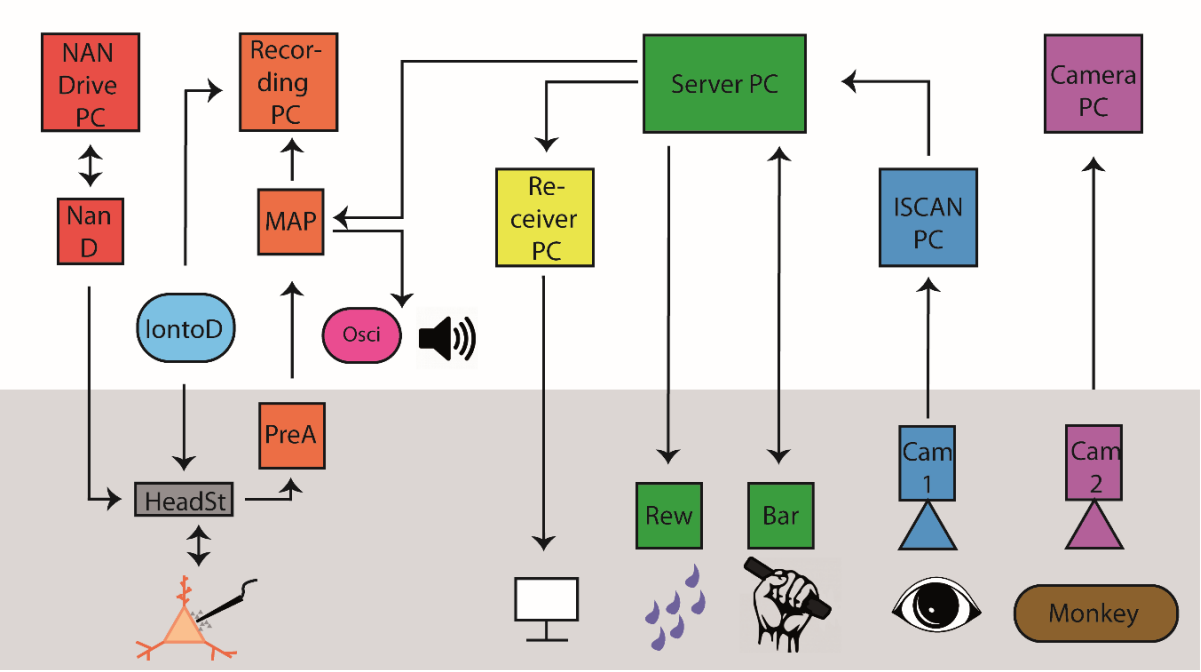

Figure 2.1:Schematic of the experimental set-up*:* gray shaded area: darkened chamber, Server PC ('Server PC' - big green box) controlled task presentation via the receiver PC ('Receiver PC' - yellow box) and the screen inside the darkened chamber, as well as assessment of response behavior (bar grab ('Bar' - second small green box, eye-tracking('ISCAN PC', 'Cam 1' - blue boxes)) and reward delivery ('Rew' - small green box). For precise placement of the recording electrodes we used the NAN drive system ('Nan Drive PC', 'Nan D' - red boxes). Iontophoresis was implemented with the iontophoresis device ('IontoD' - light blue box). Neuronal recordings were conducted through the Plexon system ('PreA' preamplifier, 'MAP' multichannel acquisition processor, 'Recording PC' - orange boxes). Monitoring of the monkey and neuronal recordings was made with a camera ('Cam2', monitoring camera, 'Camera PC' - purple boxes) and oscilloscope ('Osci' - pink box).

2.3 Task

Monkeys performed a numerical same-different decision task (**Figure 2.2**), comparing the set size of reference and test stimuli. They initiated a trial by grasping a response bar and maintaining central fixation on a screen. After a pure fixation period (500ms), a dot display (reference phase, 500ms) cued the animals for the reference numerosity (i.e., number of dots) they had to remember through a memory interval (delay, 1000ms) where no numerosities were presented. During the following display (test phase, 500ms), a test numerosity was shown with either the same or a different number of

dots as the reference numerosity. The test phase was followed by a second delay (decision, 1000ms) without visual information and a rule cue phase (1000ms). Here, the monkeys were presented with one of two rule cues (red or blue square). Correct choices depended on the seen combination of presented stimuli and rule cue. In ‘blue’ trials the monkeys had to release the lever, if the number of items in the reference and test were the same (match trials) and withhold response in trials were both presented

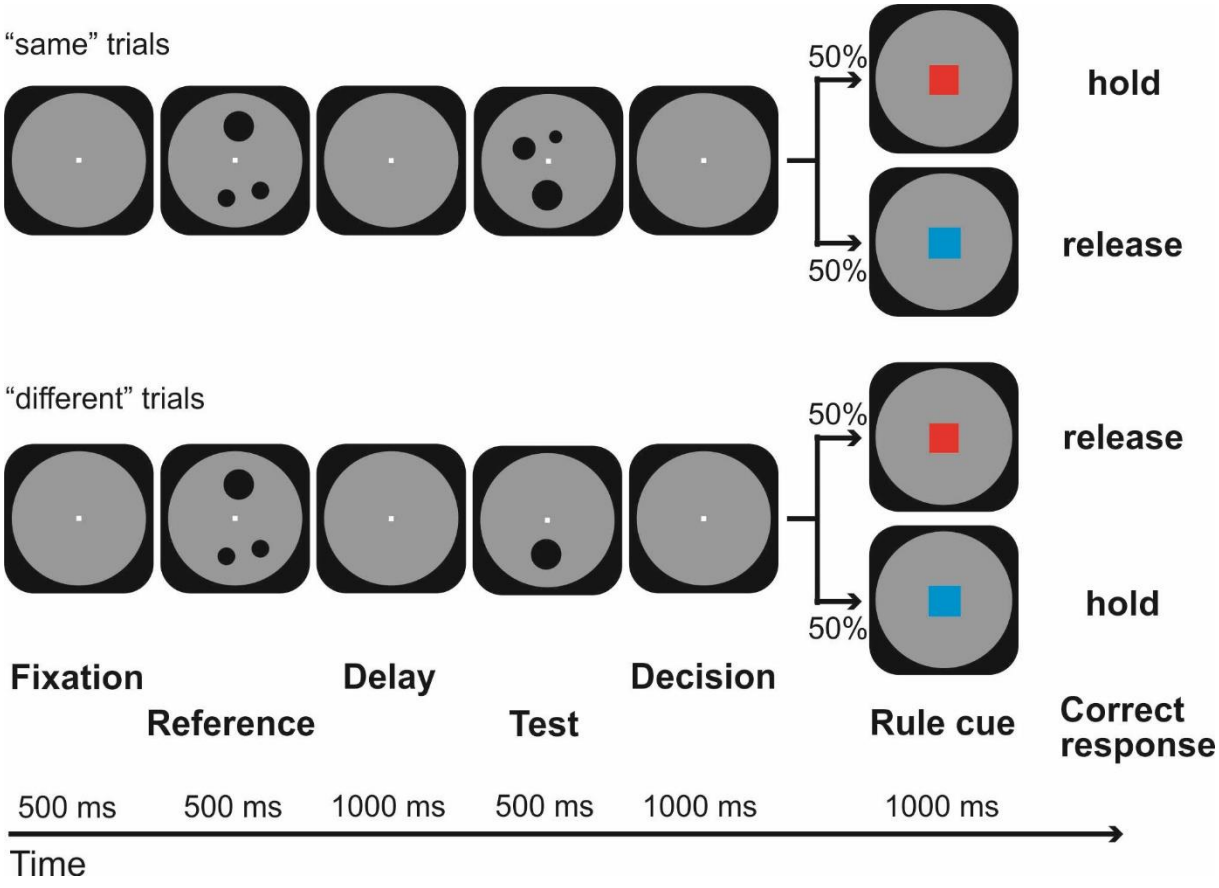

Figure 2.2 Behavioral protocol. Monkeys were required to assess and memorize the number of dots shown as reference to decide whether a second shown numerosity (test) was equal in size. The correct behavioral response was indicated by a rule cue at the end of the task. The correct action was depending on seen combination of numerosities and rule cue. In a “red” rule trial monkeys had to release a lever in “different” trials and withhold response in “same” trials, vice versa in “blue” rule trials. Thus, in this example trial the correct action was to withhold response given the red rule cue was presented while releasing the lever would be rewarded in a blue rule trial. As the rule cue was necessary to prepare a motor response, analysis was restricted to task phases before rule cue presentation.

stimuli contained different number of items (nonmatch trials). In ‘red’ trials, these conditions were reversed, monkeys were to respond to different numbers. Monkeys received a liquid reward for a correct choice. The rule cue was used so that a behavioral response was required in each trial, ensuring that the monkeys were paying attention during all completed trials.

Because both reference and test numerosities varied randomly such that all combinations of reference and sample were shown, the monkeys could only solve the task by assessing the second numerosity display relative to the three possible numerosities of the first numerosity. Monkeys had to keep their gaze within 1.75° of the fixation point from the fixation interval up to the end of the rule phase (monitored with an infrared eye-tracking system; ISCAN, Burlington, MA).

2.4 Stimuli

Numerosity stimuli consisting of multiple-dot patterns were generated by using a custom-written MATLAB script. All numerosity stimuli had a set size of either 1, 3 or 9 (diameter of 0.2°-0.6° visual angle, **Figure 2.3**). They were presented on a gray background circle with a diameter of 5° visual angle. To prevent the monkeys from exploiting low-level visual cues (e.g., dot density, total dot area), a standard numerosity protocol (with randomly selected dot sizes and positions) and a control numerosity protocol (with equal total area and average density of all dots within a trial) were used. Before each session, the stimuli were generated anew using MATLAB (Mathworks). Trials were pseudorandomized and balanced across all relevant features (‘red’ and ‘blue’ rules, reference and test numerosities, standard and control stimuli, match and nonmatch trials), resulting in a total of 48 stimulus conditions. Numerosities one, three and nine were chosen to compensate for the numerical magnitude effect (Moyer and Landauer, 1967; Dehaene, 1992; Dehaene et al., 1998; Nieder and Dehaene, 2009), which states that larger numerosities need to be more distant to be equally well discriminated as smaller numerosities. In our case, numerosities three and nine are equally well discriminable as numerosity one and three.

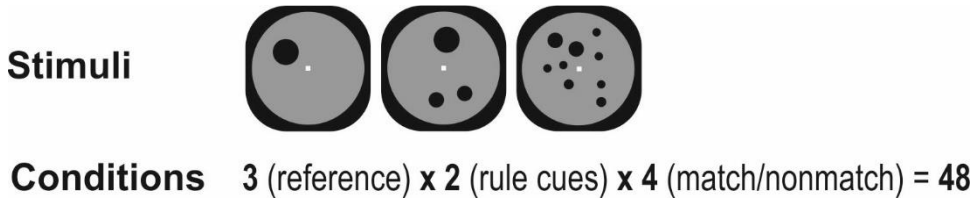

Figure 2.3*:* **The three different numerosities** were presented on a gray circular background and used as reference and test stimuli. In combination with the two rule cues there were a total of 48 conditions

2.5 Electrophysiology and Iontophoresis

Extracellular single-unit recording and microiontophoretic drug application were performed as described previously in work from our group. (Jacob et al., 2013; Ott et al., 2014). We recorded in the dorsolateral Prefrontal Cortex, above the principal sulcus (**Figure 2.4**).

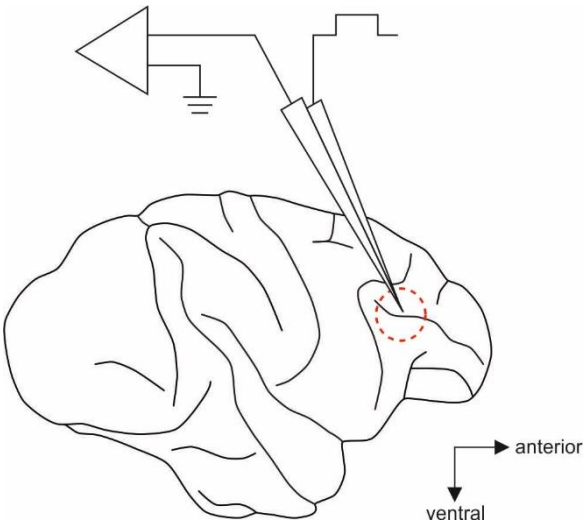

Figure 2.4: Recording location. Lateral view of a rhesus monkey brain, facing to the right. Red circle depicts the principal sulcus region (PFC), location of extracellular neuronal recordings and 5-HT mircoiontophresis

We used up to three custom-made tungsten-in-glass electrodes (**Figure 2.5**, (Thiele et al., 2006; Jacob et al., 2013; Ott et al., 2014)) in each session. The electrodes were flanked by two pipettes, which were filled with one of two serotonergic agents before

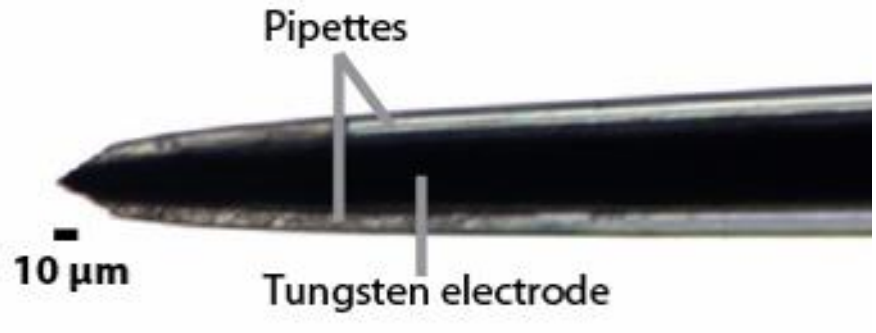

Figure 2.5: Picture of a custom-made electrode, taken through a light microscope, zoom level 40 x

recording sessions (see **Section 2.6**). To insert the electrodes transdurally we used a modified electrical microdrive (NAN Instruments). This consisted out of three towers, which each contained a rail system connected to tiny motors. These towers were mounted to the recording chamber with the help of a baseplate. Each recording

electrode was attached to a different tower's rail system and by this could be precisely positioned (in the range of one µm) on a vertical axis and individually inside the cortical tissue. Usually, the depth of recording electrodes was related to the first detectable trace of neuronal activity through visual and auditory monitoring. In some cases, recording depth of an individual electrode was adjusted to deeper levels, to yield well-isolated signals. Recorded single neurons were not preselected to task-related neuronal activity or any given drug effect. As described in **Section 2.2**, signal acquisition, amplification, filtering, and digitalization were conducted with the MAP system (Plexon). To implement drug microiontophoresis we used the MVCS

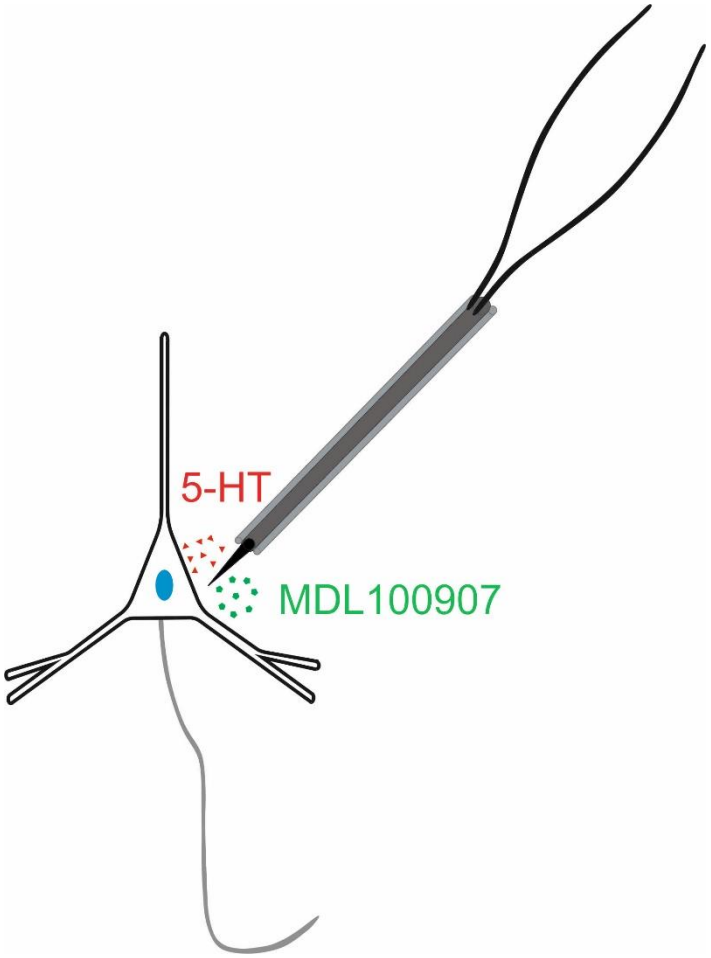

Figure 2.6: Schematic of a recording electrode, with two flanking pipettes. During drug conditions ejection currents were used to apply one of the serotonergic agents (red:5-HT, green: MDL100907) into the tissue in proximity of the recorded neuron. We used only one substance for a recording session

iontophoresis system (npi electronic, see **Section 2.2**). In each session only one flanking pipette was filled with one of the serotonergic agents (either 5-HT, MDL100907) or, for current control experiments, with 0.9% NaCl. The second pipette

was usually filled with 0.9% NaCl, as security step during the filling process, to prevent any functional substance to enter the second barrel. This was important to make sure that as little as possible of the functional drugs entered the tissue during experiments unintended. In some cases, the second barrel was not filled at all. **Figure 2.6** shows a schematic of one recording electrode during iontophoretic drug application. After each session we measured electrode impedance and pipette resistance. Electrode impedances ranged between 0.1 and 3.3 MΩ (measured at 500Hz; Omega Tip Z; World Precision Instruments, mean 1.02 MΩ, SEM ± 0.59). Mean pipette resistance was 38.52 MΩ (SEM ± 20.5), depending on opening diameter and applied drug. Recording session always started with control conditions, using the retention current, followed by drug conditions (**Figure 2.7**) in which the ejection current (see **Section 2.6**) was used to apply the drugs. Both iontophoretic conditions alternated throughout the whole recording session (**Figure 2.7**). Usually, drug conditions lasted for 10–15min, depending on the time the monkey took to complete a certain amount of trials correctly. After max. 17 minutes drug conditions were discontinued. Control or drug application block consisted of either 48 or 72 correct trials in order to yield sufficient trials for analysis. To increase recording stability and as a physical boundary to keep the dura from drying out, we filled the recording chamber with 3% agarose for the duration the recording session.

Single cells were sorted manually offline according to the waveform (Offline Sorter; Plexon). Drug application through Iontophoresis works fast and any given drug effect on neuronal firing properties usually happens quickly. Therefore, it was unnecessary to exclude trials close to iontophoresis-switching points except for baseline analysis.

Figure 2.7: Schema of iontophoretic condition sequence in a typical recording session

2.6 Iontophoretic applied drugs

For this study we used two serotonergic drugs, namely the endogenous neuromodulator 5-HT and the highly selective 5-HT2A receptor antagonist MDL100907 for iontophoretic application. Both substances were solved in ultra-pure

water and pH adjusted (to approximately pH 4) with 1 N hydrochloric acid (Sigma-Aldrich). As solutions were prepared multiple times, pH and resulting concentration varied slightly (5-HT: pH between 3.64 and 3.85, concentration between 10.0 and 10.5 mM; MDL100907: pH between 3.58 and 3.61, concentration between 9.2 and 9.9 mM). The solutions were stored in 40 µl aliquots at -20°C and defreezed as required before recording sessions. The solution was then filled into one of the adjacent barrels from where the functional component was either ejected or retained by the means of small currents during the experiment. As in previous experiments (Jacob et al., 2013; Ott et al., 2014) we used retention currents of –7nA to retain the drugs in the pipette during control conditions. In the first few recording sessions, we determined ejection currents that ensured ejection of appropriate drug amounts into the tissue. Therefore, the ejection currents for 5-HT varied between +2 and +30nA. The ejection currents for MDL100907 lay between +15 and +25nA. Drug sensitivities varied highly between the two monkeys which also resulted in different ejection current ranges for each monkey. To ensure that any given effect derived from the ejected substances and not from applied iontophoretic currents we also conducted control recordings with 0.9% physiological NaCl (pH 5.9). The barrel, usually filled with a serotonergic substance, was instead filled with saline, which was ejected with a +30nA current during drug condition. We did not investigate dosage effects and chose the strongest ejection current which would not silence the recorded cell.

2.7 Data Analysis

2.7.1 Behavioral Data

We calculated the performance (percentage correct) by determining the proportion of correct trials to all complete trials, in one case sorted after stimulus protocol (standard vs control stimuli) and in the other case sorted after seen rule (red rule vs blue rule). Next, we investigate performances for each reference-test combination individually. To this end, we compiled behavioral performance functions, which show how often an animal judged the test numerosity to be equal to the reference numerosity.

2.7.2 Modulation of Neuronal Baseline Activity

For this analysis we considered all recorded neurons which had at least 96 consecutive trials, 48 trials in each iontophoretic conditions (control/drug). Baseline discharge rates were assessed during the first 350ms of the 500ms fixation period preceding reference presentation. This was done to exclude signals related to the anticipation of visual stimuli. For this analysis, we considered only the first control and drug application blocks (48 trials prior and subsequent to the first switch of iontophoresis) to exclude changes in baseline related to potential residual substance in the tissue. The three first trials after the first switch between iontophoresis conditions were also excluded from testing, to account for the time course of drug effects (wash-in). The average spiking activity in each trial was calculated for each cell separately and then averaged across cells. To visualize the change in firing rates from control to drug phases, the resulting mean per drug trial was normalized to the mean discharge rate across control trials and smoothed with a Gaussian kernel (width of 10 trials). The mean change in spike rate was calculated by subtracting the mean control spike rate from the drug spike rate for each cell individually and then averaging the result.

2.7.3 Numerosity-selectivity in reference phase and delay phase

For this analysis we considered all well-isolated recorded single units with an average discharge rate above 0.5Hz. Additionally, each cell had to have at least three trials per reference condition (‘1’,’3’ and ‘9’) and per iontophoresis condition (control/drug conditions) to enter the analyses. The maximum number of trials was 117/114 (5-HT/MDL100907) control trials and 92/101 (5-HT/MDL100907) drug trials per reference condition, with an average of 45 ± 2 (SEM) / 42 ± 2 (SEM) (5-HT/MDL100907) control trials and 39 ± 2 (SEM) / 33 ± 2 (SEM) (5-HT/MDL100907) drug trials per one of the reference conditions (i.e., the average neuron was recorded for 253 ± 12 (SEM) / 225 ± 12 (SEM) (5-HT/ MDL100907) trials: three reference conditions for control and drug conditions, respectively). Only correct trials were included. We calculated a three-way ANOVA for each neuron to determine if a neuron’s response was correlated with the numerical identity of the reference stimulus. For the analysis of the reference phase, we used spike rates in a 500ms window beginning 100 ms after onset of the reference. We repeated these calculations for the delay, thus checking whether cells responses

represent numerosity in working memory. Here, we used an 800ms analyzing window, beginning 300ms after reference offset. The main factors of the ANOVA were reference numerosities (‘1’,’3’ or ‘9’), stimulus protocol (standard/control) and iontophoresis condition (control conditions/drug conditions). We identified numerosity-selective neurons by a significant main factor of reference numerosity, that the monkeys had to remember ($p < 0.05$). To ensure that neuronal responses varied with the abstract numerical identities rather than with the stimulus protocol, we excluded neurons with a significant main factor stimulus protocol as well as with a significant interaction of the main factors reference numerosity and stimulus protocol ($p < 0.05$). For the remaining neurons we averaged across standard and control stimuli trials. Further, we quantified the delta response, which is a neuron’s selectivity to the preferred numerosity/decision by calculating the difference between the normalized activity for the preferred and the nonpreferred stimulus separately for control conditions and drug application trials in the same analysis window as used for the ANOVA.

2.7.4 Test numerosity-selectivity in test and decision phase

To identify test numerosity-selective neurons, we employed a 4-way ANOVA with following main factors: test numerosities (‘1’,’3’ or ‘9’), decision (‘same’/’different’), stimulus protocol (standard/control) and iontophoresis condition (control conditions/drug conditions). We included all well-isolated single units with an average discharge rate above 0.5 Hertz and at least 3 trials per condition combination (test times decision) in the analysis. The maximum number was 114/115 (5-HT/MDL100907) control trials and 92/95 drug trials per test condition, with an average of 48 ± 2 (SEM) / 50 ± 3 (SEM) (5-HT/MDL100907) control trials and 42 ± 2 (SEM)/ 40 ± 2 (SEM) (5-HT/MDL100907) drug trials per one of the test conditions (i.e., the average neuron was recorded for 268 ± 12 (SEM) / 248 ± 14 (SEM) (5-HT/MDL100907) trials: three test conditions for control and drug conditions, respectively). Calculations were performed only for correct trials. To analyze selectivity during test presentation we used a 500 ms analysis window for the ANOVA starting 100 ms after test onset. The analysis window for the decision phase started 300 ms after test onset and lasted 800 ms. Test-selective neurons were identified by a significant main factor for test numerosity. All cells with a significant main factor protocol or an interaction of protocol

with test were discarded for further analysis. Further, we quantified the delta response, which is a neuron's selectivity to the preferred numerosity/decision by calculating the difference between the normalized activity for the preferred and the nonpreferred stimulus separately for control conditions and drug application trials in the same analysis window as used for the ANOVA.

2.7.5 Decision-selectivity in test and decision phase

We used the same 4-way ANOVAs as described in **Section 2.7.3** to identify decision-selective neurons. Cells were considered decision-selective if the ANOVA revealed a significant main factor for decision type, without a significant main factor protocol or an interaction of protocol with decision. Otherwise cells were discarded for further analysis. The maximum number was 177/168 (5-HT/MDL100907) control trials and 135/144 drug trials per decision condition, with an average of 72 ± 3 (SEM) / 69 ± 4 (SEM) (5-HT/MDL100907) control trials and 62 ± 3 (SEM)/ 55 ± 3 (SEM) (5-HT/MDL100907) drug trials per one of the decision conditions (i.e., the average neuron was recorded for 268 ± 12 (SEM) / 248 ± 14 (SEM) (5-HT/MDL100907) trials: two decision conditions for control and drug conditions, respectively). Further, we quantified the delta response, which is a neuron's selectivity to the preferred numerosity/decision by calculating the difference between the normalized activity for the preferred and the nonpreferred stimulus separately for control conditions and drug application trials in the same analysis window as used for the ANOVA.

2.7.6 Single-Cell and Population Responses

For plotting single-cell spike density histograms, the average firing rate in trials with one of the three different reference numerosities (correct trials only) was smoothed with a Gaussian kernel (bin width of 200 ms, steps of 1 ms). For the population responses, discharge rates of trials with rule cues signifying the same decision were averaged. A neuron's preferred numerosity was defined as the numerosity yielding the higher average spike rate in the analysis window used for the ANOVA. The nonpreferred numerosity was defined as the numerosity resulting in lowest average spike rate. Neuronal activity was normalized by subtracting the mean baseline (first

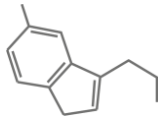

350 ms of fixation period) firing rate in the control condition and dividing by the standard deviation of the baseline firing rates in the control condition. For population histograms, normalized activity was averaged and smoothed with a Gaussian kernel (bin width of 200 ms, step of 1 ms).

2.7.7 Drug Modulation Index

To determine if drug induced modulation of a neuron's discharge rate was dependent on the neurons stimulus preference, we calculated a drug modulation index (MI) for each neuron, separately for the preferred and the nonpreferred numerosity. The MI was computed by first subtracting the mean baseline spike rate (350 ms fixation period preceding reference presentation) from each trial separately for control and drug conditions and dividing by the standard deviation of baseline spike rates to account for general shifts in baseline spike rates induced by the drugs. Next, we calculated the MI for the preferred numerosity defined as the difference between the mean response to the preferred numerosity in the drug condition and the mean response to the preferred numerosity in the control condition for each neuron. The MI for the nonpreferred numerosity was calculated in the same way. Thus, the MI reflects the amount by which the drug modulates the preferred or the nonpreferred numerosity, respectively, in comparison to the neuron's baseline activity. We conducted this analysis for neurons, recorded in 5-HT sessions and MDL100907 sessions separately.

2.7.8 Receiver Operating Characteristic Analysis

We used receiver operating characteristic (ROC) analysis derived from Signal Detection Theory (Green and Swets, 1966) to quantify coding strength. The ROC

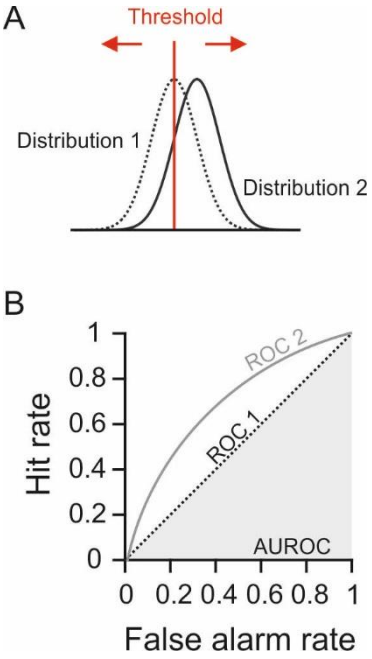

Figure 2.8: Schematic of receiver operating characteristic. A) The ratio of hits and false alarms of two distributions (dashed and solid lines) depend on adjustable threshold (red line). B) The ratios plotted against each other result in the ROC. The ROC1 depicts two indistinguishable distri-butions, whereas both distributions responsible for the ROC2 share only some overlap. Area under the ROC = AUROC

denotes the ratio between correct detections and false alarms ('detection' of non-existing stimuli) under different detection thresholds (**Figure 2.8 A**). Afterwards, the area under the receiver operating characteristic (AUROC) is determined (**Figure 2.8 B**), which value represents the probability of a correct decision between target and noise when judged by an ideal observer. This means, when AUROC is 0.5, both distributions are not distinguishable, whereas values of 1 indicate perfect discriminability. First developed as a tool during World War II for unbiased discrimination between targets and noise by radar engineers, today, the AUROC is a widely used nonparametric measure to discriminate between two distributions. In this study AUROCs were used to quantify numerosity/decision coding quality. Therefore, we calculated the AUROC for each neuron using the spike rate distributions of the preferred and the nonpreferred numerosity/decision in the same analysis window used for the ANOVA.

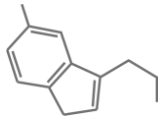

2.7.8.1Sliding ROC analysis

To determine any temporal effect of drug modulation on coding strength we performed a sliding ROC analysis for each selective neuron separately for control conditions and drug application trials. All numerosity-selective or decision-selective neurons entered the analysis. The AUROC comparing neuronal activity between preferred and non-preferred numerosity/decision was calculated for 100 ms long windows stepped in 10 ms increments. For numerosity-selective neurons in the reference phase, analysis started at the start of the trial (1 ms) and was conducted until reference offset (1000 ms), numerosity-selective neurons in the delay phase were investigated for temporal modulation effects starting at reference onset (501 ms) until delay offset (2000 ms). For both numerosity and decision coding strength in test phase the overall analysis window started in the second half of the delay (1501 ms) and lasted until the first half of the decision phase (3000 ms). Cells which were selective for either test numerosity or decision were investigated in the window starting with test onset (2001 ms) and ending after decision phase offset (3500 ms). To identify the latency of a neuron, that is the time point the neuron gets selective, we applied a permutation test. Therefore, we estimated the null-distribution by randomly shuffling labels of preferred and non-preferred groups and recalculating the AUROC 1000 times for each 100 ms window of the sliding window analysis. The latency of a neuron was defined as the first time point the actual AUROC value was larger than 95 % of the null-distribution in at least 3 consecutive windows (control for multiple comparisons). However, we only considered latencies within the time window a given neuron was identified as selective by the above described ANOVAs (Sections 2.7.3, 2.7.4 and 2.7.5). So, significant AUROC deviations from the null-distribution of neurons, selective during the reference phase, were only considered when they existed after reference onset. This was also true for all other analysis windows (delay latencies had to be later than 1001 ms, test latencies > 2001 ms, decision phase latencies > 2501 ms). The latency lengths were calculated from the start of the sliding window analysis window. Neurons of which no latency could be computed were excluded from the analysis.

2.7.9 Sliding-window ω^2 PEV analysis

We investigated the temporal variation of information about task factors namely reference numerosity, test numerosity and decision type within a neuron's discharge rate. To this end, we calculated omega square percentage explained variance (ω^2 PEV) individually for each neuron and separately for drug-application and control condition trials using one-way ANOVAs for each factor respectively in a sliding window fashion (200 msec in 20 msec steps). The measure ω^2 PEV reflects how much of the variance of a neuron's discharge rate can be explained by the respective task factor (e.g. reference numerosity). As ω^2 PEV is calculated using unbiased variance components the resulting values remain unbiased. Nevertheless, PEV values vary depending on the number of trials included in the analysis. Therefore, we balanced trial numbers over factor levels, employing only the minimum trial number across groups. However, we did not want to exclude trials of factor levels with more than minimum trials so repeated measurement 100 times, drawing a random subset of trials and calculating the PEV. The mean of the resulting 100 values was taken as overall statistic (Buschman et al., 2011; Jacob and Nieder, 2014). Cells with less than 30 trials in either iontophoresis condition did not enter the analysis. We identified the time points in a trial where individual cells carried significant information about the task factors by the means of a randomization test. We shuffled group membership labels and firing rates randomly and recalculate the ω^2 PEV. This process was repeated 1000 times for each time window of the sliding window analysis (0 - 3700 msec, 200 msec in 20 msc steps) which resulted in a null-distribution for each analysis window and iontophoresis condition. When compared to the null-distribution the actual PEV values had to be larger than 95 % of the null distribution in at least 5 consecutive windows (control for multiple comparisons) for the neuron to be considered selective for the respective task factor. Possible drug-induced differences between information content were determined with a bin-wise Wilcoxon paired signed rank test (alpha 0.05). To control for multiple comparison at least 5 consecutive bins had to be significantly different.

3 Results

To investigate the role of 5-HT in two different cognitive processes (visual working memory and decision making) in the lateral PFC, we trained two monkeys on an abstract numerical comparison task. The monkeys had to detect the number of items on a reference stimulus (reference), maintain the numerical information in working memory during a delay period and make a decision after being presented with a second stimulus (test) whether the numerosity matched the first stimulus ("same") or not ("different") (**Figure 2.2**).

3.1 Performance

53 behavioral sessions of monkey E and 75 behavioral sessions of monkey Y entered analysis. The maximum number of trials was 300 for monkey E with an average of 182 trials ± 11 [SEM] per session. In total 10934 trials of monkey E entered the analysis of which 10283 were solved correctly. Monkey Y solved 43872 out of 47084 trials correctly. The maximum number of trials was 661 with an average of 346 ± 15 [SEM] trials per session. Monkeys proficiently decided whether the second numerosity (test) matched the reference (monkey E 94% ± 0.41 [SEM] correct, monkey Y 93% ± 0.26 [SEM] correct).

To ensure the assessment of numerosity rather than low-level visual features we employed control stimuli, with equal total area and average density of all dots within a trial. Control protocol trials were shown equally often as standard trials in a pseudorandomized order. The monkeys performed for all protocol and rule types well above chance level (monkey E: $p_{std} < 0.001$, $p_{ctr} < 0.001$, $p_{red} < 0.001$, $p_{blue} < 0.01$; monkey Y: $p_{std} < 0.001$, $p_{ctr} < 0.001$, $p_{red} < 0.001$, $p_{blue} < 0.01$, binomial test against chance performance 0.5). The monkeys performances differed significantly across stimulus protocols (standard/control, **Figure 3.1 A**, $p_{Monkey\ E} = 0.0469$, t value = 2.0361, n = 53, $p_{Monkey\ Y} < 0.001$, t value = -4.4168, n = 75 ,both paired t test) but not for rule cues (red/blue, **Figure 3.1 A**, $p_{Monkey\ E} = 0.7385$, t value = -0.3356, n = 53, $p_{Monkey\ Y} = 0.8355$, t value = 0.2084, n = 74, both paired t test). **Figure 3.1 B** shows the probability the second presented numerosity (test) was judged to match the numerosity shown as reference, so called behavioral performance functions. Thus, each curve shows the performance for "same" trials (reference and test showed equal quantities, curve

peaks) and the percentage of error trials in “different” trials (reference and test showed different quantities, non-peak values). The behavioral performance functions display the numerical distance effect (Nieder and Dehaene, 2009). Monkeys made more mistakes when the numerosity was closer in value, e.g. animals misjudged test numerosity three to be equal to reference numerosity one more often than test numerosity nine (**Figure 3.1 B** orange curves).

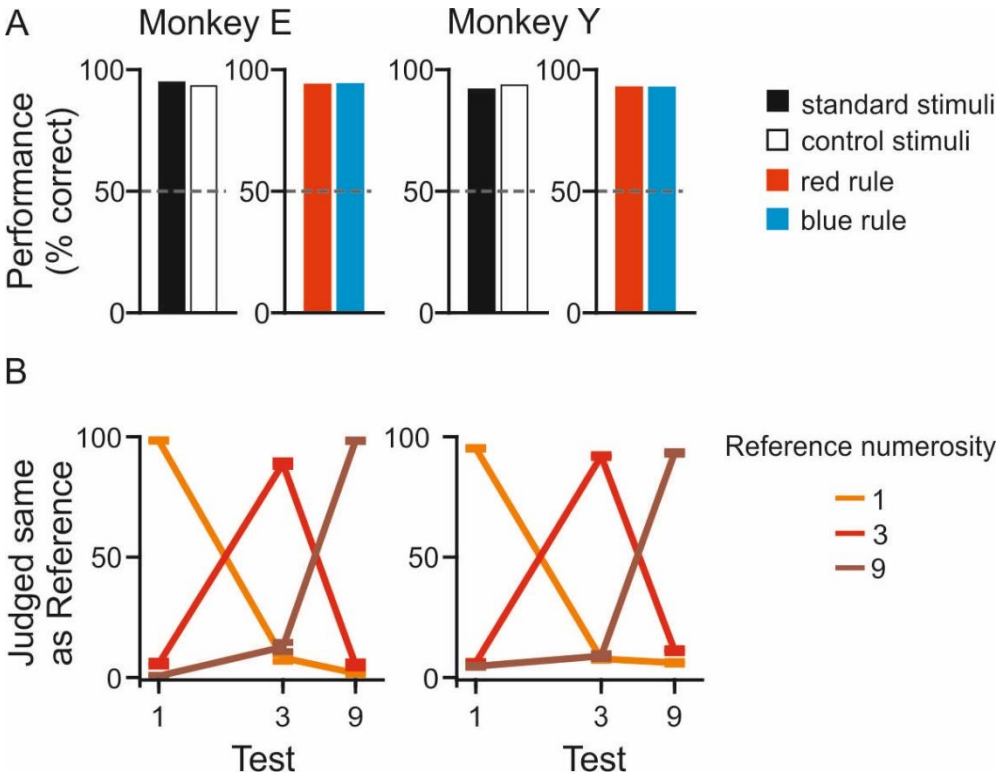

Figure 3.1: Behavioral Performance A) Percentage of correct trials for both monkeys (monkey E – left, monkey Y – right) for stimulus protocol (first and third bar graphs) and rule cue (second and fourth bar graphs). Performances for each protocol and rule type were significantly (all 8 p-values < 0.001) better than chance level (the dotted line indicates chance performance at 50%). B) Behavioral tuning curves for both monkeys (monkey E – left, monkey Y – right). Colors correspond to the reference numerosity. The curves show how often the animals judged the test numerosity to match the reference numerosity. Thus, peak values depict percentages for correct choices in “same” trials while other values show the percentages of erroneous choices in “different” trials.

3.2 Recordings

We recorded single cell activity in the lateral PFC and simultaneously applied serotonergic agents in proximity of the recorded cell using microiontophoresis while monkeys performed the task (**Figure 2.4**). Trial blocks with (drug condition) and without (control condition) pharmacological manipulations alternated (repeatedly) within one recording session (**Figure 2.7**). All recording sessions started with a control condition

block. We used one of two substances each session, either 5-HT or the 5-HT2A receptor antagonist MDL100907. Physiological saline solution (0.9% NaCl) was used for control experiments. We recorded 487 randomly selected neurons in total (180 from monkey E, 307 from monkey Y). Analyses were restricted to tasks phases before the rule cue presentation, ensuring all signals to be free of preparatory motor activity.

3.3 5-HT Application but not 5-HT2A Blockage Modulated Baseline Activity.

218 single neurons from the lateral PFC of two macaque monkeys (78 from monkey E, 140 from monkey Y) entered the analysis. We compared fixation period activity of the first drug application phase with the discharge rates during the fixation period of the first control condition. The discharge rates were assessed during the first 350 ms of the fixation period, to avoid including anticipation signals of visual input. 5-HTR stimulation significantly reduced baseline activity (**Figure 3.2 A**, ΔFR = -0.62 Hz, p = 0.007, n = 110, Wilcoxon test). No modulation of baseline activity was found after blockage of 5-HT2AR through MDL100907 application (**Figure 3.2 B**), ΔFR = -0.3 Hz, p = 0.525, n = 86, Wilcoxon test) nor after applying NaCl solution as a control (**Figure 3.2 C**, ΔFR = +0.16 Hz, p = 0.39, n = 22, Wilcoxon test). **Figure 3.2 D** (left and middle panel) shows the time-dependent baseline modulations aligned to onset (left) and offset (middle) of drug-application, that differed significantly for 5-HT (**Figure 3.2 D**, right panel, p = 0.0041, n = 110, Wilcoxon test against 0). In sum, 5-HTR stimulation decreases excitability. However, this effect seemed to be less conveyed by the 5-HT2AR, as its blockage showed no significant effect on the baseline activity.

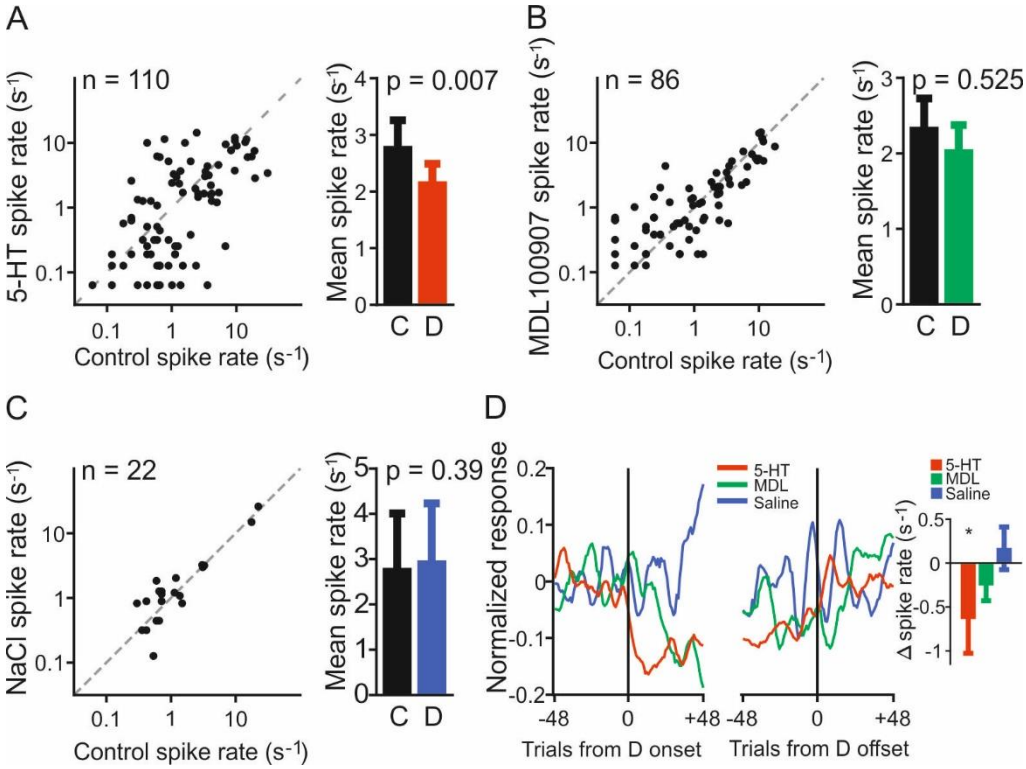

Figure 3.2: Baseline Modulation A) Comparison of average baseline spike rates of individual neurons during the first block of 5-HT application and first control condition block (left panel) and mean baseline spike rates during the first block of 5-HT application and first control condition block (right panel). 5-HT decreased baseline spike rates significantly. C, control condition; D, drug condition B) Same conventions as in (A), showing that MDL100907 showed no effect on baseline spike rates. C) Same conventions as in (A), showing that NaCl did not change baseline spike activity. D) Time-dependent drug effects (wash-in and wash-out effects for the first onset and offset of drug application) on normalized baseline activity for all neurons aligned to first onset (left) and first offset (middle) of drug application. Mean spike rate difference for drug and control conditions (right, first drug application block). Both MDL100907 (green bar) and NaCl (blue bar) show no significant effect on baseline firing rate whereas 5-HT (red bar) reduced baseline activity significantly ($p < 0.05$, Wilcoxon signed rank test). Error bars represent SEM, n denotes sample size, p values of Wilcoxon signed rank tests.

3.3.1 5-HT application reduces numerosity-selectivity during reference presentation in single cells.

To investigate the role of the serotonergic system during the visual presentation of the reference numerosity, we identified numerosity-selective neurons recorded during sessions with 5-HT and MDL100907 application as well as during control experiments with NaCl using a 3-way ANOVA (main factors: numerosity (1,3 or 9), stimulus protocol (standard or control) and drug condition (control or pharmacological application)). We identified 22 (21%, **Figure 3.3 A**) merely numerosity-selective cells recorded in sessions with 5-HT, 16 (16%, **Figure 3.3 B**) in sessions with MDL100907 and 3 (14%,

Figure 3.3 C) during the control experiments with NaCl application. **Figure 3.4 A** shows a numerosity-selective neuron with decreased numerosity-selectivity during 5-HT application (preferred numerosity = 3, red trace). 5-HT did not alter preference order but reduced discharge rates differences between presented reference

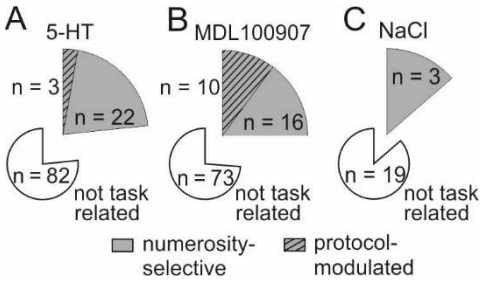

Figure 3.3: Number of recorded neurons that were numerosity-selective during the reference phase recorded in session with A) 5-HT application, B) MDL100907 application and C) in control experiments with NaCl.

numerosities (**Figure 3.4 A**, right panel). This neuron also shows a strong decrease in discharge rate for the second-preferred numerosity (numerosity 1, orange trace) during reference presentation. **Panel B** shows a numerosity-selective example neuron recorded during control conditions (left panel) and during MDL100907 application (middle panel). Blockage of 5-HT2A receptors showed no significant modulation of numerosity-selectivity, which is also evident in the tuning curves. The small decrease in neuronal activity for all numerosities is not significant. We found no modulatory effect of NaCl application on numerosity selectivity of the example neuron presented in **Figure 3.4 C**. Neuronal activity for the different numerosities did not change between control conditions (left) and NaCl application trials (middle). The tuning curve for NaCl application (blue curve) shows a small increase for the second preferred numerosity (numerosity 9) but this modulation is not significant.

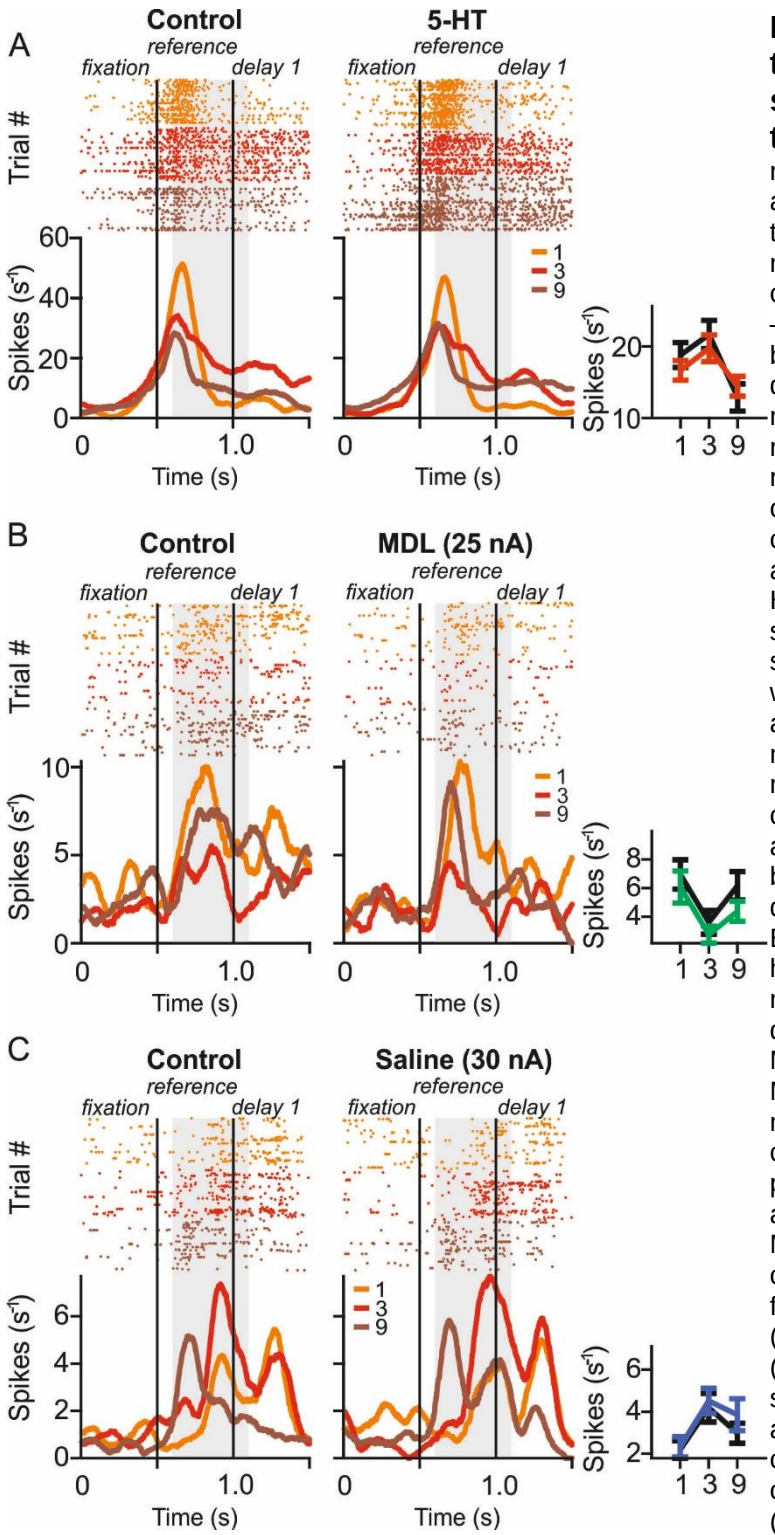

Figure 3.4: Responses of three reference numerosity-selective example cells in the reference phase A) Dot raster (top: each dot represents an action potential, each line a trial, trials sorted after presented numerosity in the reference phase, colors indicate numerosities: orange – numerosity 1; red – numerosity 3; brown – numerosity 9) and spike-density histogram (bottom) of a numerosity-selective single neuron recorded during fixation phase, reference presentation and first half of delay 1, separated for control conditions (left panel) and 5-HT application (middle panel). After 5-HT application, numerosity-selectivity was decreased. Gray shaded area depicts the analysis window. Right panel shows the averaged discharge rates for all numerosities of the same single neuron separately for control conditions (black curve) and 5-HT application (red curve). Differences between averaged spike rates were decreased during 5-HT application. B) Dot raster (top) and spike-density histogram (bottom) of an example numerosity-selective cell recorded during control conditions (left) and MDL100907 application (middle). MDL100907 showed almost no modulatory effect on numerosity coding. The tuning curve (right panel) shows a slight decrease in all average firing rates during MDL100907 application (green curve) and a small relative change for the second preferred numerosity (9) compared to control conditions (black curve). C) Dot raster (top) and spike-density histogram (bottom) of an example numerosity-selective cell recorded during control conditions (left) and NaCl application (middle). NaCl did not alter numerosity coding except for a slight increase in neuronal activity for the second preferred numerosity (numerosity 9), as also evident in the tuning curves (black curve: control conditions, blue curve: NaCl application trials).

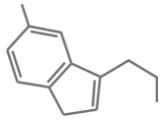

3.3.2 The Population of Numerosity-Selective Neurons show decreased numerosity coding during the reference phase after 5-HT Application

A decrease in numerosity-selectivity, as seen in the example cell in **Figure 3.4 A**, was also evident for the whole population of numerosity-selective neurons recorded during control conditions and 5-HT application (**Figure 3.5 A**). For comparison, discharge rates for preferred (red trace) and nonpreferred (blue trace) numerosity stimulus were normalized to control baseline and averaged separately for control (**Figure 3.5 A** left) and drug trials (**Figure 3.5 A** right**)**. The reduced numerosity-selectivity was due to reduced discharge rates for preferred stimuli as evident in the tuning curves (**Figure 3.5 B**, lower panel, black: averaged normalized response during control conditions, red curve: averaged normalized response during drug application). To study the impact of 5-HT on preferred and nonpreferred stimuli in more detail, we calculated the modulation index (**Figure 3.5 B,** upper panel). Modulation was not significant (mean $MI_{Nonpreferred}$ = -0.015 ± 0.113, mean $MI_{Preferred}$ = 0.064 ±0.102 [SEM], p = 0.17, n = 22, Wilcoxon paired test). We used receiver operator characteristics to assess the quality of coding in numerosity-selective neurons. The area under the curve (AUROC) was computed for control conditions and 5-HT application separately using the same analysis window as used in the ANOVA (see **Section 2.7.3**). Application of 5-HT decreased numerosity coding strength (AUROC) in 68 % (15/22) of all numerosity-selective cells recorded with 5-HT (**Figure 3.5 C**, ΔAUROC = + 0.039 ± 0.017 [SEM], p = 0.042, n = 22, Wilcoxon test). 5-HT2A blockage by MDL100907 application showed no effect on numerosity-selectivity during reference presentation in the population of reference-selective neurons (**Figure 3.5 D-F),** similar to what is shown for an example cell (**Figure 3.4 B**). Even though the averaged normalized discharge is reduced overall during MDL100907 application (**Figure 3.5 E** lower panel) MDL100907 had no effect on the MI (**Figure 3.5 E** upper panel, mean $MI_{Nonpreferred}$ = 0.1634 ± 0.0635, mean $MI_{Preferred}$ = 0.1905 ± 0.0861 [SEM], p = 0.17, n = 22, Wilcoxon paired test) nor on AUROCs (**Figure 3.5 E** ΔAUROC = - 0.012 ± 0.02 [SEM], p = 0.501, n = 16, Wilcoxon test). Further, we checked for iontophoresis-current induced effects by conducting the same analyses with data from control experiments with NaCl (**Figure 3.5 G-I**). We find no effects of applied current on MI (mean $MI_{Nonpreferred}$ = -0.0433 ± 0.0418, mean $MI_{Preferred}$ = 0.0072 ± 0.0864 [SEM], p = 0.75, n = 3, Wilcoxon paired test) or coding

strength (**Figure 3.5 I** ΔAUROC = - 0.047 ± 0.019 [SEM], p = 0.25, n = 3, Wilcoxon test).

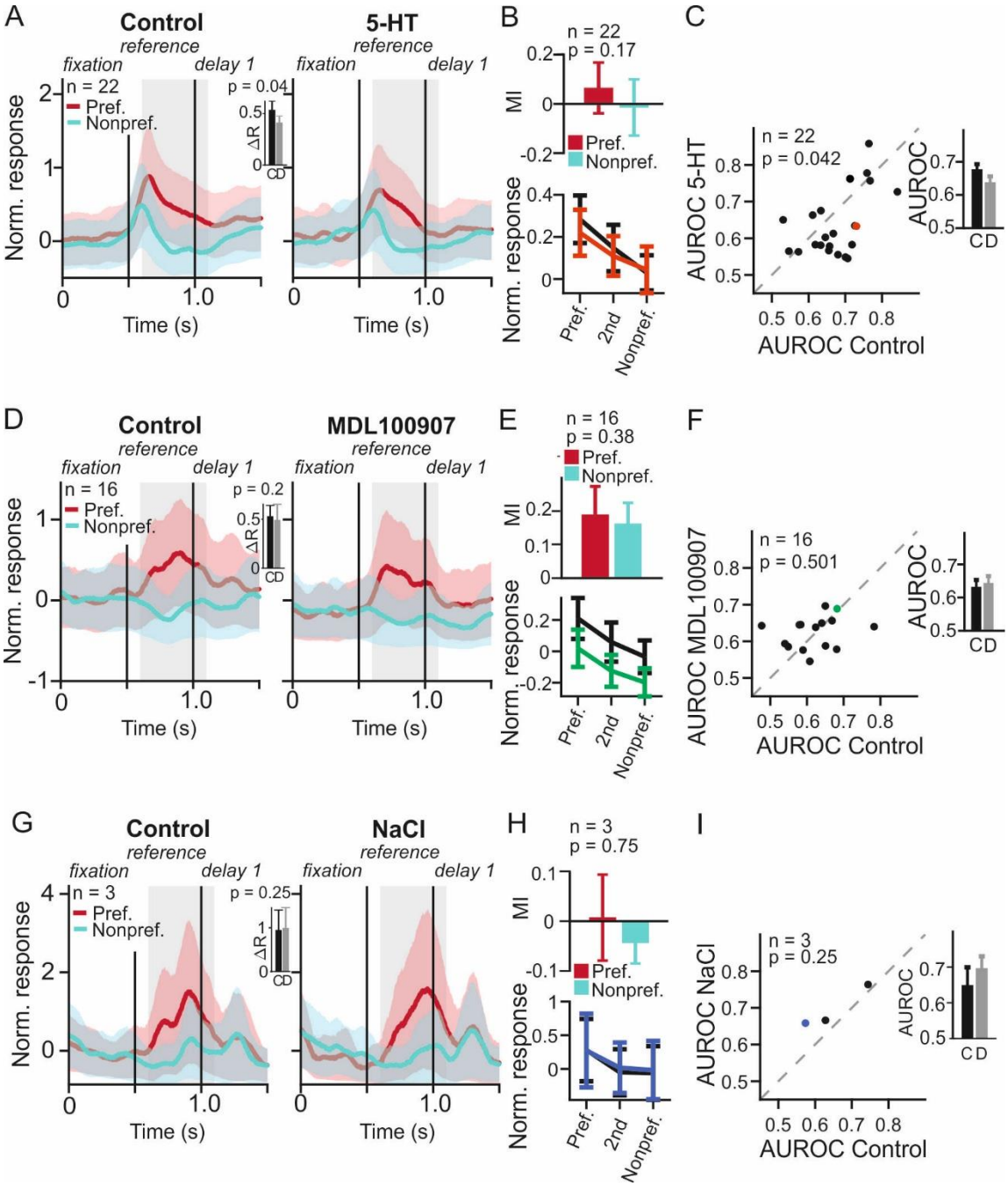

Figure 3.5: Modulation of numerosity-selective Neurons by 5-HT. A) Normalized (to baseline of control conditions) responses averaged over all numerosity-selective neurons for preferred (red trace) and nonpreferred (blue trace) numerosity, separated for control conditions (left panel) and 5-HT application (right panel; trace for second preferred numerosity not shown). Inset shows differences between normalized responses ΔR of preferred and nonpreferred numerosity for control conditions (black bar) and 5-HT application (gray bar). B) Lower panel shows averaged normalized tuning curves for all numerosity-selective neurons separately for control conditions (black curve) and 5-HT application (red curve). The normalized response for the preferred stimulus is decreased during 5-HT application, whereas the activity for the nonpreferred stimulus stayed the same.

Upper panel: 5-HT application showed no significantly different effect on preferred (red bar) and nonpreferred (blue bar) stimuli modulation. C) Distribution of AUROCs of all numerosity-selective neurons recorded during control and 5-HT application (left panel, each dot represents one neuron, red dot depicts example neuron from **Figure 3.4 A**)). AUROCs were decreased during 5-HT application in comparison to control conditions in most numerosity-selective neurons ($p = 0.042$). The average AUROC (right panel) was significantly decreased during 5-HT application (gray bar) compared to control conditions (black bar). C, control conditions; D, drug conditions. D) Same conventions as in A) for numerosity-selective neurons recorded in sessions with MDL100907 application. E) Same conventions as in B) for numerosity-selective neurons recorded in sessions with MDL100907 application (green curve). F) Distribution of AUROCs of all numerosity-selective neurons recorded during control conditions and MDL100907 application (each dot represents one neuron; green dot depicts example neuron from **Figure 3.4 B**). Inset shows mean AUROCs for control and MDL100907 conditions. MDL100907 application showed no effect on numerosity selectivity during sample presentation ($p = 0.501$). G) Same conventions as in A) for numerosity-selective neurons recorded in control experiment with NaCl application. H) Same conventions as in B) for numerosity-selective neurons recorded in sessions with NaCl application (blue curve). I) Same conventions as in C) for numerosity-selective neurons recorded in control experiments with NaCl (each dot represents one neuron; blue dot depicts example neuron from **Figure 3.4 C**). No effect on numerosity selectivity was found.

3.3.3 Temporal Dynamics of Reference Coding Strength in the Reference Phase

A sliding window ROC analysis was used to study the emergence and temporal progression of numerosity coding during reference presentation phase (**Figure 3.6 A-C**). Therefore, an analysis window from the start of the fixation period until the end of the reference presentation (as described in **Section 2.7.8.1**), was analyzed with a sliding window of 100 ms in 10 ms steps. We calculated the AUROC between the preferred and nonpreferred numerosity for each window. As expected, we found numerical coding strength increased after reference onset for control conditions (**Figure 3.6 A**, left, black curve) and 5-HT application (red curve). Coding quality was maintained throughout reference presentation without visible differences between control and 5-HT conditions. Further, we tested whether 5-HT had an influence on the time point a cell became numerosity-selective by the means of a permutation test. Therefore, we estimated the null distribution by recalculating the AUROC 1000 times with randomly shuffled reference numerosity labels for each sliding window. A neuron's latency was defined as time point the actual AUROC value was larger than 95 % of the null distribution for at least three consecutive windows, starting from reference onset. The individual latencies were then compared with a Wilcoxon paired test between drug and control conditions. We found that 5-HT had no effect on numerosity-selective neurons' latencies in the reference phase (**Figure 3.6 A**, right panel, black bar: control

conditions latency, mean latency 673 ± 17 ms, red bar: 5-HT application trials, mean latency 647 ± 13 ms, p = 0.745, n = 21, Wilcoxon paired test). We conducted the same analysis for numerosity-selective neurons recorded during MDL100907 application (**Figure 3.6 B**) and control experiments with NaCl (**Figure 3.6 C**). We find that no

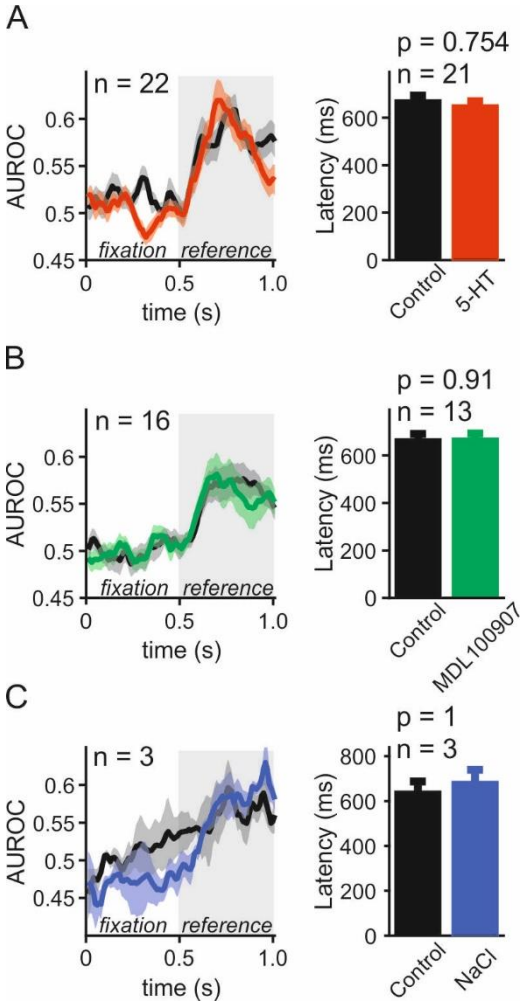

Figure 3.6: Temporal dynamics of numerosity-selectivity in the reference phase is not modulated by serotonergic agents A) Sliding ROC analysis depicting the temporal dynamics of numerosity-coding strength of control condition trials (left, black curve) and 5-HT application trials (red curve) from trial on set until the end of the reference phase. The gray bar represents the onset of the reference phase. The latency of numerosity coding was unchanged (right panel). Colored shaded area depicts the SEM. B) Same conventions as in A) for numerosity-selective cells recorded in sessions with MDL100907 application. C) Same conventions as in A) for numerosity-selective cells recorded in sessions with the control substance NaCl.

substance modulated the temporal evolution of coding strength (**Figure 3.6 B**: control condition, black bar, mean latency 668 ± 18 ms, MDL100907 application trials, green bar, mean latency 671 ± 21 ms, p = 0.91, n = 13, Wilcoxon paired test; **Figure 3.6 C**: control conditions, black bar, mean latency 644 ± 43 ms, NaCl application trials, blue bar, mean latency 691 ± 55 ms, p = 1, n = 3, Wilcoxon paired test).

3.4 5-HT2A receptor blockage enhances numerosity-selectivity during first working memory period.

Next, we investigated numerosity selectivity during delay 1, to determine the role of the serotonergic system in maintaining numerical information in working memory. We used a three-way ANOVA (main factors: numerosity (1,3 or 9), stimulus protocol (standard or control) and drug condition (control or pharmacological application)) to identify numerosity-selective neurons in this task-phase. In sessions with 5-HT application we found 16 (15%) numerosity-selective neurons (**Figure 3.7 A**), likewise in sessions with MDL100907 application (16%, **Figure 3.7 B**). During control experiments with NaCl, 7 (32%) neurons were numerosity-selective (**Figure 3.7 C**).

Figure 3.8 shows three numerosity-selective example neurons. The first neuron

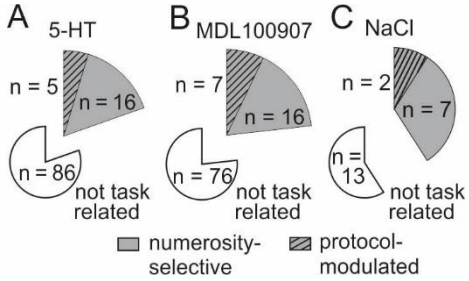

Figure 3.7: Number of recorded neurons that were numerosity-selective during the working memory phase recorded in session with A) 5-HT application, B) MDL100907 application and C) in control experiments with NaCl.

(**Figure 3.8 A**) was recorded during control conditions (left panel) and 5-HT application (middle panel). It differentiated between the different reference numerosities equally for control conditions and while 5-HT was applied. The tuning curve showed only marginal differences for the average spike rates of control conditions (black curve) and 5-HT application trials (red curve). The example cell in **Figure 3.8 B** shows a neuron with increased numerosity-selectivity during MDL100907 application. Numerosity tuning was weak during control conditions but improved highly during 5-HT2A blockage by an activity decrease for the second-preferred stimulus (red curve, numerosity = 3) and an even stronger reduction of response activity for the nonpreferred stimulus (brown curve, numerosity = 9). A cell recorded during control experiments with NaCl showed no change in numerosity tuning (**Figure 3.8 C**).

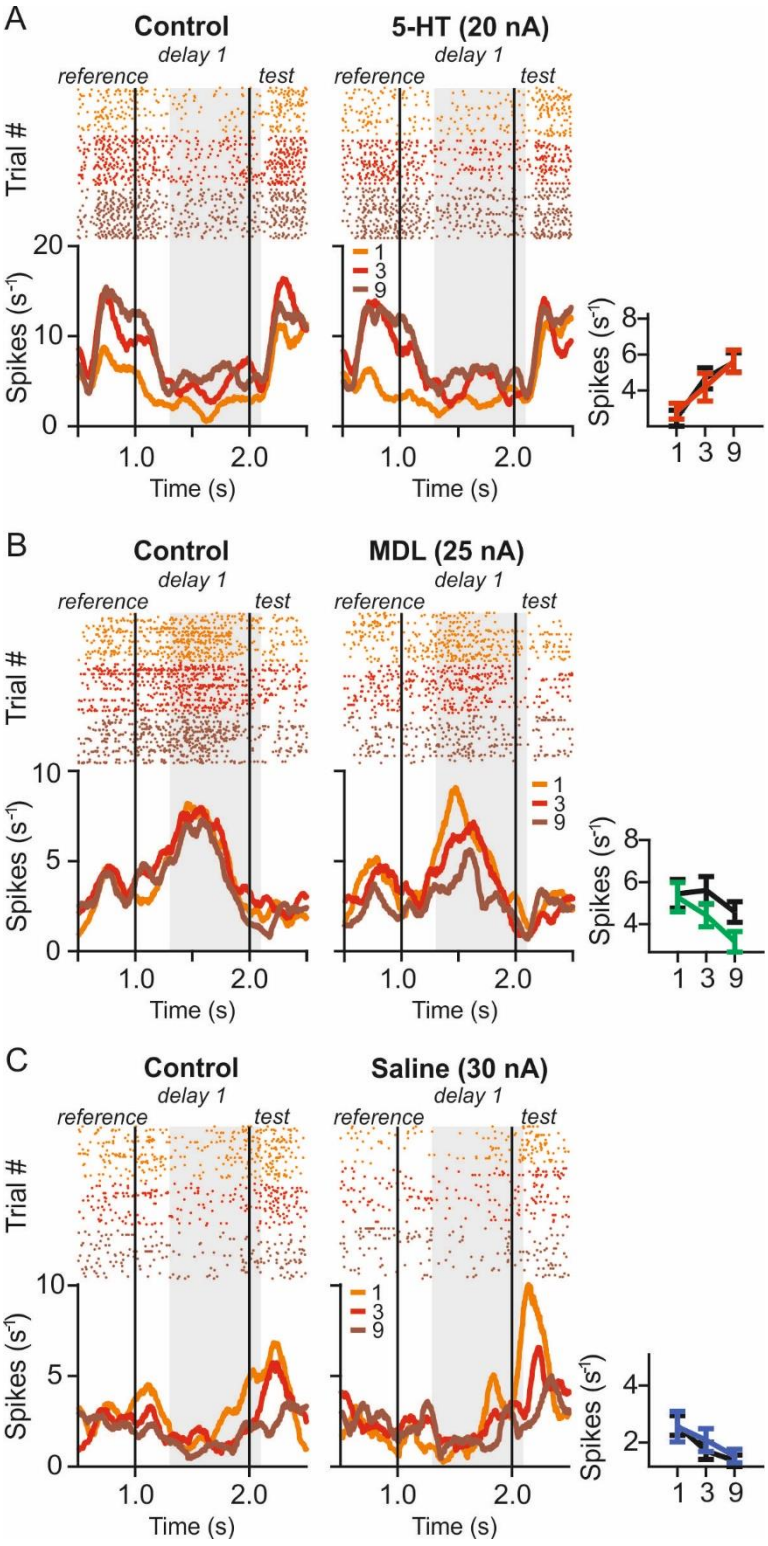

Figure 3.8: Responses of three reference numerosity-selective example cells in the delay phase A) Dot raster (top) and spike-density histogram (bottom) of an example neuron, numerosity-selective in delay 1, recorded during control conditions (left) and 5-HT application (middle). 5-HT did not affect numerosity coding. The tuning curve (right panel) shows no change in average firing rates during 5-HT application (red curve) compared to control conditions (black curve). B) Dot raster and spike-density histogram (bottom) of a numerosity-selective single neuron during delay 1, separately for control conditions (left panel) and MDL100907 application (middle panel). After MDL100907 application, numerosity-selectivity was increased. Right panel shows the averaged discharge rates for all numerosities of same single neuron separately for control conditions (black curve) and MDL100907 application (green curve). 5-HT2A blockage enhanced differences between discharge rates for different numerical stimuli. Gray shaded area depicts analysis window. C) Dot raster (top) and spike-density histogram (bottom) of an example neuron, numerosity-selective in delay 1, recorded during control conditions (left) and NaCl application (middle). Saline did not affect numerosity coding. The tuning curve (right panel) shows a slight increase in the average firing rate for the second preferred numerosity during control experiments (blue curve) compared to control conditions (black curve).

3.4.1 5-HT2A blockage increases reference encoding in the delay

Next, discharge rates for the preferred (red trace) and nonpreferred (blue trace) numerosity were normalized to control baseline and averaged for the population of

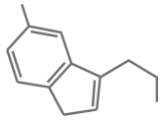

numerosity-selective neurons to investigate population responses (**Figure 3.9**) in the delay. This was done for both serotonergic substances and control experiments with NaCl. 5-HT did not modulate numerosity coding in the population of selective neurons in delay 1. **Figure 3.9 A** shows the normalized discharge rates during control conditions (left) and drug conditions (right). 5-HT did not affect firing rate differently depending on preference (**Figure 3.9 A** inset, **B**) (mean $MI_{Nonpreferred}$ = - 0.0044 ± 0.0625, mean $MI_{Preferred}$ = - 0.0726 ± 1086 [SEM], p = 0.605, n = 16, Wilcoxon paired test). Further, effects on coding strength were not consistent within the selective population (**Figure 3.9 C**, ΔAUROC = - 0.0145 ± 0.027 [SEM], p = 0.605, n = 16, Wilcoxon paired test). Regarding MDL100907, blockage of 5-HT2A receptors did not modulate the averaged normalized response for the preferred stimulus (red trace, **Figure 3.9 B**). Further, we did not find significant differences in modulation strength on preferred and nonpreferred stimuli (**Figure 3.9 D**, mean $MI_{Preferred}$ = -0.031 ± 0.075 [SEM]; mean $MI_{Nonpreferred}$ = 0.076 ± 0.043 [SEM], p = 0.088, n = 16, Wilcoxon paired test between MIs for preferred and nonpreferred reference numerosities). MDL100907 application increased numerosity-selectivity in 75% (12/16) of numerosity-selective cells during the delay 1 phase (**Figure 3.9 C**, ΔAUROC = - 0.049 ± 0.020 [SEM], p = 0.044, n = 16, Wilcoxon paired test). Control experiments with NaCl exhibited no modulation of discharge rates (**Figure 3.9 H**,**I** , mean $MI_{Nonpreferred}$ = -0.0524 ± 0.0396 [SEM], mean $MI_{Preferred}$ = -0.0044 ± 0.0662 [SEM],p = 0.219, n = 7, Wilcoxon paired test) or AUROCs of numerosity coding (**Figure 3.9 F**, ΔAUROC = - 0.0151 ± 0.008 [SEM], p = 0.219, n = 7, Wilcoxon paired test).

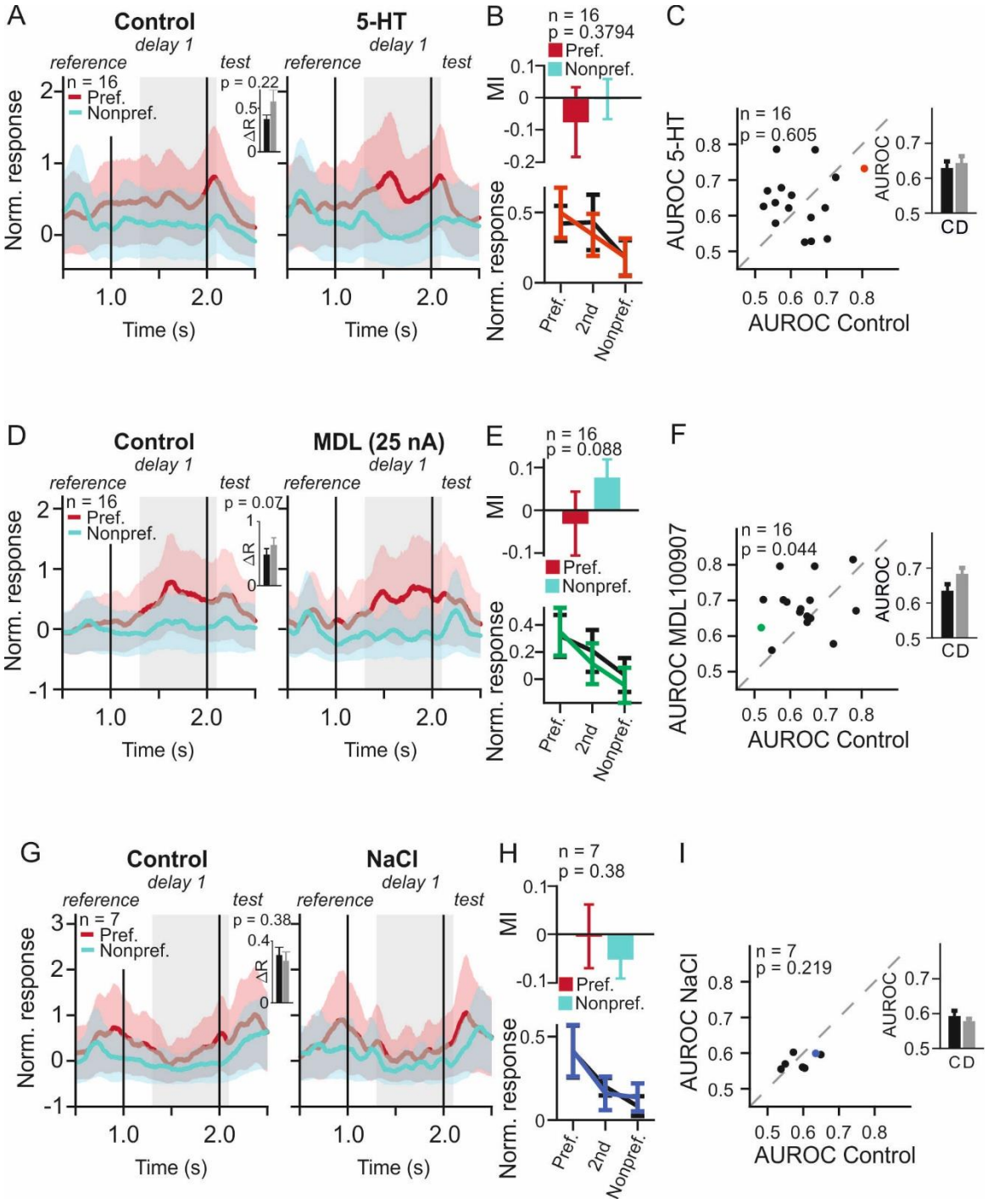

Figure 3.9: MDL100907 increases numerosity coding during working memory phase A) Normalized (to baseline of control conditions) responses averaged over all numerosity-selective neurons in delay1 for preferred (red trace) and nonpreferred (blue trace) numerosity, separated for control conditions (left panel) and 5-HT application (right panel; trace for second preferred numerosity not shown). Inset shows differences between normalized responses ΔR of preferred and nonpreferred numerosity for control conditions (black bar) and 5-HT application (gray bar). B) The lower panel shows that the averaged normalized tuning curves (bottom) for all numerosity-selective neurons recorded during 5-HT application (red curve) and control conditions (black curve). The average activity was increased for the preferred stimulus whereas activity for the second preferred stimulus was decreased compared to control conditions. Modulation Indices (top) were increased for both preferred (red bar) and nonpreferred (blue bar) numerosity. C) The distribution of AUROCs of all numerosity-selective neurons recorded during control conditions and 5-HT application (each dot represents one neuron, red dot depicts single neuron from **Figure 3.8 A**) shows that 5-HT application did not change coding quality od numerosity-selective cells during delay 1 (p = 0.605, n = 0.605, n = 16, Wilcoxon paired test).

D) The average normalized response of all numerosity-selective neurons shows a decrease for the nonpreferred (blue trace) but not for the preferred (red trace) numerosity (trace for second preferred numerosity is not shown) after MDL100907 application (middle panel) in comparison to control conditions (left panel). This difference is not selective (Inset p = 0.07, control conditions: black bar, MDL100907 application: gray bar). E) The lower panel shows that the averaged normalized tuning curves (bottom) for all numerosity-selective neurons are decreased for the 2nd and nonpreferred numerosities during MDL100907 application (green curve) when compared to control conditions (black curve). Modulation Indices (top) were increased for both preferred (red bar) and nonpreferred (blue bar) numerosity. F) AUROCs of numerosity-selective neurons were increased during MDL100907 application in comparison to control conditions in most numerosity-selective neurons (left panel, each dot represents one neuron, green dot depicts single neuron from **Figure 3.8 B**), p = 0.044, n = 16, Wilcoxon paired test). The average AUROC was significantly decreased during MDL100907 application (gray bar) compared to control conditions (black bar). G) The average normalized response of all numerosity-selective neurons recorded during control conditions (left) and control experiments with NaCl (right) for the nonpreferred (blue trace) and preferred (red trace) numerosity (trace for second preferred numerosity is not shown). NaCl did not change spike rates (Inset p = 0.38, control conditions: black bar, NaCl application: gray bar). H) The lower panel shows that the averaged normalized tuning curves (bottom) for all numerosity-selective neurons are increased for the nonpreferred numerosity during NaCl application (green curve) compared to control conditions (black curve). Modulation Indices (top) were decreased for the nonpreferred (blue bar) numerosity. I) AUROCs of numerosity-selective neurons were unchanged during NaCl application in comparison to

3.4.2 Reference-Selectivity Latencies are unaffected in the delay phase

We conducted a similar sliding window ROC analysis as in **Section 3.3.3** again to study the temporal progression of numerosity coding but for the population of numerosity-selective neurons in the delay phase (**Figure 3.10 A**-**C**). The respective delay analysis window (reference onset until delay offset, see **Section 2.7.8.1**) was analyzed with a sliding window of 100 ms with 10 ms increments. The AUROC was calculated between the preferred and nonpreferred numerosity for each window. Numerical coding strength increased after reference onset for control conditions (**Figure 3.10 A**, left, black curve) and 5-HT application (red curve) and was maintained during the delay without visible differences between control and 5-HT conditions. The permutation test revealed no differences between the selectivity latencies of control and 5-HT application trials (**Figure 3.10 A**, right panel, black bar: control conditions latency, mean latency 708 ± 61 ms, red bar: 5-HT application trials, mean latency 764 ± 63 ms, p = 0.765, n = 14, Wilcoxon paired test). There was also no significant difference in latencies for neither MDL100907 (**Figure 3.10 B**: control condition, black bar, mean latency 726 ± 58 ms, MDL100907 application trials, green bar, mean latency 630 ± 37 ms, p = 0.233, n = 15, Wilcoxon paired test) nor for control experiments with NaCl (**Figure 3.10 C**: control conditions, black bar, mean latency 861 ± 142 ms, NaCl

application trials, blue bar, mean latency 899 ± 72 ms, p = 0.628, n = 5, Wilcoxon paired test).

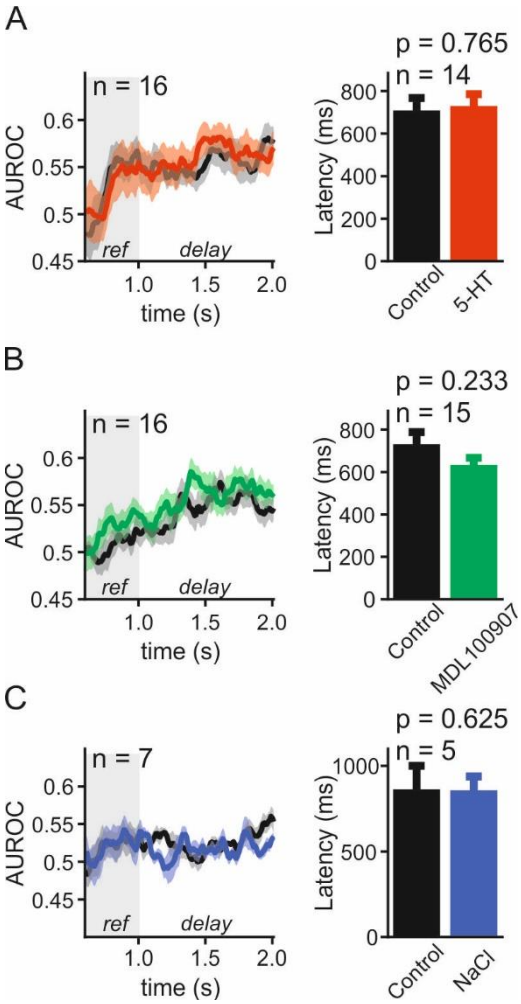

Figure 3.10: Temporal dynamics of numerosity-selectivity in the delay phase is not modulated by serotonergic agents A) Sliding ROC analysis depicting the temporal dynamics of numerosity-coding strength of control condition trials (left, black curve) and 5-HT application trials (red curve) from reference onset until the end of the delay phase. The gray bar represents the onset of the delay. The latency of numerosity coding was unchanged (right panel). Colored shaded area depicts the SEM. B) Same conventions as in A) for numerosity-selective cells recorded in sessions with MDL100907 application. C) Same conventions as in A) for numerosity-selective cells recorded in sessions with the control substance NaCl.

3.4.3 MDL100907 decreases information about the reference during its visual presentation

To explore the temporal dynamics of reference information processing, we conducted a sliding-window ω^2 PEV analysis. Therefore, we calculated the ω^2 PEV value for reference in overlapping 200 ms windows with 20 ms increments throughout the whole trial, separately for drug-application trials and corresponding control conditions for

each recorded neuron (see **Section 2.7.9**).). Bars above the curves denote time bins in which the respective information was significantly different between drug application and control conditions (paired Wilcoxon signed rank test, p = 0.05, black bar: information was larger in control trials, colored bar: information was smaller in control trials). **Figure 3.11 A** shows the reference information during control conditions (black curve) and 5-HT application trials (red curve) of an example neuron. After reference on-set information increases rapidly for both iontophoresis conditions and decreases again, after reaching a peak mid-reference presentation. Next, we looked at the modulation effect on reference information within the whole population of neurons, recorded in sessions with 5-HT application (**Figure 3.11 B**). Information peaks shortly after reference numerosity presentation onset for both, 5-HT application trials and control conditions, but drops by half after stimulus off-set. When averaged over all recorded neurons with 5-HT, we see no difference between reference information of control and 5-HT application trials (**Figure 3.11 B**). **Figure 3.11 C** shows an example neuron, which's information about the reference numerosity is decreased during application of MDL100907 in comparison to control trials. On a population level temporal dynamics were similar to cells recorded with 5-HT. Reference information peaked after onset of the reference presentation (**Figure 3.11 D**), however, it

decreased rapidly again in MDL100907 trials compared to control conditions which altered information significantly between MDL100907 and control trials. During the delay reference information remained stable for both iontophoresis conditions. To control whether the applied iontophoretic currents had any influence on a cell's information we looked at our population of cells recorded under control conditions and NaCl application. The sliding window ω^2 PEV analysis of an example cell regarding

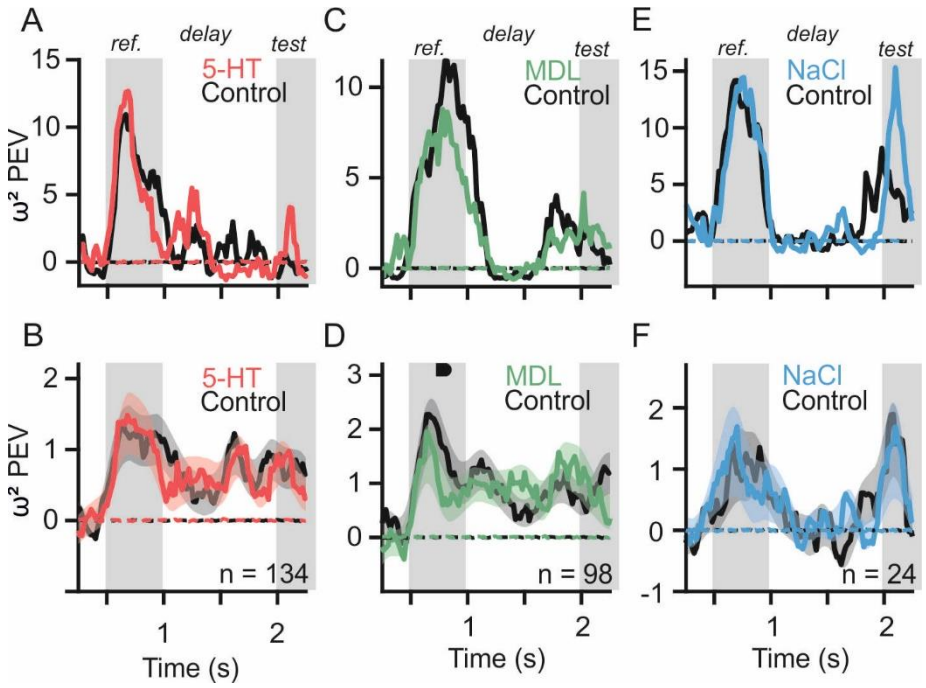

Figure 3.11: MDL100907 decreases reference information during visual presentation. A) Sliding window ω^2 PEV of an example cell showing control trials (black curve) and 5-HT application trials (red curve) quantifying information about the reference numerosity across a factor-relevant task period of an example neuron. B) Average sliding window ω^2 PEV of control trials (black curve) and 5-HT application trials (red curve) quantifying information about the reference numerosity across a factor-relevant task period of all neurons, recorded in sessions with 5-HT application. Dashed lines show mean PEV values of null distribution respectively for control trials (black line) and 5-HT application trials (red line). C) Sliding window ω^2 PEV of control trials (black curve) and MDL100907 application trials (green curve) quantifying information about the reference numerosity across a factor-relevant task period of an example neuron. D) Average sliding window ω^2 PEV of control trials (black curve) and MDL100907 application trials (green curve) quantifying information about the reference numerosity across a factor-relevant task period of all neurons, recorded in sessions with MDL100907 application. Dashed lines show mean PEV values of null distribution respectively for control trials (black line) and MDL100907 application trials (green line). Reference information is significantly decreased during the reference phase. E) Sliding window ω^2 PEV of an example cell showing control trials (black curve) and NaCl application trials (blue curve) quantifying information about the reference numerosity across a factor-relevant task period of an example neuron. F) Average sliding window ω^2 PEV of control trials (black curve) and NaCl application trials (blue curve) quantifying information about the reference numerosity across a factor-relevant task period of all neurons, recorded in sessions with NaCl application. Dashed lines show mean PEV values of null distribution respectively for control trials (black line) and NaCl application trials (blue line). Colored/black bars above the curves marks time bins in which information was significantly larger/smaller ($p = 0.05$) during drug application trials than control trials. Colored shaded areas denote the SEM. Gray shaded rectangulars depict stimuli presentations phases (either reference or test stimulus).

information about the reference numerosity is shown in **Figure 3.11 E**. The blue curve depicts the temporal information progression during NaCl application whereas the black curve shows information during control conditions. For both conditions information went up during reference presentation, declined to zero during the delay period and went up again during, for control trials even shortly before, test numerosity presentation. The information averaged across the whole population shows a similar temporal profile (**Figure 3.11 F**). Reference information peaked during reference presentation, went back to zero and peaked again during test numerosity presentation without significant differences between control and NaCl conditions.

3.5 Modulation of Test-Selectivity by Serotonergic Agents

3.5.1.1 Numerosity-selective population is not modulated by serotonergic agents during presentation of the test numerosity

We determined the influence of serotonin on the population of test-numerosity-selective neurons, during visual presentation of the second numerosity stimulus. Therefore, we calculated a four-way ANOVA (main factors: test numerosity (1,3 or 9), decision (same/different), stimulus protocol (standard or control) and drug condition (control or pharmacological application)) to identify numerosity-selective single units (significant main factor test-numerosity, no significant main factor or interaction for protocol). We did this separately for each investigated task phase (test phase, decision phase (**Section 2.7.4**)) and serotonergic agent as well as for the control experiments with NaCl. In session with 5-HT, we found 12 (12 %) neurons which selectively encoded the test numerosity in the test phase (**Figure 3.12 A**). Stimulation of 5-HT receptors seemed to have no influence on the average firing rate of the whole selective population (**Figure 3.12 A**, right panel). Further, 5-HT application had no effect on coding strength of test-numerosity-selective cells significantly (**Figure 3.12 B**, ΔAUROC = 0.0047 ± 0.0265 [SEM], p = 1, n = 12, Wilcoxon test). We also found no significant differences in sessions with MDL100907 application. Here, 18 (23 %) units were test-selective (**Figure 3.12 C**). On average, activity for the preferred numerosity was reduced during MDL100907 application (**Figure 3.12 C** right) but this had no consistent effect on test-selectivity (**Figure 3.12 D**, ΔAUROC = - 0.0112 ± 0.0152 [SEM], p = 0.396, n = 18, Wilcoxon test). We also looked at the population of

numerosity-selective cells recorded in control experiments with NaCl (**Figure 3.12 E**). NaCl had no effect on average firing rates (**Figure 3.12 E** right) nor on coding-strength (**Figure 3.12** F, ΔAUROC = - 0.0199 ± 0.0124 [SEM], p = 0.563, n = 6, Wilcoxon test). The gray shaded area depicts the phase of interest.

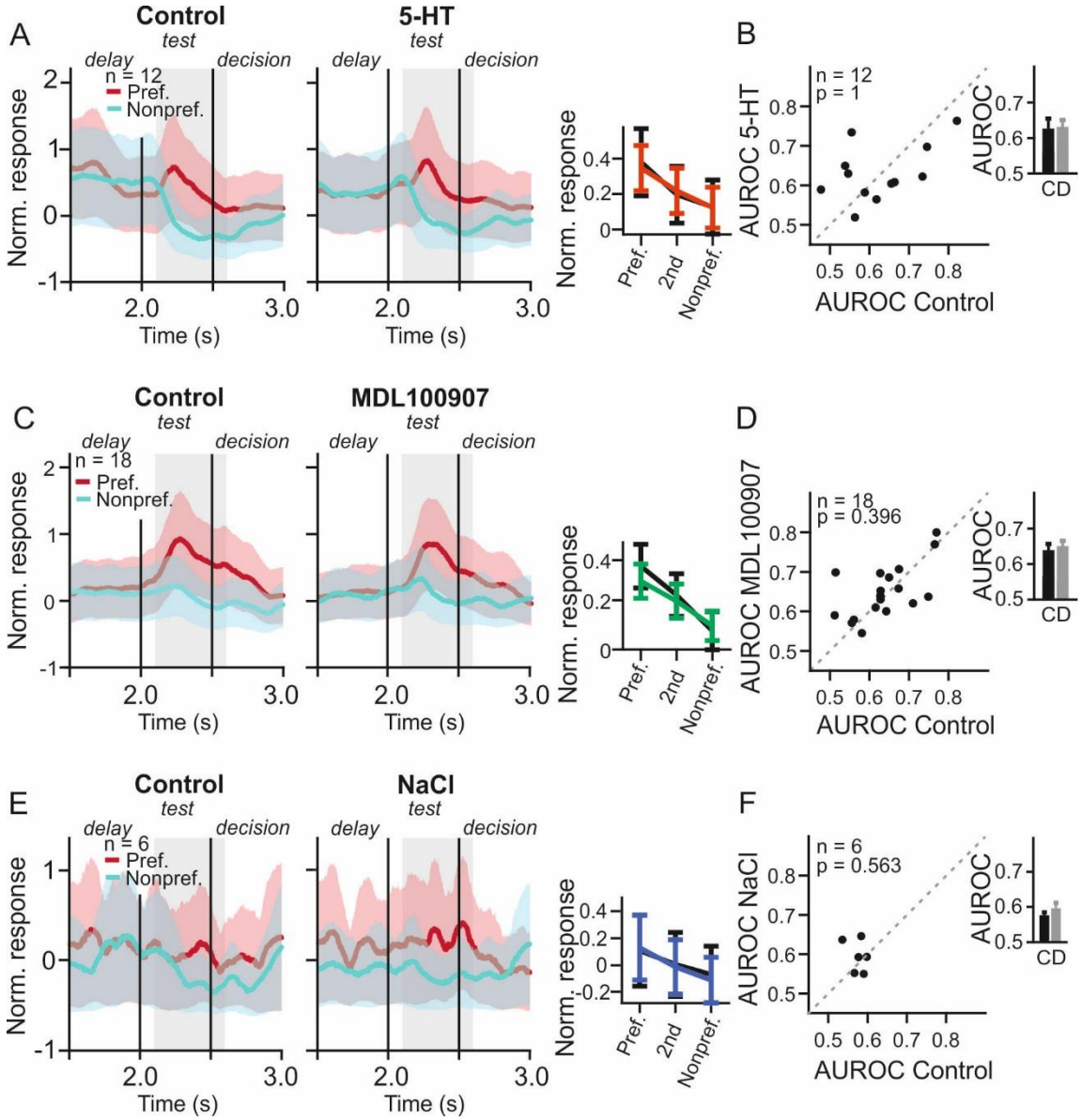

Figure 3.12: Test numerosity-selectivity in the test phase is not modulated by serotonergic agents A) Averaged normalized responses of the population of neurons, which were test numerosity-selective in the test phase for the nonpreferred (blue trace) and preferred (red trace) decision during control conditions (left panel) and 5-HT conditions (middle panel). The right panel shows that the averaged normalized tuning curves for all test numerosity-selective neurons for control conditions (black curve) and 5-HT application (red curve). B) The distribution of AUROCs of all test numerosity-selective neurons recorded during control conditions and 5-HT application (each dot represents one neuron) shows that 5-HT application did not change coding quality of numerosity-selective cells during the test phase. C) Same conventions as in A) for population of test-selective neurons recorded in sessions with MDL100907. D) Same conventions as in B) for the population of test selective neurons recorded in sessions with MDL100907. E) Same conventions as in A) for population of test-selective neurons recorded in sessions with NaCl. F) Same conventions as in B) for the population of test selective neurons recorded in sessions with NaCl.

3.5.1.2 Test Selectivity across Time was Unaffected by Application of Serotonergic Agents

Next, we checked whether any serotonergic substance had any effect on test selectivity latency (**Figure 3.13**). We used a similar sliding window ROC analysis as described in **Section 3.3.3**, this time starting 1.5 section into the trial until end of the decision phase (3.5 sec). Selectivity increases shortly after test onset for control conditions (**Figure 3.13 A**, left, black curve) and 5-HT application trials (red curve). Afterwards it reaches its peak before decreasing slowly during the first half of the decision phase. Cells did not reach selectivity faster when compared to control

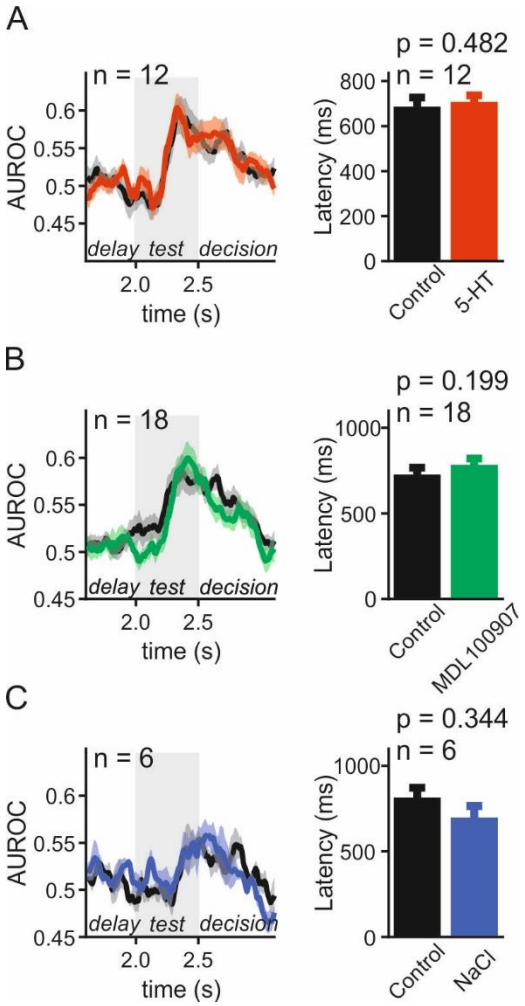

Figure 3.13: Temporal dynamics of test numerosity-selectivity in the test phase is not modulated by serotonergic agents A) Sliding ROC analysis depicting the temporal dynamics of test numerosity-coding strength of control condition trials (left, black curve) and 5-HT application trials (red curve) beginning in the second half of the delay until the first half of the decision phase. The gray bar represents the onset of the test. The latency of numerosity coding was unchanged (right panel). Colored shaded area depicts the SEM. B) Same conventions as in A) for test numerosity-selective cells recorded in sessions with MDL100907 application. C) Same conventions as in B) for test numerosity-selective cells recorded in sessions with MDL100907 application. D) Same conventions as in A) for test numerosity-selective cells recorded in sessions with NaCl application. E) Same conventions as in B) for test numerosity-selective cells recorded in sessions with the control substance NaCl.

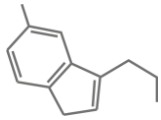

conditions (**Figure 3.13 A**, right, black bar: control conditions latency, mean latency 684 ± 44 ms, red bar: 5-HT application trials, mean latency 705 ± 31 ms, p = 0.482, n = 12, Wilcoxon paired test). Likewise, the AUROC of cells recorded during MDL100907 application showed only small deviations from control conditions (**Figure 3.13 B**, left) but without modulatory effect on the temporal evolution of selectivity (**Figure 3.13 B**, right, black bar: control conditions latency, mean latency 706 ± 42 ms, MDL100907 application trials, green bar, mean latency 768 ± 40 ms, p = 0.199, n = 18, Wilcoxon paired test). Control experiments with NaCl showed no differences between control conditions and NaCl application trials (**Figure 3.13 C**, black bar: control conditions latency, mean latency 814 ± 61 ms, NaCl application trials, blue bar, mean latency 694 ± 70 ms, p = 0.344, n = 6, Wilcoxon paired test).

3.5.3.1Test Numerosity coding is Unaffected in the Decision Phase

We applied the same analyses for test numerosity-selective neurons in the decision phase. First, we identified numerosity-selectivity by the means of a 4-way ANOVA (main factors: test numerosity (1,3 or 9), decision (same/different), stimulus protocol (standard or control) and drug condition (control or pharmacological application)). Of all cells, recorded in session with 5-HT application 14 (14 %) neurons were test numerosity-selective. **Figure 3.14 A** shows the normalized average discharge rates of the population of test-selective neurons for control conditions (left) and 5-HT application trials (middle) for the preferred (red curve) and nonpreferred (blue curve) stimuli. The gray shaded area depicts the phase of interest. Differences in normalized activity between control and drug conditions seemed to be not affected by 5-HT application. When averaged over time activity was the same for 5-HT (red curve) and control trials (black curve) for both preferred and non-preferred stimuli (**Figure 3.14 A**, right). We also assessed coding strength with an AUROC analysis. We found no consistent effect of 5-HT on selectivity (**Figure 3.14 B**, ΔAUROC = - 0.0335 ± 0.0256 [SEM], p = 0.385, n = 14, Wilcoxon paired test). The same type of ANOVA identified 11 (14 %) test numerosity-selective neurons from session with MDL100907 application. Blockage of 5-HT2A receptors decreased the differences between the normalized average spike rates of the preferred and nonpreferred stimuli (**Figure 3.14 C**, middle) in comparison to control conditions (**Figure 3.14 C**, left). This is also evident

in the tuning curve (**Figure 3.14 C**, right). Here, the green curve (MDL100907 trials) is slightly decreased for the preferred and second preferred numerosity in comparison to

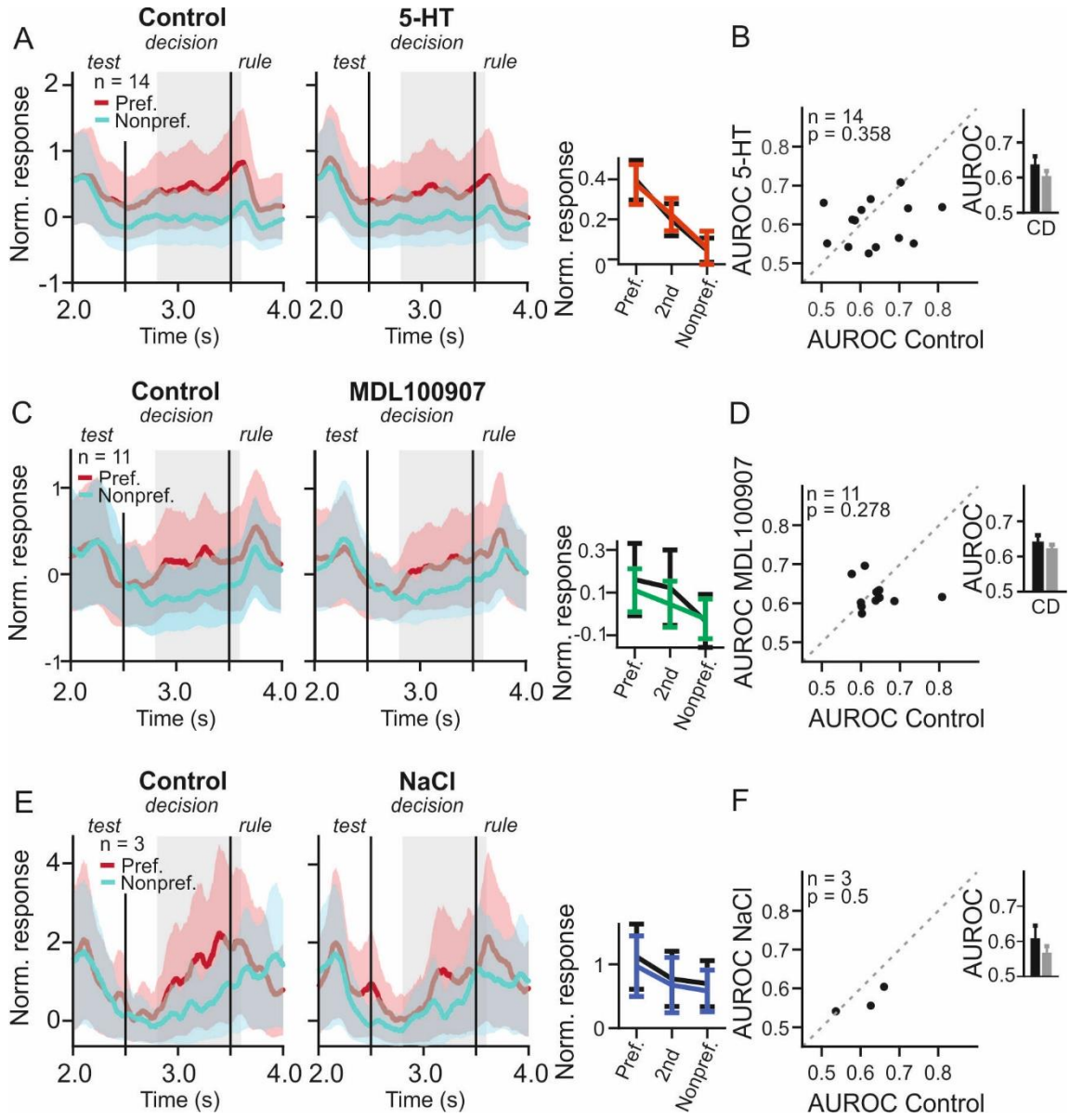

Figure 3.14: **Test numerosity-selectivity in the decision phase is not modulated by serotonergic agents** A) Averaged normalized responses of the population of neurons, which were test numerosity-selective in the test phase for the nonpreferred (blue trace) and preferred (red trace) decision during control conditions (left panel) and MDL100907 conditions (middle panel). The right panel shows that the averaged normalized tuning curves for all test numerosity-selective neurons for control conditions (black curve) and 5-HT application (green curve). B) The distribution of AUROCs of all test numerosity-selective neurons recorded during control conditions and 5-HT application (each dot represents one neuron) shows that 5-HT application did not change coding quality of numerosity-selective cells during the decision phase. C) Same conventions as in A) for population of test-selective neurons recorded in MDL100907 session in the decision phase. D) Same conventions as in B) for population of test-selective neurons recorded in MDL100907 session in the decision phase. E) Same conventions as in A) for population of test-selective neurons recorded in MDL100907 session in the decision phase. F) Same conventions as in B) for population of test-selective neurons recorded in NaCl session in the decision phase

control trials (black curve). This, however, is not affecting selectivity in a significant manner (**Figure 3.14 D**, ΔAUROC = 0.0194 ± 0.0232 [SEM], p = 0.278, n = 11, Wilcoxon paired test). In control experiments with NaCl we recorded three test-numerosity-selective neurons in the decision phase. These cells did not alter their activity noticeably during NaCl application (**Figure 3.14 E**, **F**, ΔAUROC = 0.0408 ± 0.0231 [SEM], p = 0.5, n = 3, Wilcoxon paired test).

3.5.3.2 Coding Strength of Test-Selectivity is not modulated in the Decision Phase

We investigated possible drug effects on the temporal progression of selectivity again by the means of a sliding window ROC analysis combined with a permutation test. In session with 5-HT application, selectivity increased shortly after the onset of the test stimulus and remained at the same level throughout the decision phase for both, control conditions and 5-HT application trials (**Figure 3.15 A**). When tested against an estimated null distribution we found no differences in latencies between control and

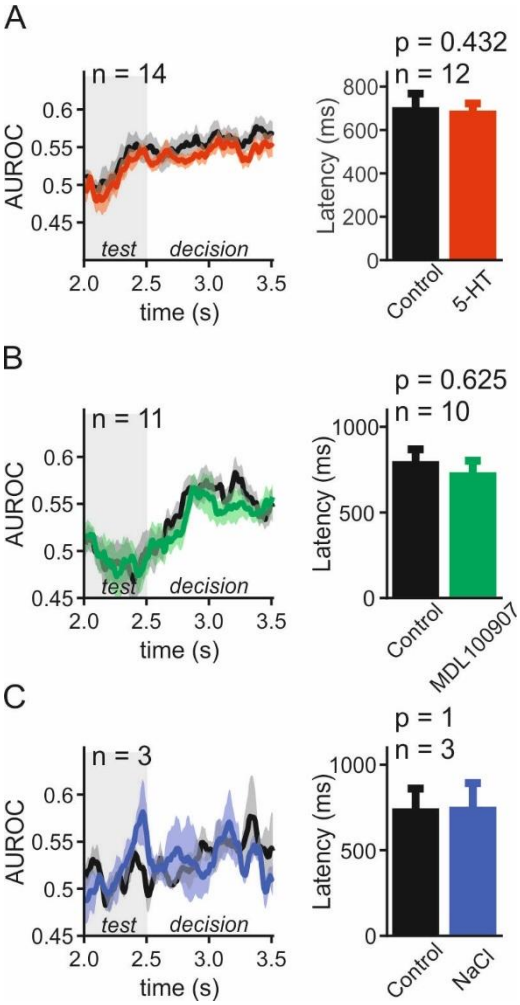

Figure 3.15: Temporal dynamics of test numerosity-selectivity in the decision phase is not modulated by serotonergic agents A) Sliding ROC analysis depicting the temporal dynamics of test numerosity-coding strength of control condition trials (left, black curve) and 5-HT application trials (red curve) beginning at the offset of the test phase until the end of the decision phase. The gray bar represents the offset of the test. The latency of numerosity coding was unchanged (right panel). Colored shaded area depicts the SEM. B) Same conventions as in A) for test numerosity-selective cells recorded in sessions with MDL100907 application. C) Same conventions as in B) for test numerosity-selective cells recorded in sessions with MDL100907 application. D) Same conventions as in A) for test numerosity-selective cells recorded in sessions with NaCl application. E) Same conventions as in B) for test numerosity-selective cells recorded in sessions with the control substance NaCl.

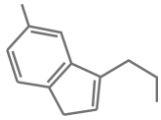

drug conditions (**Figure 3.15 A**, right, black bar: control conditions latency, mean latency 754 ± 80 ms, 5-HT application trials, red bar, mean latency 688 ± 37 ms, p = 0.432, n = 12, Wilcoxon paired test). Interestingly, cells recorded in MDL100907 session showed a different temporal progression of selectivity (**Figure 3.15 B**, left). While the test numerosity was shown, AUROCs went down slightly for both, control conditions and MDL100907 application trials. Selectivity started to increase only after offset of the visual stimulus and remained heightened until the end of the decision phase. When latencies were compared, we found no effect of MDL100907 on the timing on selectivity evolution (**Figure 3.15 B**, right, black bar: control conditions latency, mean latency 796 ± 73 ms, MDL100907 application trials, green bar, mean latency 738 ± 69 ms, p = 0.625, n = 10, Wilcoxon paired test). We performed the same analysis for our control experiments with NaCl. The temporal selectivity evolution oscillated strongly for control conditions and especially for NaCl application trials (**Figure 3.15 C**, left). However, this was possibly due to the small number of analyzed cells (n = 3). We found no evidence for an effect on latencies in our control experiment data (**Figure 3.15 C**, right, black bar: control conditions latency, mean latency 758 ± 123 ms, NaCl application trials, blue bar, mean latency 751 ± 141 ms, p = 1, n = 3, Wilcoxon paired test).

3.5.4 MDL100907 decreases information about the test stimulus during its visual presentation

Next, we investigated the temporal progression of test information. Therefore, we replicated the sliding-window ω^2 PEV analysis for information about the test (**see Section 3.5.4.**). **Figure 3.16 A** shows an example neuron encoding test information, during control conditions (black curve) and 5-HT application (red curve). After test onset information goes up, peaks and goes down again without noticeable difference between the iontophoresis conditions. The averaged information for test information increases shortly after test-onset, resembling the reference information progression (**Figure 3.16 B**), though locked to the test-onset. Test information does not differ significantly between 5-HT trials and control conditions at any given time point of the trial. The second example neuron (**Figure 3.16 C**) shows reduced sensory information upon MDL100907 application during test numerosity presentation.

The population plot in **Figure 3.16 D** shows that test information increased sharply during test presentation for both MDL100907 trials and control conditions but dropped earlier in MDL100907 trials, resulting in significantly larger test information in control trials towards the end of the test phase. This showed that MDL100907 decreased information about the visual stimulus also during the second presentation of a numerosity stimulus. The test information of an example cell (**Figure 3.16 E**) recorded in control experiments with NaCl increased strongly during test presentation, sunk back to zero after test offset, but increased briefly again during the decision phase for both iontophoretic conditions. Within the recorded population, test information for control and NaCl trials goes up during test presentation and decreases slowly during the

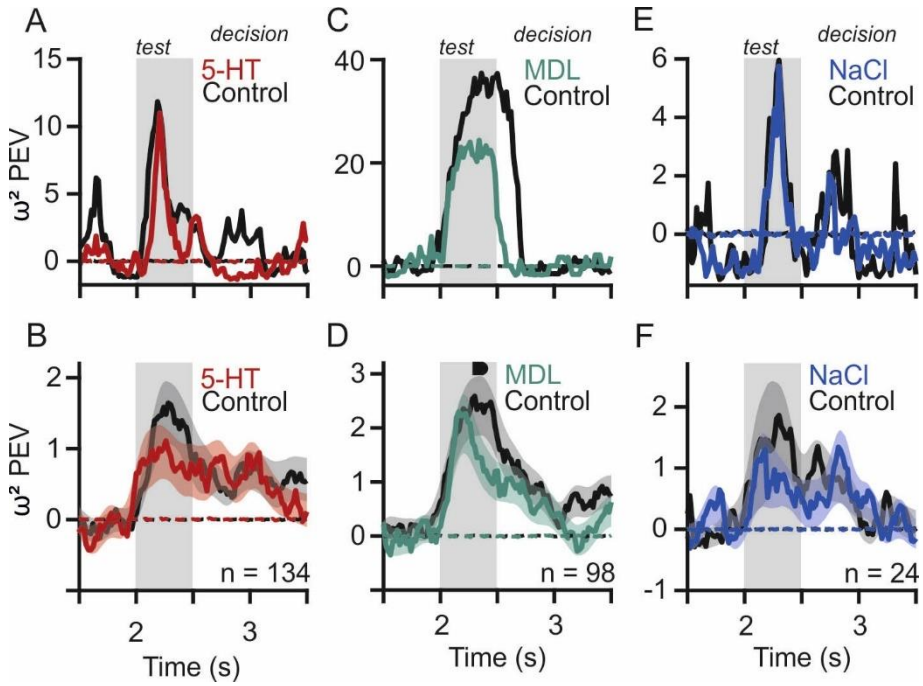

Figure 3.16: MDL100907 decreases test information during its visual presentation. A) Sliding window ω^2 PEV of an example cell showing control trials (black curve) and 5-HT application trials (red curve) quantifying test information across a factor-relevant task period of an example neuron. B) Average sliding window ω^2 PEV of control trials (black curve) and 5-HT application trials (red curve) quantifying information about the test numerosity across a factor-relevant task period of all neurons, recorded in sessions with 5-HT application. Dashed lines show mean PEV values of null distribution respectively for control trials (black line) and 5-HT application trials (red line). C) Same conventions as in A) for an example neuron recorded during control conditions (black curve) and MDL100907 application (green curve). D) Same conventions as in B) for neurons, recorded during control conditions (black curve) and MDL100907 application (green curve) Test information is significantly decreased during the test phase. E) Same conventions as in A) for an example neuron recorded during control conditions (black curve) and NaCl application (blue curve). F) Same conventions as in B) for neurons, recorded during control conditions (black curve) and NaCl application (blue curve). Colored/black bars above the curves marks time bins in which information was significantly larger/smaller ($p = 0.05$) during drug application trials than control trials. Colored shaded areas denote the SEM. Gray shaded rectangulars depict test presentations phases.

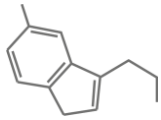

decision phase (**Figure 3.16 F**). Even though test information was smaller in trials with NaCl application, this difference is not significant.

3.6 Modulation of Decision-Selective Neurons by Serotonergic Agents

3.6.1.1 Population of decision-selective neurons is not modulated by serotonergic agents.

To gain insight into the role of 5-HT in the neuronal process of decision-making, we next analyzed decision-related activity in the two task phases after test stimulus on-set (test phase and decision phase). We used the same four-way ANOVA as described above (**Section 2.7.5**) to identify decision-selective neurons separately for test and decision phase. In sessions with 5-HT application, 13 neurons (13 %) significantly modulated their discharge rate according to the decision type (“same” vs “different”) in the test phase. Their normalized and averaged discharge rate is shown in **Figure 3.17 A**, separately for control trials (left) and 5-HT application trials (middle) and for the preferred (red curve) and nonpreferred (blue curve) decision. The gray shaded area depicts the phase of interest. 5-HT did not modulate firing rates, as also seen in the tuning curves (**Figure 3.17 A**, right, black: control trials, red: 5-HT application trials). We performed a ROC analysis to assess any drug effect on coding strength. 5-HT seemed to increase selectivity, however, not in a significant manner (**Figure 3.17 B**, ΔAUROC = - 0.0346 ± 0.0156 [SEM], $p = 0.057$, $n = 13$, Wilcoxon paired test). In sessions with MDL100907 application we identified 12 decision-selective neurons (15 %) in the test phase. Blockage of 5-HT2A receptors decreased firing rates for the nonpreferred decision (**Figure 3.17 C**), but this had no effect on decision coding strength (**Figure 3.17 D**, ΔAUROC = 0.0051 ± 0.018 [SEM], $p = 0.97$, $n = 12$, Wilcoxon paired test) in the test phase. NaCl application (**Figure 3.17 E, F**) decreased neuronal activity for the preferred decision. However, coding strength did not decrease but was unaffected (**Figure 3.17 F**, ΔAUROC = 0.0171 ± 0.013 [SEM], $p = 0.301$, $n = 9$, Wilcoxon paired test)

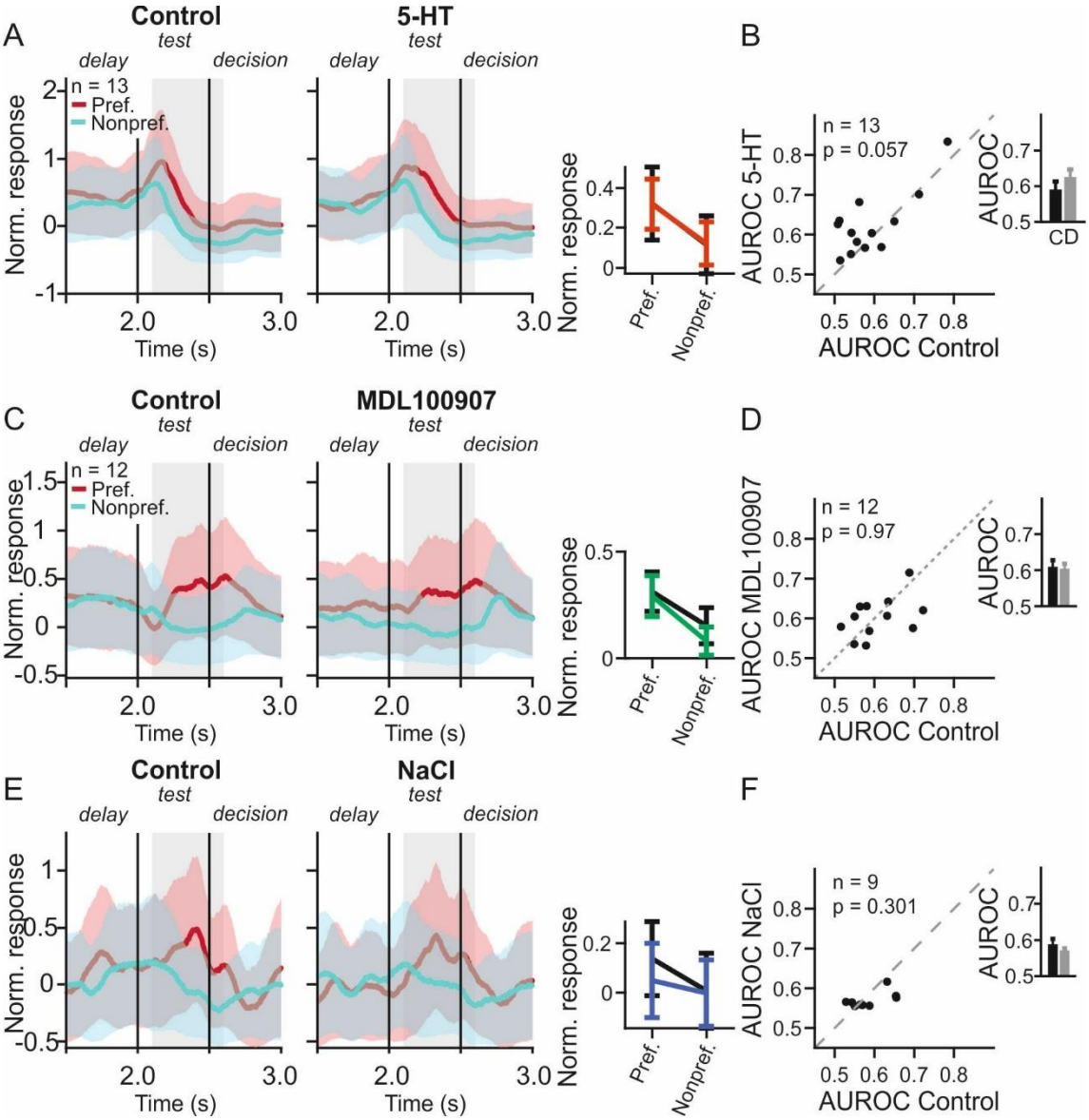

Figure 3.17: Decision-selectivity in the test phase is not modulated by serotonergic agents A) Averaged normalized responses of the population of neurons, which were decision-selective in the test phase, sorted by decision preference (nonpreferred = blue trace, preferred = red trace) during control conditions (left panel) and 5-HT conditions (middle panel). The right panel shows that the averaged normalized tuning curves for all test decision-selective neurons for control conditions (black curve) and 5-HT application (red curve). B) The distribution of AUROCs of all decision-selective neurons recorded during control conditions and 5-HT application (each dot represents one neuron) shows that 5-HT application did not change coding quality of decision-selective cells during the test phase. C) Same conventions as in A) for population of decision-selective neurons recorded in sessions with MDL100907 in the test phase. D) Same conventions as in B) for population of decision-selective neurons recorded in sessions with MDL100907 in the test phase. E) Same conventions as in A) for population of decision-selective neurons recorded in sessions with NaCl in the test phase. F) Same conventions as in B) for population of decision-selective neurons recorded in sessions with NaCl in the test phase

3.6.1.2Evolution of decision coding strength during test presentation

We repeated the sliding window ROC analysis for decision-selective cells in the test phase. We found, that in cells recorded in 5-HT sessions decision-selectivity started to come about after onset of the test stimulus, both during control and drug trials. It peaks towards the end of the test phase and decreases slowly afterwards throughout the decision phase (**Figure 3.18 A**, left). Selectivity for 5-HT application trials was higher after the peak compared to control conditions, but at the end coding strength was similar for both iontophoretic conditions. Latencies were not significantly different

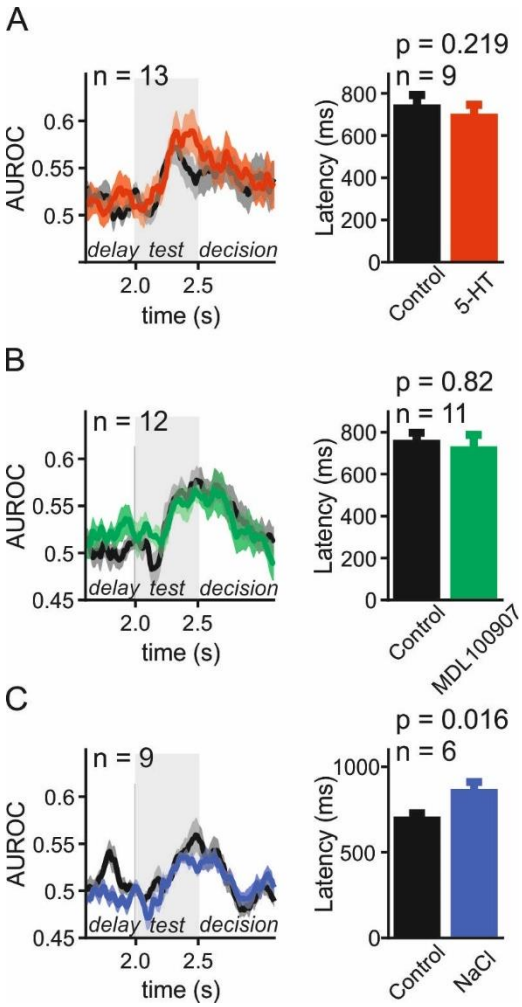

Figure 3.18: Temporal dynamics of decision-selectivity in the test phase are not modulated by serotonergic agents A) Sliding ROC analysis depicting the temporal dynamics of test numerosity-coding strength of control condition trials (left, black curve) and 5-HT application trials (red curve) beginning in the second half of the delay until the first half of the decision phase. The gray bar represents the onset of the test. The latency of numerosity coding was unchanged (right panel). Colored shaded area depicts the SEM. B) Same conventions as in A) for test numerosity-selective cells recorded in sessions with MDL100907 application. C) Same conventions as in B) for test numerosity-selective cells recorded in sessions with MDL100907 application. D) Same conventions as in A) for test numerosity-selective cells recorded in sessions with NaCl application. E) Same conventions as in B) for test numerosity-selective cells recorded in sessions with the control substance NaCl.

(**Figure 3.18 A**, right, black bar: control conditions latency, mean latency 753 ± 32 ms, 5-HT application trials, blue bar, mean latency 739 ± 42 ms, p = 0.219, n = 9, Wilcoxon paired test). MDL100907 application increased decision selectivity before the visual presentation of the test stimulus, however, shortly after test onset, ROC values for control and drug conditions showed an equal progression (**Figure 3.18 B**, left). MDL100907 also did not modulate decision selectivity latencies (**Figure 3.18 B**, right, black bar: control conditions latency, mean latency 760 ± 38 ms, MDL100907 application trials, blue bar, mean latency 724 ± 56 ms, p = 0.82, n = 11, Wilcoxon paired test). When we applied the same analysis on cells, recorded in control experiments with NaCl application, we found that ROC values fluctuated during the test phase. After test onset selectivity for both conditions rose, but slightly more during control conditions. Selectivity dropped to baseline again towards the decision phase. We compared individual cells latencies of control and drug trials and found a significant effect. Cells became significant earlier during control trials (**Figure 3.18 C**, right, black bar: control conditions latency, mean latency 729 ± 30 ms, NaCl application trials, blue bar, mean latency 887 ± 49 ms, p = 0.016, n = 6, Wilcoxon paired test).

Decision-selective cells were unmodulated by Serotonergic Agents in the Decision Phase

Next, we analyzed decision-selective cells in the decision phase. As mentioned above (**Section 3.5.1.1**) a 4-way ANOVA was used to identify decision-selective neurons. We found 19 neurons (19 %), which were selective for decision in decision phase in 5-HT sessions. However, the normalized firing rates for preferred (red trace) and nonpreferred (blue trace) decision of control (**Figure 3.19 A**, left) and drug conditions (**Figure 3.19 A**, middle) as well as the tuning curves (black: control conditions, red: 5-HT application trials) showed no difference. Neither did we find an effect of 5-HT on coding strength (**Figure 3.19 B**, ΔAUROC < 0.001 ± 0.0223 [SEM], p = 0.968, n = 19, Wilcoxon paired test). Next, we investigated whether MDL100907 had an influence on the 24 (30 %) decision-selective neurons in the decision phase (**Figure 3.19 C, D**). Overall, it seemed as if MDL100907 (**Figure 3.19 C**, middle) decreased neuronal activity for both the preferred (red curve) and the nonpreferred (blue curve) decision compared to control trials (left). This can also be seen in the tuning curve (**Figure 3.19 C**, right). The curve for MDL100907 trials (green curve) is lower for both, preferred and nonpreferred decision, than the curve for control trials (black curve). The ROC analysis

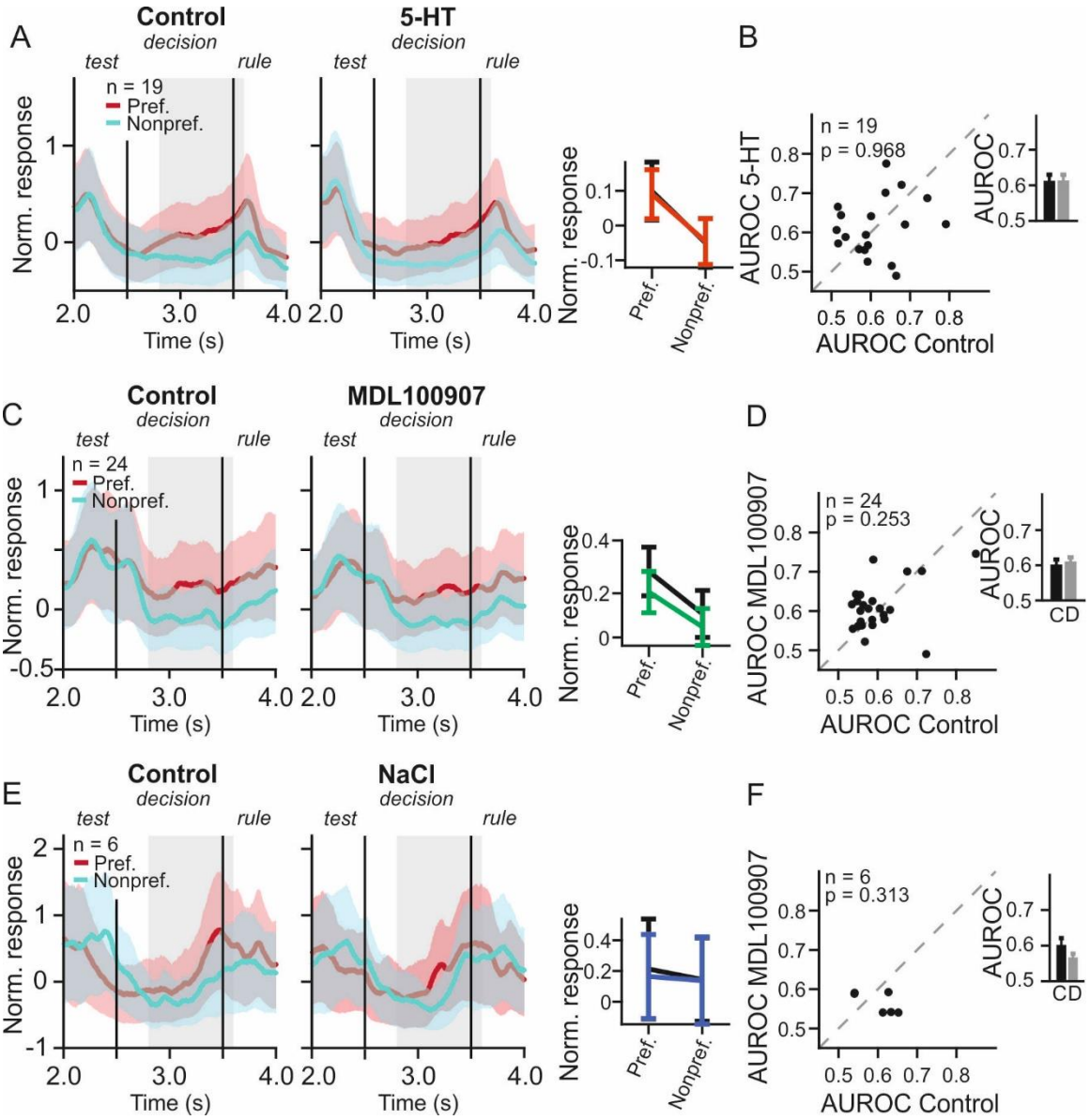

Figure 3.19: Decision-selectivity in the decision phase is not modulated by serotonergic agents A) Averaged normalized responses of the population of neurons, which were decision-selective in the decision phase for the nonpreferred (blue trace) and preferred (red trace) decision during control conditions (left panel) and 5-HT conditions (middle panel). The right panel shows that the averaged normalized tuning curves for all decision-selective neurons for control conditions (black curve) and 5-HT application (red curve). B) The distribution of AUROCs of all decision-selective neurons recorded during control conditions and 5-HT application (each dot represents one neuron) shows that 5-HT application did not change coding quality of decision-selective cells during the decision phase. C) Same conventions as in A) for population of decision-selective neurons recorded in sessions with MDL100907 in the decision phase. D) Same conventions as in B) for population of decision-selective neurons recorded in sessions with MDL100907 in the decision phase. E) Same conventions as in A) for population of decision-selective neurons recorded in sessions with NaCl in the decision phase. F) Same conventions as in b) for population of decision-selective neurons recorded in sessions with NaCl in the decision phase

(**Figure 3.19 D**) showed no general effect of MDL100907 on selectivity (ΔAUROC = -0.0086 ± 0.0152 [SEM], p = 0.253, n = 24, Wilcoxon paired test). Control experiments

with NaCl showed also no effect of the used current on discharge rate (**Figure 3.19 E**) nor AURC values (**Figure 3.19 F**, ΔAUROC = 0.0353 ± 0.0286 [SEM], p = 0.313, n = 6, Wilcoxon paired test)

3.6.1.4Decision Selectivity across Time was altered by 5-HT application

We also investigated whether any substance or the control experiments had any effect on the temporal decision selectivity progression. Decision-selectivity increased from the beginning of the test presentation and continued to increase throughout the

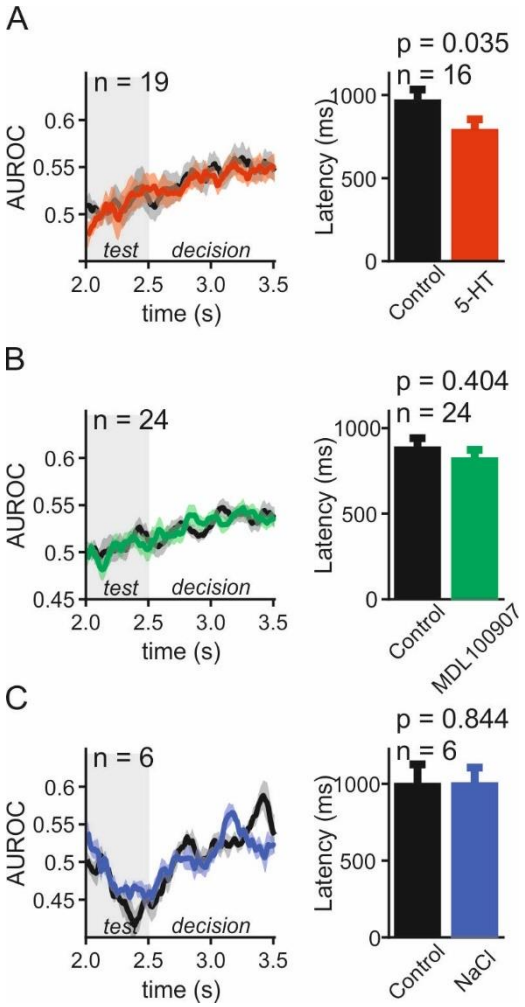

Figure 3.20: Temporal dynamics of decision-selectivity in the decision phase is modulated by 5-HT A) Sliding ROC analysis depicting the temporal dynamics of decision-coding strength of control condition trials (left, black curve) and 5-HT application trials (red curve) beginning at the offset of the test phase until the end of the decision phase. The gray bar represents the offset of the test. The latency of decision coding was unchanged (right panel). Colored shaded area depicts the SEM. B) Same conventions as in A) for decision-selective cells recorded in sessions with MDL100907 application. C) Same conventions as in B) for decision-selective cells recorded in sessions with MDL100907 application. D) Same conventions as in A) for decision-selective cells recorded in sessions with NaCl application. E) Same conventions as in B) for decision-selective cells recorded in sessions with the control substance NaCl.

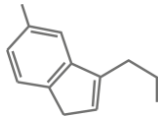

decision phase in a very similar manner for both control conditions (**Figure 3.20 A**, black curve) and 5-HT application trials (red curve). Comparing latencies of control and drug trials against an estimated null-distribution, however, revealed that 5-HT application decreased the temporal progression of decision-selectivity significantly (**Figure 3.20 A**, right, black bar: control conditions latency, mean latency 942 ± 58 ms, 5-HT application trials, red bar, mean latency 791 ± 60 ms, $p = 0.035$, $n = 16$, Wilcoxon paired test). Cells, recorded in session with MDL100907 showed a similar temporal profile (**Figure 3.20 B**, left), showing that selectivity for decision started to rise slowly during test presentation, and continued to incline throughout the decision phase. Nevertheless, MDL100907 had no visible effects on the temporal progression nor on the latencies (**Figure 3.20 B**, right, black bar: control conditions latency, mean latency 901 ± 55 ms, MDL100907 application trials, green bar, mean latency 840 ± 48 ms, $p = 0.404$, $n = 24$, Wilcoxon paired test). The same analyses applied on our control experiments revealed an interesting temporal profile of decision-selectivity. AUROC values went down during the test phase, especially for control trials (**Figure 3.20 C**, black curve). However, after test offset, coding strength started to increase throughout the decision phase. No effects on latencies was found (**Figure 3.20 C**, right, black bar: control conditions latency, mean latency 1006 ± 122 ms, NaCl application trials, blue bar, mean latency 1029 ± 96 ms, $p = 0.844$, $n = 6$, Wilcoxon paired test).

3.7 5-HT modulates Abstract Decision Information in the Whole Population of Recorded Neurons

To determine whether decision information was modulated by one of the serotonergic agents, we employed a sliding-window ω^2 PEV analysis (**Section 2.7.9**). Information was considered to be significantly different for control and drug-application trials if a bin wise computed Wilcoxon signed rank test (alpha 0.05) showed significant differences for at least five consecutive bins. **Figure 3.21 A** shows an example neuron, recorded with 5-HT application. This neuron increased information about the abstract decision during presentation of the test numerosity, for both, control conditions and 5-HT application, however, the increase was stronger for 5-HT application trials. When information about the decision is compared between 5-HT application trials and control conditions for the whole population of recorded neurons, we find that 5-HT application

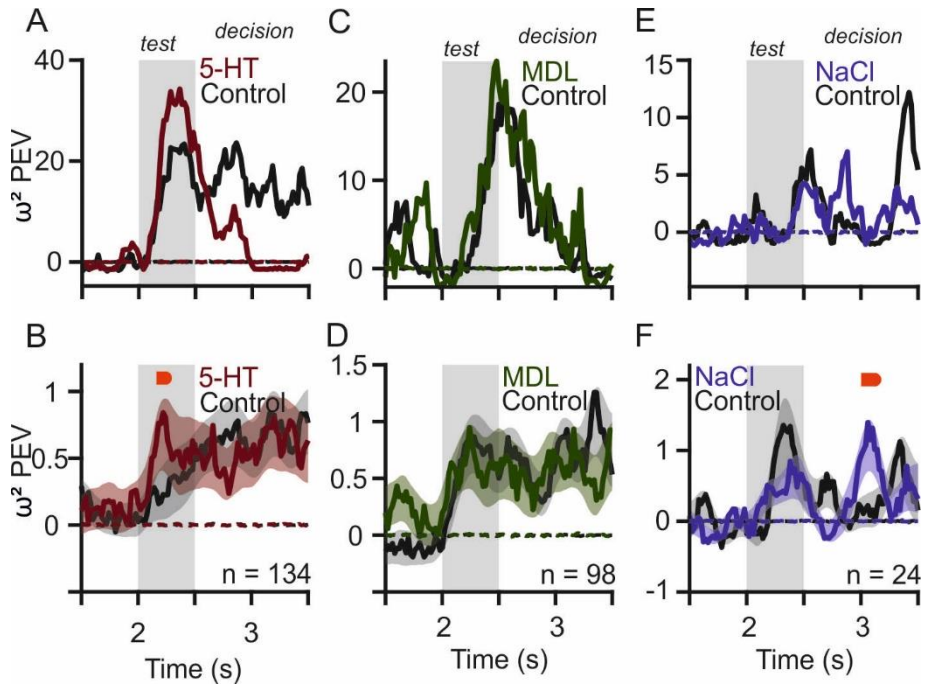

Figure 3.21: Decision information is increased significantly by 5-HT as well as during control experiments A) Sliding window ω^2 PEV of an example cell showing control trials (black curve) and 5-HT application trials (red curve) quantifying decision information across a factor-relevant task period of an example neuron. B) Average sliding window ω^2 PEV of control trials (black curve) and 5-HT application trials (red curve) quantifying information about the decision across a factor-relevant task period of all neurons, recorded in sessions with 5-HT application. Decision information is significantly increased during 5-HT application during the test presentation. Dashed lines show mean PEV values of null distribution respectively for control trials (black line) and 5-HT application trials (red line). C) Same conventions as in A) for an example neuron recorded during control conditions (black curve) and MDL100907 application (green curve). D) Same conventions as in B) for neurons, recorded during control conditions (black curve) and MDL100907 application (green curve). E) Same conventions as in A) for an example neuron recorded during control conditions (black curve) and NaCl application (blue curve). F) Same conventions as in B) for neurons, recorded during control conditions (black curve) and NaCl application (blue curve). Decision information is increased during the decision phase. Colored/black bars above the curves marks time bins in which information was significantly larger/smaller (p = 0.05) during drug application trials than control trials. Colored shaded areas denote the SEM. Gray shaded rectangular depict test presentation phase.

increases decision information significantly for a brief period of time, shortly after onset of the test stimulus (**Figure 3.21 B**). Information about the decision did not different for both iontophoresis conditions in an example neuron (**Figure 3.21 C**) recorded with MDL100907 application. Also, in the population of cells, recorded with MDL100907, we find no modulatory influence on decision information (**Figure 3.21 D**). Both curves increased slightly after test onset and sustained during the decision phase. Next, we checked for current-induced differences regarding decision information. **Figure 3.21 E** shows an example neuron recorded during control experiments with NaCl application. Here, decision information rises after test offset and fluctuates during the decision

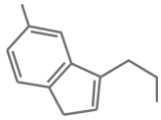

phase. This is also the case for the whole population (**Figure 3.21 F**). Decision information increases during test presentation, more so for control trials, while fluctuating during the decision phase. At one point, information about the decision is significantly larger in NaCl trials.

These results show that stimulation of all 5-HT receptors increases early cognitive information while blockage of the 5-HT2A receptor via MDL100907 application decreases information about sensory stimulus identity. We also find an effect on decision encoding within the population of recorded neurons during control experiments.

4 Discussion

The aim of our study was to investigate the role of the serotonergic system in various cognitive processes in the dlPFC necessary to solve an abstract decision task. Thus, we trained two monkeys to compare and assess two sequentially presented numerosities in a same-different decision task and manipulated the recorded neuronal activity by iontophoretic application of exogenous 5-HT or the selective 5-HT2A receptor antagonist MDL100907. The analyses were restricted to task phases before the rule cue presentation to ensure the neuronal activity would be free from motor preparatory signals. We found that, when we looked at the population of selective cells, reference-selectivity was decreased by 5-HT during reference presentation and increased by blockage of 5-HT2A by MDL100907 during working memory delay. However, neither substance modulated test-selectivity nor decision-selectivity. Temporal evolution of selectivity was mostly unmodulated by both serotonergic substances; however, we found evidence that decision-selectivity evolved later during 5-HT application. When we investigated whether serotonergic agents influence information about different task-relevant features within the discharge rates of all recorded neurons, we found sensory information is reduced when solely 5-HT2A receptors are blocked, while information about the decision is enhanced by higher 5-HT levels. Thus, our results highlight diverging effects of 5-HT depending on cell populations. Further, we find evidence for a distinct role of the 5-HT2A receptors in sensory processing and working memory.

4.1 Behavioral Performance

Both monkeys were very proficient solving the task, regardless of protocol type (standard/control) and rule (red/blue). They performed well above chance level (50 %), despite showing differences in performance according to stimulus protocol. The animals were very well trained, given that the same monkeys performed the tasks with iontophoretic application of dopamine. Thus, any effect of stimulus protocol is likely due to overtraining and the test being overpowered. Further, even though both monkeys showed significantly different accuracies, they performed better for different stimulus protocols with small effect sizes.

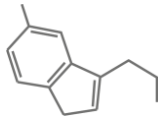

The behavioral performance functions show the numerical distance effect very clearly (Merten and Nieder, 2009). The difficulty of numerosity discrimination decreases with increasing numerical distance. Monkeys misjudged test numerosity nine less often to be equal to reference numerosity one in comparison than to reference numerosity three. But as mentioned above, the animals were very well trained, which resulted in a small number of erroneous trials.

Assessment and processing of numerosity (number of items in a set) constitutes a widespread skill in the animal kingdom (Koehler, 1956; Davis and Albert, 1986; Brannon and Terrace, 1998; Uller et al., 2003; Dacke and Srinivasan, 2008; Gross et al., 2009; Rugani et al., 2009; Agrillo et al., 2011; Vonk and Beran, 2012; Potrich et al., 2015) It is exceedingly important for many cognitive functions - whether it is to meet one's basic need like to choose the profitable food source or complex requirements like to determine the ability of a bridge to support the loads of crossing vehicles. Therefore, numerosity stimuli are well suited to investigate different cognitive processes. However, in the case of the present study, we were less interested in the neuronal processing of numerosity but investigated the modulatory effects 5-HT and MDL100907 had on neuronal activity. Thus, this thesis will not go into detail about numerical processing but concentrates on the role of the serotonergic system in the overarching cognitive processes.

4.2 Modulation of Baseline Activity

We found that iontophoretic application of 5-HT decreases neuronal baseline activity. This has been shown before in anesthetized rats (Puig et al., 2005, 2010) and for other cortical regions in the macaque brain (Seillier et al., 2017). A possible explanation is that the decreases of neuronal activity is 5-HT1A-mediated which, due to the receptors' location on the soma and the axon hillock, effectively inhibits action potential generation. After blockage of the 5-HT2A receptor we find no significant effect on neuronal baseline activity. MDL100907 reduces excitatory postsynaptic currents (Aghajanian and Marek, 1997), however, not to the extent that baseline activity is affected. This might be due to the generally small excitatory effect that activation of 5-HT2A has on its own, depolarizing the resting membrane potential only by a few millivolts (Araneda and Andrade, 1991; Tanaka and North, 1993; Zhang and Arsenault,

2005). Further, our data demonstrates that modulation of neuronal baseline activity was not caused simply by iontophoretic currents, as we see no effect in control experiments with NaCl.

4.3 Modulation of numerosity-selectivity reference phase

4.3.1 By 5-HT

We investigated the effect of 5-HT on numerosity-selectivity during the reference phase. We find, that 5-HT application decreases neuronal representation of numerosity in selective cells during the visual presentation of a reference numerosity, mainly by decreasing responses to preferred numerosities. Very little is known about whether and if so, how 5-HT modulates visual processing in the PFC. Two studies in the monkey V1 showed an involvement of 5-HT in visual processing in cortical neurons. The first study, conducted in anesthetized animals, suggests that the serotonergic system controls visual processing by the antagonistic interplay of 5-HT1 and 5-HT2 receptors (Watakabe et al., 2009). The second study involved awake monkeys performing a fixation task. Their data showed that 5-HT decreased the gain of visual responses (Seillier et al., 2017). In our case, numerosity-selectivity is affected, thus indicating a direct modulation of selectivity by 5-HT.

Studies in rats and cats showed that serotonergic cells in the dorsal raphe nucleus (DRN) exhibit an increase in activity related to visual stimulation (Heym et al., 1982; Rasmussen et al., 1986; Ranade and Mainen, 2009; Li et al., 2013), which in turn leads to an increase of 5-HT release in several cortical areas (Müller et al., 2006; Pum et al., 2008), including the rat medial PFC. Further, Ranade and Mainen (Ranade and Mainen, 2009) showed the transient nature of DRN neurons responses to visual stimuli. Serotonergic projection neurons in the DRN strongly innervate the PFC (Törk, 1990; Jacobs and Azmitia, 1992). As a consequence, one possible explanation for our findings could be an enhancement of the preferential inhibitory effect of 5-HT on cortical neurons (Zhou and Hablitz, 1999), mediated by the activation of inhibitory 5-HT1A receptors (Puig et al., 2005, 2010; Seillier et al., 2017). This is consistent with the ‘motor hypothesis’ by Jacobs and Fornal (Jacobs and Fornal, 1997) which suggests that increased 5-HT levels are related to a suppression of sensory processing.

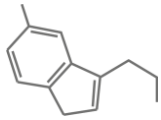

4.3.2 by MDL100907

Blockage of 5-HT2A receptors had no effect on numerosity-selectivity during reference presentation. Activation of 5-HT2A receptors through systemic administration has been shown to influence visual perception. In humans 5-HT2 receptor agonists like 2,5-dimethoxy-4-iodoamphetamine (DOI) (Shulgin and Shulgin, 1995; reviewed by Nichols, 2016), mescaline (Fleming, 1936; Hermle et al., 1992) and psilocybin (Wasson, 1957) act as a strong psychedelics, eliciting visual illusion or hallucinations. Evidence from studies in the V1 suggest that these altered visual percepts stem from altered neuronal activity in early visual areas. Micro iontophoretically application of DOI in the V1 of anesthetized monkeys (Watakabe et al., 2009) revealed a bidirectional modulation effect on firing rate of cortical neurons, which might be enough to explain the neurophysiological effects of systemic DOI. A recent study in awake mice by Michaiel and colleagues (Michaiel et al., 2019) confirmed the bidirectional modulatory effect on firing rate. They performed wide-field and two photon calcium imaging as well as single cell recordings. They moreover found evidence that activation of 5-HT2A receptors lead to an overall decreased in visual responding and surround suppressing in mouse V1 neurons, similar to what was found in awake monkeys during iontophoresis of 5-HT (Seillier et al., 2017), suggesting that, at least partly, the observed effect is 5-HT2A mediated. These results support the hypothesis that altered visual perception during hallucinations stems from reduced bottom-up (external) signaling and not from top-down (internal) signals.

However, psychedelics alter not only perception but also mood and numerous cognitive processes. Therefore, the PFC, as the conductor of the mammalian brain, is a likely target area. A fMRI study in healthy humans revealed decreased BOLD signals in the anterior cingulate cortex (ACC), a part of the medial PFC, after oral administration of psilocybin (Carhart-Harris et al., 2012). The subjectively perceived effect strength negatively correlated with the decrease in activity. Further, they showed that psilocybin reduced positive coupling between the mPFC and posterior cingulate cortex (PCC), which they claim is responsible for altered cognition. All this taken together one would expect an increase in selectivity in case the 5-HT2A receptors are involved in visual processing in the PFC, after application of the 5-HT2A antagonist MDL100907.

To our knowledge the present study is the first investigating how 5-HT2A receptors affect visual signals in higher brain areas. Our data suggests that the serotonin system is involved in processing visual input in the dlPFC (see **Section 4.3**), however, contrary to the V1, this modulation is not mediated by the 5-HT2A receptors.

4.4 Modulation of numerosity-selectivity during the working memory delay

4.4.1 By 5-HT

5-HT's role in working memory has been implicated in rats (Winter and Petti, 1987; Bonaventure et al., 2011), pigeons (Karakuyu et al., 2007) and humans (Luciana et al., 1998; Carter et al., 2005). These studies focused on modulation caused by systemic administration of serotonergic agents or naturally occurring fluctuation in 5-HT levels. Even though they demonstrated a clear connection between the serotonergic system and working memory, it remains elusive whether these are direct or indirect effects. Meanwhile, one study investigated the effects of serotonergic agents on response properties of single cells during a spatial working memory task in nonhuman primates (Williams et al 2002). As they found iontophoretic application of the 5-HT2A antagonist MDL100907 reduced spatial tuning in an oculomotor delayed response task (see **Section 4.4.2**) they also recorded one single cell with application of 5-HT. During control conditions the recorded neuron showed barely any spatial tuning, however, during application of 5-HT the cell discharge rate for one particular location was severely enhanced, resulting in spatial tuning during the delay period. Unfortunately, no further analyses were conducted on the effects of 5-HT itself on a populational level. As described above (**Section 1.3**), 5-HT receptors trigger a various number of intracellular responses upon activation, strongly depending on receptor type and receptor location. Therefore, it is possible working memory is modulated very distinctively by specific 5-HT receptor types. Our data allows the assumption that we stimulated different kinds of 5-HT receptors as numerosity-selectivity is broadly modulated during the delay.

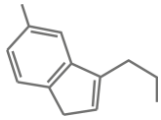

4.4.2 by MDL100907

As reported in **Section 4.3.2** MDL100907 had no influence on numerosity-selectivity during the visual presentation of the stimuli. However, numerosity tuning was improved during the delay in trials with MDL100907. This modulation was achieved by decreasing activity towards the non-preferred numerosity in working memory. Our finding seemingly contradicts two other studies investigating the role of 5-HT2A receptors in working memory. The first study, conducted by Williams and colleagues (Williams et al., 2002), found that blocking 5-HT2A receptors affected activity towards both, the preferred and non-preferred stimulus during the delay. They trained monkeys on an oculomotor delayed response task and recorded single cell activity in the dlPFC while applying different 5-HT2A targeting substances with microiontophoresis. Blocking 5-HT2A receptors caused cells to fire less for the preferred location but also increased their activity for nonpreferred locations, effectively decreasing spatial working memory. It is important to note that they observe this effect despite using a considerably weaker ejection current (10 nA) compared to our study (25 nA). They also showed that activating the 5-HT2 receptors with a modest ejection current strength (50 nA) increased spatial tuning of a weakly tuned cell but using higher currents (100 nA) lead to the loss of spatial tuning in a weakly tuned cell.

The second study used a conditional discrimination task to investigate working memory in rats (Herremans et al., 1995). The animals were systemically injected with three different doses of the high-affinity non-selective 5-HT2 antagonist Ketanserin. Afterwards their performance was compared to a control group. None of the doses showed a modulatory effect on the animals' performance, suggesting that 5-HT2A receptors are not involved in mnemonic processes. In this case, the doses were high (at least 0.3 mg/kg) compared to the dose of around 0.08 mg/kg MDL100907 shown to be enough to achieve 90% 5-HT2A receptor occupancy in the human brain (Andrée et al., 1998). A dosage effect reconciles our results with these studies and suggests that blockage of 5-HT2A receptors, similar to D1 receptors (Vijayraghavan et al., 2007), follows an inverted u-shaped function as suggest by a computational network model (Cano-Colino et al., 2013).

Coinciding with our study, it was shown that 5-HT2A receptor stimulation through the psychedelic drug psilocybin (dose-dependently) inhibited working memory

performance in humans (Barrett et al., 2018). But what is the mechanism of action of a 5-HT2A receptor in working memory? A possible explanation could be the seemingly antagonistic interplay between 5-HT1A and 5-HT2A receptors, resulting out of the opposing effect on membrane potential upon their activation and receptor expression location. As mentioned above, most pyramidal neurons express both receptor types in the primate brain. The excitatory 5-HT2A is located at the apical dendrites and thought to amplify excitatory synaptic input after activation. The 5-HT1A receptors are expressed at soma and the axon hillhock. Their activation impedes action potential generation by opening rectifying potassium channels (Bockaert et al., 2006). These opposing effects provide a potent tool to modulate and shape a neurons response depending on temporal dynamics of receptor activation and the resulting computation of excitatory and inhibitory postsynaptic currents. As MDL100907 application increased working memory in selective cells in our study it is conceivable that blocking 5-HT2A receptors suspend a kind of uncertainty filter preventing premature responses. High levels of 5-HT and resulting strong activation of 5-HT1A receptors would superimpose any EPSP by 5-HT2A activation, due to their efficient location. Optogenetic studies in rats (Miyazaki et al., 2012, 2014; Fonseca et al., 2015) showed that 5-HT plays an important role in patience, with the PFC, a major hub for goal directed behavior, being a likely candidate for this function. However, these are mere speculations and a similar study with both 5-HT1A and 5-HT2A targeting substances could shed light in this question.

4.5 No Modulation of test-numerosity selectivity by 5-HT and MDL100907

The behavioral protocol in the present study provides the possibility to compare modulatory effects of the used serotonergic agents onto two sequentially shown numerosity stimuli separately. Importantly, even though both stimuli are similar or even match in their physical numerosity, they differ strongly in their contextual interpretation for the task. There are two likely strategies to solve the comparison-task between reference and test numerosity. In either one the physical numerosity of the reference stimulus must be remembered. However, there are two options for assessing the second shown numerosity (test). 1. Either the monkey also remembers the test

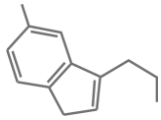

numerosity, and compares it to the reference stimulus, or 2. it judges test-numerosities directly into two categories, namely whether it was the ‘same’ or a ‘different’ numerosity. From our data it is not possible to infer which strategy the monkeys used, however, in case the first strategy pertains, one would expect two distinct subsets of neurons encoding reference and test numerosity. Consequently, application of 5-HT would lead to similar drug effects during test-numerosity presentation as seen during reference presentation. The second strategy does not necessarily involve test-selective neurons in the comparison process. It is possible that this process takes place in one circuit. Interestingly, we found no modulation of test-numerosity-selectivity by neither 5-HT nor MDL100907 application during the presentation of the test stimulus even though 5-HT modulated reference numerosity processing during the visual presentation of the reference stimulus (see **Section 4.3**). One explanation could be an increasing cognitive component of the neuronal signal, superimposing any serotonin-effect on visual processing of the test numerosity. A second possible explanation could be that test-selective neurons are not involved in the comparison process, but merely representing a perceptual category as shown for naïve monkeys (Viswanathan and Nieder, 2013). Therefore, no substance has a consistent effect on test-selectivity in this population of neurons.

Test-selectivity was also not modulated by either serotonergic agent used in the present study during the decision phase. As mentioned above the behavioral task consists out of two repetitions of a visual presentation of a numerosity stimulus followed by a delay, without any external sensory stimulation. However, during test and decision phase the cognitive demand increases due to the necessary comparison process. It is possible that the increasing cognitive demand is mirrored in the neuronal signal, superimposing any drug effect also during the decision phase.

4.6 Decision-selectivity is not modulated by 5-HT and MDL100907

We investigated whether iontophoretical application of exogenous 5-HT or MDL100907 modulated the abstract decision tuning within the population of decision-selective neurons. However, decision-selectivity in dlPFC neurons was neither modulated by 5-HT nor MDL100907, with the exception of temporal evolution of decision-selectivity in the decision phase, which was extended by 5-HT.

Often, the capability for assessment of situations and adequate reactions seem to be impaired in patients suffering from mental disorders with accompanying cognitive impairments. This is possibly related to altered evaluation of reward or reward valence. The serotonergic system has been implicated both in mental disorders (Deakin, 1991; Graeff et al., 1996) as well as in various function which are important for decision making (Homberg, 2012). These functions include cognitive flexibility, which increases with increasing 5-HT levels in marmosets (Clarke, 2004) and rats (Bari et al., 2010; Boulougouris and Robbins, 2010), attentional set shifting in marmosets (Clarke et al., 2005) and humans (Rogers et al., 1999) and response inhibition, which is decreased when 5-HT levels are globally reduced in rats (Harrison et al., 1997; Puumala and Sirviö, 1998) but increased after a rise of endogenous 5-HT levels in the rat mPFC, measured with micro dialysis (Dalley et al., 2002). However, to our knowledge this is the first study to investigate the serotonergic modulation of abstract decisions. Therefore, it is hard to conclude that the serotonergic system is not involved in decision making, even with negative results. By application of exogenous 5-HT we target all available 5-HT receptor types, which trigger a variety of cell responses vastly depending on cell type (pyramidal vs interneuron, (Puig and Gulledge, 2011)) and expression location (quelle). Further, it cannot be ruled out, that 5-HT influences other aspects of the neuronal activity than its frequency. Maybe complex temporal (Thorpe, 1990; Gerstner et al., 1997; Aur and Jog, 2007) or populational coding (Maunsell and Van Essen, 1983) schemes are affected.

4.7 Modulation of task feature information within the whole recorded population

We tested the modulatory effects of 5-HT and MDL100907 on task relevant information within the whole population of recorded dlPFC neurons. We find that blockage of 5-HT2A receptors decreased information about the visually presented numerosity stimuli but did not modulate decision information. 5-HT has been implicated in sensory processing in hierarchically lower brain areas (Heym et al., 1982; Rasmussen et al., 1986; Müller et al., 2006; Ranade and Mainen, 2009; Li et al., 2013). Studies in early visual areas of monkeys showed that 5-HT decreased visual responses (Watakabe et al., 2009), primarily by gain change of neuronal tuning curves (Seillier et al., 2017).

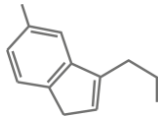

One hypothesis is that by reducing the saliency of a visual stimulus, 5-HT functions as a promotor of behavioral inhibition and patience (Miyazaki et al., 2012; Fonseca et al., 2015; Lottem et al., 2018). However, only little is known about how 5-HT modulates prefrontal visual signals.

A perceptual inference study by Costa and colleagues (Costa et al., 2016) injected monkeys intramuscular with a 5-HT reuptake inhibitor. The animals showed reduced impulsive answering, while also the perceptual performance suffered, indicating attenuated sensory processing. This is compatible with our results which suggest that 5-HT2A receptors are important for accurate information complement/integration of sensory input in the PFC, probably by fine tuning how neurons encode incoming signals into firing response. The involvement in sensory processing becomes also evident as blocking 5-HT2A receptors only affect sensory properties of the information signal, whereas information about the abstract decision remains unaffected. Our findings allow the assumption that the 5-HT2A receptor might be a key structure for reduction of visual saliency in the population signal of prefrontal cortex neurons.

Further it is also known that blockage of 5-HT2A receptors in the rat PFC reduced dopaminergic release in the mPFC (Bortolozzi et al., 2005). A study in monkeys from our lab showed that numerosity-selectivity decreases upon dopamine d1 receptor blockage (Ott et al., 2014), which mirrors the situation of reduced dopamine levels. It is questionable, whether blockage of 5-HT2A elicit an indirect dopamine effect, which in turn, is responsible for decreased sensory information, however, it cannot be ruled out that reduced DA levels contribute to information loss about sensory signal properties.

Application of 5-HT had a distinct impact on whole population information. Sensory information was unaffected. 5-HT is the endogenous ligand for all 5-HT receptor types, responsible for various intracellular responses/ signaling cascades. 5-HT1A and 5-HT2A receptors are the most abundant receptor types in the PFC (De Almeida and Mengod, 2007, 2008) and affect the membrane potential in opposing directions (Araneda and Andrade, 1991; Puig and Gulledge, 2011). It is very likely, that any effects were canceled out (as we cannot be sure which receptor type was activated by 5-HT application in the respective recorded cell) on the populational or even a cellular level.

The present study is the first to our knowledge investigating the role of 5-HT in abstract decisions. The fact that additional 5-HT modulated decision information is compatible with previous findings. Such as, 5-HT modulates different fundamental operation of decision making. 5-HT depletion in marmosets (Clarke, 2004; Clarke et al., 2005) and humans (Rogers et al., 1999; Evers et al., 2005) impaired cognitive flexibility, which is a key prerequisite for decision making. Another important function is suppression of mere stimulus-response associations and premature reactions. In a delayed response study in rats it was shown that optogenetic stimulation of serotonergic neurons in the DRN prolonged time animals would wait for a signaled reward (Miyazaki et al., 2014), effectively enabling the execution of goal-directed behavior. We find that 5-HT increased information about the abstract decision. 5-HT beneficial impact on decision making was already implicated by the fact that 5-HT reuptake inhibitors (SSRI) often show positive therapeutic effects as treatment for mental illnesses with accompanying cognitive inhibition, including impaired decision making (Cáceda et al., 2014).

We find that decision information is significantly increased in control experiments with NaCl application during the decision phase. In all other control analyses investigating effects of the mere current, we found no evidence for a current-induced modulation. It is likely, that due to the relatively small number of cells recorded with NaCl application any strong effect of one or two cells influences the population activity significantly. Our results implicate that 5-HT2A receptors are involved primarily in processing of sensory signals whereas modulation of decision information is carried by other 5-HT receptor types on a populational level.

5 Conclusion

We recorded single cell activity with simultaneous micro-iontophoretical application of serotonergic agents in the monkey dorsolateral prefrontal cortex, while animals performed an abstract decision task. To our knowledge our study is the first investigating the role of serotonin in visual/numerical working memory and decisions related single cell activity.

We find heterogeneous modulatory effects in different subpopulations of neurons. 5-HT is involved in decision making, as application of 5-HT increased information about

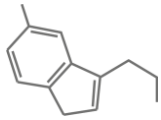

the decision in the whole population of recorded neurons. However, this effect was not conveyed through modulation of decision-selective neurons. Furthermore, our findings highlight the role of 5-HT in prefrontal visual processing. During visual presentation higher levels of 5-HT inhibited stimulus-selective neurons. Blockage of 5-HT2A receptors contributed to activity maintenance of numerical information processing circuits. Further, application of MDL100907 increased sensory information within the whole population of recorded neurons. Our results show no involvement of 5-HT2A receptors in decision making, albeit their role in working memory. These findings suggest that 5-HT receptor subtypes contribute differently to cognitive and sensory processes in prefrontal cortex and highlight the importance of further research to tackle mental illnesses with accompanying cognitive impairment.

6 References

Abrams JK, Johnson PL, Hollis JH, Lowry CA (2004) Anatomic and functional topography of the dorsal raphe nucleus. In: Annals of the New York Academy of Sciences, pp 46–57. New York Academy of Sciences.

Adell A, Carceller A, Artigas F (1991) Regional Distribution of Extracellular 5 Ż Hydroxytryptamine and 5 Ż Hydroxyindoleacetic Acid in the Brain of Freely Moving Rats. J Neurochem 56:709–712.

Aggleton JP, Burton MJ, Passingham RE (1980) Cortical and subcortical afferents to the amygdala of the rhesus monkey (Macaca mulatta). Brain Res 190:347–368.

Aghajanian GK, Foote WE, Sheard MH (1968) Lysergic acid diethylamide: Sensitive neuronal units in the midbrain raphe. Science (80-) 161:706–708.

Aghajanian GK, Marek GJ (1997) Serotonin induces excitatory postsynaptic potentials in apical dendrites of neocortical pyramidal cells. Neuropharmacology 36:589–599.

Agrillo C, Piffer L, Bisazza A (2011) Number versus continuous quantity in numerosity judgments by fish. Cognition 119:281–287.

Akert K (1964) Comparative anatomy of frontal cortex and thalamofrontal connection. Front Granul cortex Behav:372–396.

Albert PR, Sajedi N, Lemonde S, Ghahremani MH (1999) Constitutive G i2-dependent Activation of Adenylyl Cyclase Type II by the 5-HT1A Receptor. Inhibition by Anxiolytic Partial Agonists*.

Amargós-Bosch M, Bortolozzi A, Puig MV, Serrats J, Adell A, Celada P, Toth M, Mengod G, Artigas F (2004) Co-expression and In Vivo Interaction of Serotonin1A and Serotonin2A Receptors in Pyramidal Neurons of Pre-frontal Cortex. Cereb Cortex 14:281–299.

Amin AH, Crawford TBB, Gaddum JH (1954) The distribution of substance P and 5 Ż hydroxytryptamine in the central nervous system of the dog. J Physiol 126:596–618.

Anctil M (1989) The Antiquity of Monoaminergic Neurotransmitters: Evidence from Cnidaria. In: Evolution of the First Nervous Systems, pp 141–155. Springer US.

Andrade R, Nicoll RA (1987) Pharmacologically distinct actions of serotonin on single pyramidal neurones of the rat hippocampus recorded in vitro. J Physiol 394:99–124.

Andrée B, Nyberg S, Ito H, Ginovart N, Brunner F, Jaquet F, Halldin C, Farde L (1998) Positron emission tomographic analysis of dose-dependent MDL 100,907 binding to 5-hydroxytryptamine-2A receptors in the human brain. J Clin Psychopharmacol 18:317–323.

Angiolillo PJ, Vanderkooi JM (1996) Hydrogen atoms are produced when tryptophan within a protein is irradiated with ultraviolet light. Photochem Photobiol 64:492–495.

Aoyagi M, Arvai AS, Ghosh S, Stuehr DJ, Tainer JA, Getzoff ED (2001) Structures of tetrahydrobiopterin binding-site mutants of inducible nitric oxide synthase oxygenase dimer and implicated roles of Trp457. Biochemistry 40:12826–12832.

Araneda R, Andrade R (1991) 5-Hydroxytryptamine2 and 5-hydroxytryptamine1A receptors mediate opposing responses on membrane excitability in rat association cortex. Neuroscience 40:399–412.

Aur D, Jog M (2007) Reading the Neural Code: What do Spikes Mean for Behavior? Nat

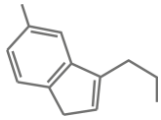

Preced.

Azmitia EC (1999) Serotonin Neurons, Neuroplasticity, and Homeostasis of Neural Tissue.

Azmitia EC (2001) Modern views on an ancient chemical: Serotonin effects on cell proliferation, maturation, and apoptosis. In: Brain Research Bulletin.

Azmitia EC, Gannon PJ (1983) The ultrastructural localization of serotonin immunoreactivity in myelinated and unmyelinated axons within the medial forebrain bundle of rat and monkey. J Neurosci 3:2083–2090.

Azmitia EC, Gannon PJ (1986) The primate serotonergic system: a review of human and animal studies and a report on Macaca fascicularis. Adv Neurol 43:407–468.

Azmitia EC, Gannon PJ, Kheck NM, Whitaker-Azmitia PM (1996) Cellular localization of the 5-HT(1A) receptor in primate brain neurons and glial cells. Neuropsychopharmacology 14:35–46.

Azmitia EC, Segal M (1978) An autoradiographic analysis of the differential ascending projections of the dorsal and median raphe nuclei in the rat. J Comp Neurol 179:641–667.

Bailey P, von Bonin G (1951) The isocortex of man.

Baker KG, Halliday GM, Hornung JP, Geffen LB, Cotton RGH, Törk I (1991) Distribution, morphology and number of monoamine-synthesizing and substance P-containing neurons in the human dorsal raphe nucleus. Neuroscience 42:757–775.

Baker KG, Halliday GM, Törk I (1990) Cytoarchitecture of the human dorsal raphe nucleus. J Comp Neurol 301:147–161.

Bari A, Theobald DE, Caprioli D, Mar AC, Aidoo-Micah A, Dalley JW, Robbins TW (2010) Serotonin modulates sensitivity to reward and negative feedback in a probabilistic reversal learning task in rats. Neuropsychopharmacology 35:1290–1301.

Barrett FS, Carbonaro TM, Hurwitz E, Johnson MW, Griffiths RR (2018) Double-blind comparison of the two hallucinogens psilocybin and dextromethorphan: effects on cognition. Psychopharmacology (Berl) 235:2915–2927.

Béıque J-CB, Campbell B, Perring P, Hamblin MW, Walker P, Mladenovic L, Andrade R (2004) Behavioral/Systems/Cognitive Serotonergic Regulation of Membrane Potential in Developing Rat Prefrontal Cortex: Coordinated Expression of 5-Hydroxytryptamine (5-HT) 1A , 5-HT 2A , and 5-HT 7 Receptors.

Belin MF, Aguera M, Tappaz M, McRae-Degueurce A, Bobillier P, Pujol JF (1979) GABA-accumulating neurons in the nucleus raphe dorsalis and periaqueductal gray in the rat: A biochemical and radioautographic study. Brain Res 170:279–297.

Beliveau V, Ganz M, Feng L, Ozenne B, Højgaard L, Fisher PM, Svarer C, Greve DN, Knudsen GM (2017) A high-resolution in vivo atlas of the human brain's serotonin system. J Neurosci 37:120–128.

Berger B, Trottier S, Verney C, Gaspar P, Alvarez C (1988) Regional and laminar distribution of the dopamine and serotonin innervation in the macaque cerebral cortex: A radioautographic study. J Comp Neurol 273:99–119.

Berger M, Gray JA, Roth BL (2009) The Expanded Biology of Serotonin. Annu Rev Med 60:355–366.

Bigham MH, Lidow MS (1995) Adrenergic and serotonergic receptors in aged monkey neocortex. Neurobiol Aging 16:91–104.

Blundell JE (1977) Is there a role for serotonin (5-hydroxytryptamine) in feeding? Int J Obes 1:15–42.

Bockaert J, Claeysen S, Bécamel C, Dumuis A, Marin P (2006) Neuronal 5-HT metabotropic receptors: Fine-tuning of their structure, signaling, and roles in synaptic modulation. Cell Tissue Res 326:553–572.

Bogdanski DF, Weissbach H, Udenfriend S (1957) The Distribution Of Serotonin, 5 Ż Hydroxytryptophan Decarboxylase, And Monoamine Oxidase In Brain. J Neurochem 1:272–278.

Bonaventure P, Aluisio L, Shoblock J, Boggs JD, Fraser IC, Lord B, Lovenberg TW, Galici R (2011) Pharmacological blockade of serotonin 5-HT7 receptor reverses working memory deficits in rats by normalizing cortical glutamate neurotransmission. PLoS One 6.

Bortolozzi A, D??az-Mataix L, Scorza MC, Celada P, Artigas F (2005) The activation of 5-HT2A receptors in prefrontal cortex enhances dopaminergic activity. J Neurochem 95:1597–1607.

Boulougouris V, Glennon JC, Robbins TW (2008) Dissociable Effects of Selective 5-HT2A and 5-HT2C Receptor Antagonists on Serial Spatial Reversal Learning in Rats. Neuropsychopharmacology 33:2007–2019.

Boulougouris V, Robbins TW (2010) Enhancement of Spatial Reversal Learning by 5-HT2C Receptor Antagonism Is Neuroanatomically Specific. J Neurosci 30:930–938.

Bradley PB, Hance AJ (1956) The effect of amphetamine and D-lysergic acid diethylamide (LSD 25) on the electrical activity of the brain of the conscious cat. J Physiol 120:13P-14P.

Brannon EM, Terrace HS (1998) Ordering of the numerosities 1 to 9 by monkeys. Science (80-) 282:746–749.

Brodal A (1981) Neurological anatomy in relation to clinical medicine. Oxford University Press.

Buschman TJ, Miller EK (2007) Top-down versus bottom-up control of attention in the prefrontal and posterior parietal cortices. Science (80-) 315:1860–1864.

Buschman TJ, Siegel M, Roy JE, Miller EK (2011) Neural substrates of cognitive capacity limitations. Proc Natl Acad Sci U S A 108:11252–11255.

Cáceda R, Nemeroff CB, Harvey PD (2014) Toward an understanding of decision making in severe mental illness. J Neuropsychiatry Clin Neurosci 26:196–213.

Cajal S (1999) Texture of the Nervous System of Man and the Vertebrates. An Annotated and Edited Translation (Pasik P, Pasik T, eds)., II. Wien: Springer-Verlag.

Cajal S y (1904) Textura del sistema nervioso del Hombre y de los vertebrados. Moya Madrid.

Campbell MJ, Lewis DA, Foote SL, Morrison JH (1987) Distribution of choline acetyltransferase Ż, serotonin Ż, dopamine ß Ż hydroxylase Ż, tyrosine hydroxylase Ż, immunoreactive fibers in monkey primary auditory cortex. J Comp Neurol 261:209–220.

Cano-Colino M, Almeida R, Gomez-Cabrero D, Artigas F, Compte A (2013) Serotonin regulates performance nonmonotonically in a spatial working memory network. Cereb Cortex 24:2449–2463.

Carhart-Harris RL, Erritzoe D, Williams T, Stone JM, Reed LJ, Colasanti A, Tyacke RJ, Leech R, Malizia AL, Murphy K, Hobden P, Evans J, Feilding A, Wise RG, Nutt DJ (2012) Neural correlates of the psychedelic state as determined by fMRI studies with psilocybin. Proc Natl Acad Sci 109:2138–2143.

Carli M, Baviera M, Invernizzi RW, Balducci C (2006) Dissociable contribution of 5-HT1A and 5-HT2A receptors in the medial prefrontal cortex to different aspects of executive control such as impulsivity and compulsive perseveration in rats. Neuropsychopharmacology 31:757–767.

Carlsson A, Falck B, Hillarp NA (1962) Cellular localization of brain monoamines. Acta Physiol Scand Suppl 56:1–28.

Carmichael ST, Price JL (1994) Architectonic subdivision of the orbital and medial prefrontal cortex in the macaque monkey. J Comp Neurol 346:366–402.

Carter OL, Burr DC, Pettigrew JD, Wallis GM, Hasler F, Vollenweider FX (2005) Using psilocybin to investigate the relationship between attention, working memory, and the serotonin 1A and 2A receptors. J Cogn Neurosci 17:1497–1508.

Cases O, Seif I, Grimsby J, Gaspar P, Chen K, Pournin S, Muller U, Aguet M, Babinet C, Shih J, Al. E (1995) Aggressive behavior and altered amounts of brain serotonin and norepinephrine in mice lacking MAOA. Science (80-) 268:1763–1766.

Casey BJ, Forman SD, Franzen P, Berkowitz A, Braver TS, Nystrom LE, Thomas KM, Noll DC (2001) Sensitivity of prefrontal cortex to changes in target probability: A functional MRI study. Hum Brain Mapp 13:26–33.

Chiba T, Kayahara T, Nakano K (2001) Efferent projections of infralimbic and prelimbic areas of the medial prefrontal cortex in the Japanese monkey, Macaca fuscata. Brain Res 888:83–101.

Choi DS, Ward SJ, Messaddeq N, Launay JM, Maroteaux L (1997) 5-HT2B receptor-mediated serotonin morphogenetic functions in mouse cranial neural crest and myocardiac cells. Development 124:1745–1755.

Clarke HF (2004) Cognitive Inflexibility After Prefrontal Serotonin Depletion. Science (80-) 304:878–880.

Clarke HF, Walker SC, Crofts HS, Dalley JW, Robbins TW, Roberts AC (2005) Prefrontal serotonin depletion affects reversal learning but not attentional set shifting. J Neurosci 25:532–538.

Clarke WP, Yocca FD, Maayani S (1996) Lack of 5-hydroxytryptamine1A-mediated inhibition of adenylyl cyclase in dorsal raphe of male and female rats. J Pharmacol Exp Ther 277:1259–1266.

Colino A, Halliwell J V. (1988) Differential modulation of three separate K-conductances in hippocampal ca1 neurons by serotonin. Nature 328:73–77.

Corvaja N, Doucet G, Bolam JP (1993) Ultrastructure and synaptic targets of the raphe-nigral projection in the rat. Neuroscience 55:417–427.

Costa VD, Kakalios LC, Averbeck BB (2016) Blocking serotonin but not dopamine reuptake alters neural processing during perceptual decision making. Behav Neurosci 130:461–468.

Cruz DA, Eggan SM, Azmitia EC, Lewis DA (2004) Serotonin 1A Receptors at the Axon Initial Segment of Prefrontal Pyramidal Neurons in Schizophrenia. Am J Psychiatry 161:739–742.

Csaba G (1993) Presence in and effects of pineal indoleamines at very low level of phylogeny. Experientia 49:627–634.

Dacke M, Srinivasan M V. (2008) Evidence for counting in insects. Anim Cogn 11:683–689.

Dahlström A, Fuxe K (1964) Evidedence For The Existence Of Monoamine Neurons In The Central Nervous System. I. Demonstration Of Monoamines in The Cell Bodies Of Brain Stem Neurons. Acta Physiol Scand Suppl:SUPPL 232:1-55.

Dahlström A, Fuxe K (1965) Evidedence For The Existence Of Monoamine Neurons In The Central Nervous System. II. Experimentally Induced Changes In The Intraneural Amine Levels Of Bulbospinal Neuron Systems. Acta Physiol Scand Suppl:SUPPL 247:1-36.

Dalley JW, Theobald DE, Pereira EAC, Li PMMC, Robbins TW (2002) Specific abnormalities in serotonin release in the prefrontal cortex of isolation-reared rats measured during behavioural performance of a task assessing visuospatial attention and impulsivity. Psychopharmacology (Berl) 164:329–340.

Datiche F, Luppi PH, Cattarelli M (1995) Serotonergic and non-serotonergic projections from the raphe nuclei to the piriform cortex in the rat: a cholera toxin B subunit (CTb) and 5-HT immunohistochemical study. Brain Res 671:27–37.

Davis H, Albert M (1986) Numerical discrimination by rats using sequential auditory stimuli.

De Almeida J, Mengod G (2007) Quantitative analysis of glutamatergic and GABAergic neurons expressing 5-HT2A receptors in human and monkey prefrontal cortex. J Neurochem 103:475–486.

De Almeida J, Mengod G (2008) Serotonin 1A receptors in human and monkey prefrontal cortex are mainly expressed in pyramidal neurons and in a GABAergic interneuron subpopulation: Implications for schizophrenia and its treatment. J Neurochem 107:488–496.

de Olmos J, Heimer L (1980) Double and triple labeling of neurons with fluorescent substances; The study of collateral pathways in the ascending raphe system. Neurosci Lett 19:7–12.

Deakin JFW (1991) Depression and 5HT. Int Clin Psychopharmacol 6:23–31.

DeFelipe J, Arellano JI, Gómez A, Azmitia EC, Muñoz A (2001) Pyramidal cell axons show a local specialization for GABA and 5-HT inputs in monkey and human cerebral cortex. J Comp Neurol 433:148–155.

Defelipe J, Jones EG (1988) Exoerimental Brain Research A light and electron microscopic study of serotonin-immunoreactive fibers and terminals in the monkey sensory-motor cortex.

Dehaene S (1992) Varieties of numerical abilities. Cognition 44:1–42.

Dehaene S, Dehaene-Lambertz G, Cohen L (1998) Abstract representations of numbers in the animal and human brain. Trends Neurosci 21:355–361.

Dewhurst SA, Croker SG, Ikeda K, McCaman RE (1972) Metabolism of biogenetic amines in drosophila nervous tissue. Comp Biochem Physiol - Part B Biochem 43:975–981.

Ding YQ, Marklund U, Yuan W, Yin J, Wegman L, Ericson J, Deneris E, Johnson RL, Chen ZF (2003) Lmx1b is essential for the development of serotonergic neurons. Nat Neurosci 6:933–938.

Erspamer V (1953) Über den 5-Hydroxytryptamin-(Enteramin)-Gehalt des Magen-

Darmtraktes bei den Wirbeltieren. In: Naturwissenschaften. Springer.

Erspamer V (1966) Occurrence of indolealkylamines in nature. In: 5-Hydroxytryptamine and Related Indolealkylamines, pp 132–181. Springer Berlin Heidelberg.

Essen LO, Perisic O, Katan M, Yiqin W, Roberts MF, Williams RL (1997) Structural mapping of the catalytic mechanism for a mammalian phosphoinositide-specific phospholipase C. Biochemistry 36:1704–1718.

Evers EAT, Cools R, Clark L, Van Der Veen FM, Jolles J, Sahakian BJ, Robbins TW (2005) Serotonergic modulation of prefrontal cortex during negative feedback in probabilistic reversal learning. Neuropsychopharmacology 30:1138–1147.

Falck B (1964) Cellular Localization of Monoamines. Prog Brain Res 8:28–44.

Fallon JH, Loughlin SE (1982) Monoamine innervation of the forebrain: Collateralization. Brain Res Bull 9:295–307.

Fargin A, Raymond JR, Lohse MJ, Kobilka BK, Caron MG, Lefkowitz RJ (1988) The genomic clone G-21 which resembles a β-adrenergic receptor sequence encodes the 5-HT1A receptor. Nature 335:358–360.

Feldberg W, Toh CC (1953) Distribution of 5 Hydroxytryptamine (serotonin, enteramine) in the wall of the digestive tract. J Physiol 119:352–362.

Felten DL, Sladek JR (1983) Monoamine distribution in primate brain V. Monoaminergic nuclei: Anatomy, pathways and local organization. Brain Res Bull 10.

Fleming GWTH (1936) Mescaline and Depersonalization. J Ment Sci 82:287–287.

Fonseca MS, Murakami M, Mainen ZF (2015) Activation of dorsal raphe serotonergic neurons promotes waiting but is not reinforcing. Curr Biol 25:306–315.

Fredriksson R, Lagerström MC, Lundin LG, Schiöth HB (2003) The G-protein-coupled receptors in the human genome form five main families. Phylogenetic analysis, paralogon groups, and fingerprints. Mol Pharmacol 63:1256–1272.

French AS, Simcock KL, Rolke D, Gartside SE, Blenau W, Wright GA (2014) The role of serotonin in feeding and gut contractions in the honeybee. J Insect Physiol 61:8–15.

Funahashi S, Bruce CJ, Goldman-Rakic PS (1989) Mnemonic coding of visual space in the monkey's dorsolateral prefrontal cortex. J Neurophysiol 61:331–349.

Fuster J (2015) The prefrontal cortex.

Fuster JM (1973) Unit activity in prefrontal cortex during delayed-response performance: neuronal correlates of transient memory. J Neurophysiol 36:61–78.

Fuster JM (2001) The prefrontal cortex - An update: Time is of the essence. Neuron 30:319–333.

Fuster JM, Alexander GE (1971) Neuron activity related to short-term memory. Science (80-) 173:652–654.

Fuxe K (1965) Evidedence For The Existence Of Monoamine Neurons In The Central Nervous System. IV. Distribution Of Monoamine Nerve Terminals In The Central Nervous System. Acta Physiol Scand Suppl:SUPPL 247:37+.

Fuxe K, Borroto-Escuela DO, Romero-Fernandez W, Zhang WB, Agnati LF (2013) Volume transmission and its different forms in the central nervous system. Chin J Integr Med 19:323–329.

Gaddum JH, Picarelli ZP (1957) Two Kinds of Tryptamine Receptor. Br J Pharmacol Chemother 12:323–328.

Garattini S, Valzelli L (1965) Serotonin. Serotonin.

Gerschenfeld HM, Stefani E (1965) 5-Hydroxytryptamine receptors and synaptic transmission in molluscan neurones [15]. Nature 205:1216–1218.

Gershon MD, Drakontides AB, Ross LL (1965) Serotonin: Synthesis and release from the myenteric plexus of the mouse intestine. Science (80-) 149:197–199.

Gershon MD, Tack J (2007) The Serotonin Signaling System: From Basic Understanding To Drug Development for Functional GI Disorders. Gastroenterology 132:397–414.

Gerstner W, Kreiter AK, Markram H, Herz AVM (1997) Neural codes: Firing rates and beyond. Proc Natl Acad Sci U S A 94:12740–12741.

Ghashghaei HT, Barbas H (2002) Pathways for emotion: Interactions of prefrontal and anterior temporal pathways in the amygdala of the rhesus monkey. Neuroscience 115:1261–1279.

Goldman-Rakic PS (1987) Circuitry of primate prefrontal cortex and regulation of representational memory. In: Handbook of Physiology, pp 373–417. Washington DC: The American Physiological Society.

Goldman-Rakic PS, Lidow MS, Gallager DW (1990) Overlap of dopaminergic, adrenergic, and serotoninergic receptors and complementarity of their subtypes in primate prefrontal cortex. J Neurosci 10:2125–2138.

Golebiewska U, Scarlata S (2008) Gαq binds two effectors separately in cells: Evidence for predetermined signaling pathways. Biophys J 95:2575–2582.

Graeff FG, Guimarães FS, De Andrade TGCS, Deakin JFW (1996) Role of 5-HT in stress, anxiety, and depression. In: Pharmacology Biochemistry and Behavior, pp 129–141. Elsevier Inc.

Green DM, Swets JA (1966) Signal Detection Therory and Psychophysics.

Green MF (2006) Cognitive impairment and functional outcome in schizophrenia and bipolar disorder. J Clin Psychiatry 67:3–8.

Grønstad KO, Demagistris L, Dahlstroum A, Nilsson O, Price B, Zinner MJ, Jaffe BM, Ahlman H (1985) The effects of vagal nerve stimulation on endoluminal release of serotonin and substance p into the feline small intestine. Scand J Gastroenterol 20:163–169.

Gross HJ, Pahl M, Si A, Zhu H, Tautz J (2009) Number-Based Visual Generalisation in the Honeybee. PLoS One 4:4263.

Hamlin KE, Fischer FE (1951) The Synthesis of 5-Hydroxytryptamine. J Am Chem Soc 73:5007–5008.

Hamon M, Gozlan H, el Mestikawy S, Emerit MB, Bolanos F, Schechter L (1990) The Central 5-HT1A Receptors: Pharmacological, Biochemical, Functional, and Regulatory Properties. Ann N Y Acad Sci 600:114–129.

Harrison AA, Everitt BJ, Robbins TW (1997) Central 5-HT depletion enhances impulsive responding without affecting the accuracy of attentional performance: Interactions with dopaminergic mechanisms. Psychopharmacology (Berl) 133:329–342.

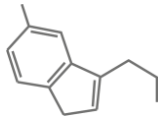

Hermle L, Fünfgeld M, Oepen G, Botsch H, Borchardt D, Gouzoulis E, Fehrenbach RA, Spitzer M (1992) Mescaline-induced psychopathological, neuropsychological, and neurometabolic effects in normal subjects: Experimental psychosis as a tool for psychiatric research. Biol Psychiatry 32:976–991.

Herremans AH, Hijzen TH, Olivier B, Slangen JL (1995) Serotonergic drug effects on a delayed conditional discrimination task in the rat; involvement of the 5-HT1A receptor in working memory. J Psychopharmacol 9:242–250.

Heym J, Trulson ME, Jacobs BL (1982) Raphe unit activity in freely moving cats: Effects of phasic auditory and visual stimuli. Brain Res 232:29–39.

Hofmann A (1996) LSD: Completely Personal. Worlds Conscious Conf 6.

Hökfelt T, Fuxe K, Goldstein M (1973) Immunohistochemical localization of aromatic L-amino acid decarboxylase (DOPA decarboxylase) in central dopamine and 5-hydroxytryptamine nerve cell bodies of the rat. Brain Res 53:175–180.

Hökfelt T, Ljungdahl Å (1972) Modification of the Falck-Hillarp formaldehyde fluorescence method using the vibratome ®: simple, rapid and sensitive localization of catecholamines in sections of unfixed or formalin fixed brain tissue. Histochemie 29:325–339.

Homberg JR (2012) Serotonin and decision making processes. Neurosci Biobehav Rev 36:218–236.

Hornung J (2003) The human raphe nuclei and the serotonergic system. In: Journal of Chemical Neuroanatomy, pp 331–343. Elsevier.

Hornung J, Celio MR (1992) The Selective innervation by serotoninergic axons of calbindin Ƶ containing interneurons in the neocortex and hippocampus of the marmoset. J Comp Neurol 320:457–467.

Hornung J, Fritschy J, Törk I (1990) Distribution of two morphologically distinct subsets of serotoninergic axons in the cerebral cortex of the marmoset. J Comp Neurol 297:165–181.

Hubbard JE, di Carlo V (1974) Fluorescence histochemistry of monoamine Ƶcontaining cell bodies in the brain stem of the squirrel monkey (Saimiri sciureus). III. Serotonin Ƶ containing groups. J Comp Neurol 153:385–398.

Hussar CR, Pasternak T (2012) Memory-guided sensory comparisons in the prefrontal cortex: Contribution of putative pyramidal cells and interneurons. J Neurosci 32:2747–2761.

Ikeda M, Tsuji H, Nakamura S, Ichiyama A, Nishizuka Y, Hayaishi O (1965) Studies on the Biosynthesis of Nicotinamide Adenine Dinucleotide. II. A Role of Picolinic Carboxylase in the Biosynthesis of Nicotinamide Adenine Dinucleotide from Tryptophan in Mammals. J Biol Chem 240:1395–1401.

Imai H, Steindler DA, Kitai ST (1986) The organization of divergent axonal projections from the midbrain raphe nuclei in the rat. J Comp Neurol 243:363–380.

Iversen SD, Mishkin M (1970) Perseverative interference in monkeys following selective lesions of the inferior prefrontal convexity. Exp Brain Res 11:376–386.

Jacob SN, Nieder A (2014) Complementary roles for primate frontal and parietal cortex in guarding working memory from distractor stimuli. Neuron 83:226–237.

Jacob SN, Ott T, Nieder A (2013) Dopamine regulates two classes of primate prefrontal

neurons that represent sensory signals. J Neurosci 33:13724–13734.

Jacobs BL, Azmitia EC (1992) Structure and function of the brain serotonin system. Physiol Rev 72:165–230.

Jacobs BL, Cannon PJ, Azmitia EC (1984) Atlas of serotonergic cell bodies in the cat brainstem: An immunocytochemical analysis. Brain Res Bull 13:1–31.

Jacobs BL, Foote SL, Bloom FE (1978) Differential projections of neurons within the dorsal raphe nucleus of the rat: a horseradish peroxidase (HRP) study. Brain Res 147:149–153.

Jacobs BL, Fornal CA (1997) Serotonin and motor activity. Curr Opin Neurobiol 7:820–825.

Jakab RL, Goldman-Rakic PS (1998) 5-Hydroxytryptamine 2A serotonin receptors in the primate cerebral cortex : Possible site of action of hallucinogenic and antipsychotic drugs in pyramidal cell apical dendrites. Proc Natl Acad Sci 95:735–740.

Jakab RL, Goldman-Rakic PS (2000) Segregation of serotonin 5-HT2A and 5-HT3 receptors in inhibitory circuits of the primate cerebral cortex. J Comp Neurol 417:337–348.

Kaneko T, Akiyama H, Nagatsu I, Mizuno N (1990) Immunohistochemical demonstration of glutaminase in catecholaminergic and serotoninergic neurons of rat brain. Brain Res 507:151–154.

Karakuyu D, Herold C, Güntürkün O, Diekamp B (2007) Differential increase of extracellular dopamine and serotonin in the “prefrontal cortex” and striatum of pigeons during working memory. Eur J Neurosci 26:2293–2302.

Kerkut GA, Cottrell GA (1963) Acetylcholine and 5-hydroxytryptamine in the snail brain. Comp Biochem Physiol 8.

Kerkut GA, Sedden CB, Walker RJ (1967) Cellular localization of monoamines by fluorescence microscopy in Hirudo medicinalis and Lumbricus terrestris. Comp Biochem Physiol 21.

Khan JA, Tao X, Tong L (2006) Molecular basis for the inhibition of human NMPRTase, a novel target for anticancer agents. Nat Struct Mol Biol 13:582–588.

Kievit J, Kuypers HGJM (1975) Subcortical afferents to the frontal lobe in the rhesus monkey studied by means of retrograde horseradish peroxidase transport. Brain Res 85:261–266.

Kim JN, Shadlen MN (1999) Neural correlates of a decision in the dorsolateral prefrontal cortex of the macaque. Nat Neurosci 2:176–185.

Koehler O (1956) The Ability of Birds to Count. In: The World of Mathematics. Volume One, pp 489–496.

Köhler C, Steinbusch H (1982) Identification of serotonin and non-serotonin-containing neurons of the mid-brain raphe projecting to the entorhinal area and the hippocampal formation. A combined immunohistochemical and fluorescent retrograde tracing study in the rat brain. Neuroscience 7.

Kosofsky BE, Molliver ME (1987) The serotoninergic innervation of cerebral cortex: Different classes of axon terminals arise from dorsal and median raphe nuclei. Synapse 1:153–168.

Kringelbach ML (2005) The human orbitofrontal cortex: Linking reward to hedonic experience. Nat Rev Neurosci 6:691–702.

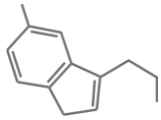

Kristensson K, Olsson Y (1971) Uptake and retrograde axonal transport of peroxidase in hypoglossal neurones - Electron microscopical localization in the neuronal perikaryon. Acta Neuropathol 19:1–9.

Krnjević K, Phillis JW (1963a) Actions of certain amines on cerebral cortical neurones. Br J Pharmacol Chemother 20:471–490.

Krnjević K, Phillis JW (1963b) Iontophoretic studies of neurones in the mammalian cerebral cortex. J Physiol 165:274–304.

Kuntzman R, Shore PA, Bogdanski D, Brodle BB (1961) Microanalytical procedures for fluorometric assay of brain DOPA-5HTP decarboxylase, norepinephrine and serotonin, and a detailed mapping of decarboxylase activity in brain. J Neurochem 6:226–231.

Lee SB, Rhee SG (1995) Significance of PIP2 hydrolysis and regulation of phospholipase C isozymes. Curr Opin Cell Biol 7:183–189.

Li Y, Dalphin N, Hyland BI (2013) Systems/Circuits Association with Reward Negatively Modulates Short Latency Phasic Conditioned Responses of Dorsal Raphe Nucleus Neurons in Freely Moving Rats.

Liddle PF, Kiehl KA, Smith AM (2001) An event-related fMRI study of response inhibition. Hum Brain Mapp 12:100–109.

Lidow MS, Goldman-Rakic PS, Gallager DW, Geschwind DH, Rakic P (1989a) Distribution of major neurotransmitter receptors in the motor and somatosensory cortex of the rhesus monkey. Neuroscience 32:609–627.

Lidow MS, Goldman-Rakic PS, Gallager DW, Rakic P (1989b) Quantitative autoradiographic mapping of serotonin 5-HT1 and 5-HT2 receptors and uptake sites in the neocortex of the rhesus monkey. J Comp Neurol 280:27–42.

Lieben CKJ, Oorsouw K Van, Deutz NEP, Blokland A (2004) Acute tryptophan depletion induced by a gelatin-based mixture impairs object memory but not affective behavior and spatial learning in the rat. Behav Brain Res 151:53–64.

Lillesaar C (2011) The serotonergic system in fish. J Chem Neuroanat 41:294–308.

Lin SH, Lee LT, Yang YK (2014) Serotonin and mental disorders: A concise review on molecular neuroimaging evidence. Clin Psychopharmacol Neurosci 12:196–202.

Lindvall O, Bjorklund A (1974) The organization of the ascending catecholamine neuron systems in the rat brain. Acta Physiol Scand 412:1–48.

Liu YF, Ghahremani MH, Rasenick MM, Jakobs KH, Albert PR (1999) Stimulation of cAMP synthesis by G(i)-coupled receptors upon ablation of distinct Gα(i) protein expression. G(i) subtype specificity of the 5-HT1A receptor. J Biol Chem 274:16444–16450.

Lottem E, Banerjee D, Vertechi P, Sarra D, Lohuis M oude, Mainen ZF (2018) Activation of serotonin neurons promotes active persistence in a probabilistic foraging task. Nat Commun 9:1000.

Luciana M, Collins PF, Depue RA (1998) Opposing Roles for Dopamine and Serotonin in the Moduation of Human Spatial Working Memory Functions. Cereb Cortex April/May:218–226.

Mai JK., Paxinos G. (2011) The Human Nerouvs System, 3rd ed. Academic Press, 2011.

Mannoury La Cour C, El Mestikawy S, Hanoun N, Hamon M, Lanfumey L (2006) Regional differences in the coupling of 5-hydroxytryptamine-1A receptors to G proteins in the rat brain. Mol Pharmacol 70:1013–1021.

Marazziti D, Consoli G, Picchetti M, Carlini M, Faravelli L (2010) Cognitive impairment in major depression. Eur J Pharmacol 626:83–86.

Marek GJ, Aghajanian GK (1999) 5-HT2A receptor or α1-adrenoceptor activation induces excitatory postsynaptic currents in layer V pyramidal cells of the medial prefrontal cortex. Eur J Pharmacol 367:197–206.

Marsden CA, Kerkut GA (1969) Fluorescent microscopy of the 5HT- and catecholamine-containing cells in the central nervous system of the leech Hirudo medicinalis. Comp Biochem Physiol 31.

Marson L, McKenna KE (1992) A role for 5-hydroxytryptamine in descending inhibition of spinal sexual reflexes. Exp brain Res 88:313–320.

Martín-Ruiz R, Victoria Puig M, Celada P, Shapiro DA, Roth BL, Mengod G, Artigas F (2001) Control of Serotonergic Function in Medial Prefrontal Cortex by Serotonin-2A Receptors through a Glutamate-Dependent Mechanism.

Mattevi A (2006) A close look at NAD biosynthesis. Nat Struct Mol Biol 13:563–564.

Maunsell JHR, Van Essen DC (1983) Functional properties of neurons in middle temporal visual area of the macaque monkey. I. Selectivity for stimulus direction, speed, and orientation. J Neurophysiol 49:1127–1147.

Maynert EW, Levi R, de Lorenzo AJD (1964) The presence of norepinephrine and 5-hydroxytryptamine in vesicles from disrupted nerve-ending particles. J Pharmacol Exp Ther 144.

Mejia JM, Ervin FR, Baker GB, Palmour RM (2002) Monoamine oxidase inhibition during brain development induces pathological aggressive behavior in mice. Biol Psychiatry 52:811–821.

Merten K, Nieder A (2009) Compressed scaling of abstract numerosity representations in adult humans and monkeys. J Cogn Neurosci 21:333–346.

Messing RB, Lytle LD (1977) Serotonin-containing neurons: their possible role in pain and analgesia. Pain 4:1–21.

Michaelson IA, Whittaker VP (1963) The subcellular localization of 5-hydroxytryptamine in guinea pig brain. Biochem Pharmacol 12:203–211.

Michaiel AM, Parker PRL, Correspondence CMN, Niell CM (2019) A Hallucinogenic Serotonin-2A Receptor Agonist Reduces Visual Response Gain and Alters Temporal Dynamics in Mouse V1. Cell Rep 26:3475–3483.

Millan MJ, Marin P, Bockaert J, Mannoury la Cour C (2008) Signaling at G-protein-coupled serotonin receptors: recent advances and future research directions. Trends Pharmacol Sci 29:454–464.

Miller EK (2000) The prefontral cortex and cognitive control. Nat Rev Neurosci 1:59–65.

Miller EK, Erickson CA, Desimone R (1996) Neural Mechanisms of Visual Working Memory in Prefrontal Cortex of the Macaque.

Miller JJ, Richardson TL, Fibiger HC, McLennan H (1975) Anatomical and electrophysiological identification of a projection from the mesencephalic raphe to the caudate-putamen in the rat. Brain Res 97:133–138.

Miyazaki K, Miyazaki KW, Doya K (2012) The role of serotonin in the regulation of patience and impulsivity. Mol Neurobiol 45:213–224.

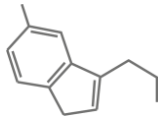

Miyazaki KW, Miyazaki K, Tanaka KF, Yamanaka A, Takahashi A, Tabuchi S, Doya K (2014) Optogenetic Activation of Dorsal Raphe Serotonin Neurons Enhances Patience for Future Rewards. Curr Biol 24:2033–2040.

Moiseiwitsch JR, Lauder JM (1995) Serotonin regulates mouse cranial neural crest migration. Proc Natl Acad Sci 92:7182–7186.

Morrison JH, Foote SL, Molliver ME, Bloom FE, Lidov HG (1982) Noradrenergic and serotonergic fibers innervate complementary layers in monkey primary visual cortex: An immunohistochemical study. Proc Natl Acad Sci U S A 79:2401–2405.

Morrissey JJ, Walker MN, Lovenberg W (1977) The Absence of Tryptophan Hydroxylase Activity in Blood Platelets. Proc Soc Exp Biol Med 154:496–499.

Moyer RS, Landauer TK (1967) Time required for judgements of numerical inequality [47]. Nature 215:1519–1520.

Mück-Seler D, Pivac N (2011) Serotonin. Period Biol UDC 57:29–41.

Müller CP, De Souza Silva MA, Huston JP (2006) Double dissociating effects of sensory stimulation and cocaine on serotonin activity in the occipital and temporal cortices. Neuropharmacology 52:854–862.

Negri L (2006) Vittorio Erspamer (1909-1999). Med Secoli 18:97–113.

Neher E, Sakaba T (2008) Multiple Roles of Calcium Ions in the Regulation of Neurotransmitter Release. Neuron 59:861–872.

Nichols CD (2006) Drosophila melanogaster neurobiology, neuropharmacology, and how the fly can inform central nervous system drug discovery.

Nichols DE (2016) Psychedelics.

Nicoll RA, Malenka RC, Andrade R (1986) A G Protein Couples Serotonin and GABA-B Receptors to the Same Channels in Hippocampus. Science (80-) 234:1261–1265.

Nieder A, Dehaene S (2009) Representation of Number in the Brain.

Normandin JJ, Murphy AZ (2011) Serotonergic lesions of the periaqueductal gray, a primary source of serotonin to the nucleus paragigantocellularis, facilitate sexual behavior in male rats. Pharmacol Biochem Behav.

O'Hearn E, Battaglia G, De Souza EB, Kuhar MJ, Molliver ME (1988) Methylenedioxyamphetamine (MDA) and methylenedioxymethamphetamine (MDMA) cause selective ablation of serotonergic axon terminals in forebrain: Immunocytochemical evidence for neurotoxicity. J Neurosci 8:2788–2803.

Oleskevich S (1995) G(αo1) decapeptide modulates the hippocampal 5-HT(1A) potassium current. J Neurophysiol 74:2189–2193.

Ongur D, Price JL (2000) The Organization of Networks within the Orbital and Medial Prefrontal Cortex of Rats, Monkeys and Humans. Cereb Cortex 10:206–219.

Ott T, Jacob SN, Nieder A (2014) Dopamine Receptors Differentially Enhance Rule Coding in Primate Prefrontal Cortex Neurons. Neuron 84:1317–1328.

Paczoska-Eliasiewicz H, Rzasa J (1983) Blood levels of serotonin in birds. Folia Biol (Praha) 31:329–335.

Paterniti S, Dufouil C, Bisserbe JC, Alpérovitch A (1999) Anxiety, depression, psychotropic drug use and cognitive impairment. Psychol Med 29:421–428.

Peroutka SJ, Howell TA (1994) The molecular evolution of G protein-coupled receptors: Focus on 5-hydroxytryptamine receptors. Neuropharmacology 33:319–324.

Petrides M, Pandya DN (1994) Comparative architectonic analysis of the human and the macaque frontal cortex. In: Handbook of Neuropsychology, 9th ed. (Boller F, Grafman J, eds), pp 17–58. Amsterdam: Elsevier.

Poitras D, Parent A (1978) Atlas of the distribution of monoamine Z containing nerve cell bodies in the brain stem of the cat. J Comp Neurol 179:699–717.

Porrino LJ, Goldman Z Rakic PS (1982) Brainstem innervation of prefrontal and anterior cingulate cortex in the rhesus monkey revealed by retrograde transport of HRP. J Comp Neurol 205:63–76.

Potrich D, Gionata S, Vallortigara G (2015) Quantity Discrimination by Zebrafish (Danio rerio) Structural and functional investigations of the avian hippocampal formation View project Origin of the social brain PRIN 2016 View project. Artic J Comp Psychol.

Praag H Van, Lemus C (1986) Nutrition and the Brain.

Puig MV, Gulledge AT (2011) Serotonin and Prefrontal Cortex Function: Neurons, Networks and Circuits. Mol Neurobiol 257:2432–2437.

Puig MV, Watakabe A, Ushimaru M, Yamamori T, Kawaguchi Y (2010) Serotonin modulates fast-spiking interneuron and synchronous activity in the rat prefrontal cortex through 5-HT1A and 5-HT2A receptors. J Neurosci 30:2211–2222.

Puig M V., Artigas F, Celada P (2005) Modulation of the Activity of Pyramidal Neurons in Rat Prefrontal Cortex by Raphe Stimulation In Vivo: Involvement of Serotonin and GABA. Cereb Cortex 15:1–14.

Pum ME, Huston JP, De Souza Silva MA, Müller CP (2008) Visual sensory-motor gating by serotonin activation in the medial prefrontal and occipital, but not in the rhinal, cortices in rats. Neuroscience 153:361–372.

Puumala T, Sirviö J (1998) Changes in activities of dopamine and serotonin systems in the frontal cortex underlie poor choice accuracy and impulsivity of rats in an attention task. Neuroscience 83:489–499.

Quay WB, Wilhoft DC (1964) Comparative and Regional Differences in Serotonin Content of Reptilian Brains. J Neurochem 11:805–811.

Quintana J, Yajeya J, Fuster JM (1988) Prefrontal representation of stimulus attributes during delay tasks. I. Unit activity in cross-temporal integration of sensory and sensory-motor information. Brain Res 474:211–221.

Ranade SP, Mainen ZF (2009) Transient Firing of Dorsal Raphe Neurons Encodes Diverse and Specific Sensory, Motor, and Reward Events. J Neurophysiol 102:3026–3037.

Rand M, Reid G (1951) Source of “Serotonin” in serum. Nature 168:385.

Rapport MM, Green AA, Page IH (1948) Serum vasoconstrictor, serotonin; isolation and characterization. J Biol Chem 176:1243–1251.

Rasmussen K, Strecker RE, Jacobs BL (1986) Single unit response of noradrenergic, serotonergic and dopaminergic neurons in freely moving cats to simple sensory stimuli. Brain Res 369:336–340.

Richard DM, Dawes MA, Mathias CW, Acheson A, Hill-Kapturczak N, Dougherty DM (2009) L-tryptophan: Basic metabolic functions, behavioral research and therapeutic

indications. Int J Tryptophan Res 2:45–60.

Roberts MHT, Straughan DW (1967) Excitation and depression of cortical neurones by 5 Ẓ hydroxytryptamine. J Physiol 193:269–294.

Rodríguez JJ, Noristani HN, Verkhratsky A (2012) The serotonergic system in ageing and Alzheimer's disease. Prog Neurobiol 99:15–41.

Rogers RD, Blackshaw AJ, Middleton HC, Matthews K, Hawtin K, Crowley C, Hopwood A, Wallace C, Deakin JFW, Sahakian BJ, Robbins TW (1999) Tryptophan depletion impairs stimulus-reward learning while methylphenidate disrupts attentional control in healthy young adults: implications for the monoaminergic basis of impulsive behaviour. Psychopharmacology (Berl) 146:482–491.

Rolls ET (2016) A non-reward attractor theory of depression. Neurosci Biobehav Rev 68:47–58.

Rolls ET, Grabenhorst F (2008) The orbitofrontal cortex and beyond: From affect to decision-making. Prog Neurobiol 86:216–244.

Römpler H, Stäubert C, Thor D, Schulz A, Hofreiter M, Schöneberg T (2007) G protein-coupled time travel: Evolutionary aspects of GPCR research. Mol Interv 7:17–25.

Rugani R, Fontanari L, Simoni E, Regolin L, Vallortigara G (2009) Arithmetic in newborn chicks. Proc R Soc B Biol Sci 276:2451–2460.

Rushworth MFS, Behrens TEJ, Rudebeck PH, Walton ME (2007) Contrasting roles for cingulate and orbitofrontal cortex in decisions and social behaviour. Trends Cogn Sci 11:168–176.

Santana N, Artigas F (2017) Laminar and cellular distribution of monoamine receptors in rat medial prefrontal cortex. Front Neuroanat 11.

Santana N, Bortolozzi A, Serrats J, Mengod G, Artigas F (2004) Expression of Serotonin1A and Serotonin2A Receptors in Pyramidal and GABAergic Neurons of the Rat Prefrontal Cortex. Cereb Cortex 14:1100–1109.

Saxena PR, Tangri KK, Bhargava KP (1966) Identification of Acetylcholine, Histamine, and 5-Hydroxytryptamine in Girarddina Heterophylla (Decne.). Can J Physiol Pharmacol 44:621–627.

Schaechter JD, Wurtman RJ (1990) Serotonin release varies with brain tryptophan levels. Brain Res 532:203–210.

Schofield SP, Dixson AF (1982) Distribution of catecholamine and indoleamine neurons in the brain of the common marmoset (Callithrix jacchus). J Anat 134:315–338.

Schofield SPM, Everitt BJ (1981) The organization of indoleamine neurons in the brain of the rhesus monkey Macaca mulatta. J Comp Neurol 197:369–383.

Scholes KE, Harrison BJ, O'Neill B, Leung S, Croft RJ, Pipingas A, Phan KL, Nathan PJ (2007) Acute serotonin and dopamine depletion improves attentional control: findings from the stroop task. Neuropsychopharmacology 32:1600–1610.

Seillier L, Lorenz C, Kawaguchi K, Ott T, Nieder A, Pourriahi P, Nienborg H (2017) Systems/Circuits Serotonin Decreases the Gain of Visual Responses in Awake Macaque V1.

Shulgin A, Shulgin A (1995) PIHKAL: a chemical love story.

Simansky KJ, Nicklous DM (2002) Parabrachial infusion of d-fenfluramine reduces food

intake: Blockade by the 5-HT1B antagonist SB-216641. Pharmacol Biochem Behav 71:681–690.

Smiley JF, Goldman-Rakic PS (1996) Serotonergic axons in monkey prefrontal cerebral cortex synapse predominantly on interneurons as demonstrated by serial section electron microscopy. J Comp Neurol 367:431–443.

Smith TA (1971) The occurrence, metabolism and functions of amines in plants. Biol Rev 46:201–241.

Sommer C (2004) Serotonin in Pain and Analgesia: Actions in the Periphery. Mol Neurobiol 30:117–126.

Stefanacci L, Amaral DG (2002) Some observations on cortical inputs to the macaque monkey amygdala: An anterograde tracing study. J Comp Neurol 451:301–323.

Steinbusch HWM (1981) Distribution of serotonin-immunoreactivity in the central nervous system of the rat-Cell bodies and terminals. Neuroscience 6:557–618.

Steinbusch HWM, Niewenhuys R, Verhofstad AAJ, Van Der Kooy D (1981) The nucleus raphe dorsalis of the rat and its projection upon the caudatoputamen. A combined cytoarchitectonic, immunohistochemical and retrograde transport study. J Physiol (Paris) 77:157–174.

Steinbusch HWM, Van der Kooy D, Verhofstad AAJ, Pellegrino A (1980) Serotonergic and non-serotonergic projections from the nucleus raphe dorsalis to the caudate-putamen complex in the rat, studied by a combined immunofluorescence and fluorescent retrograde axonal labeling technique. Neurosci Lett 19:137–142.

Steinbusch HWM, Verhofstad AAJ, Joosten HWJ (1978) Localization of serotonin in the central nervous system by immunohistochemistry: description of a specific and sensitive technique and some applications. Neuroscience.

Stepanova AN, Robertson-Hoyt J, Yun J, Benavente LM, Xie DY, Doležal K, Schlereth A, Jürgens G, Alonso JM (2008) TAA1-Mediated Auxin Biosynthesis Is Essential for Hormone Crosstalk and Plant Development. Cell 133:177–191.

Sue Goo Rhee, Kang Duk Choi (1992) Regulation of inositol phospholipid-specific phospholipase C isozymes. J Biol Chem 267:12393–12396.

Syrovatkina V, Alegre KO, Dey R, Huang XY (2016) Regulation, Signaling, and Physiological Functions of G-Proteins. J Mol Biol 428:3850–3868.

Takeuchi Y, Sano Y (1984) Serotonin nerve fibers in the primary visual cortex of the monkey - Quantitative and immunoelectronmicroscopical analysis. Anat Embryol (Berl) 169:1–8.

Tamir H, Payette RF, Huang YL, Liu KP, Gershon MD (1985) Human serotonectin: a blood glycoprotein that binds serotonin and is associated with platelets and white blood cells. J Cell Sci 73:187–206.

Tanaka E, North RA (1993) Actions of 5-hydroxytryptamine on neurons of the rat cingulate cortex. J Neurophysiol 69:1749–1757.

Tanji J, Hoshi E (2001) Behavioral planning in the prefrontal cortex. Curr Opin Neurobiol 11:164–170.

Tanji J, Hoshi E (2008) Role of the Lateral Prefrontal Cortex in Executive Behavioral Control.

Tao Y, Ferrer JL, Ljung K, Pojer F, Hong F, Long JA, Li L, Moreno JE, Bowman ME, Ivans LJ, Cheng Y, Lim J, Zhao Y, Ballaré CL, Sandberg G, Noel JP, Chory J (2008) Rapid

Synthesis of Auxin via a New Tryptophan-Dependent Pathway Is Required for Shade Avoidance in Plants. Cell 133:164–176.

Terry A V., Buccafusco JJ, Wilson C (2008) Cognitive dysfunction in neuropsychiatric disorders: Selected serotonin receptor subtypes as therapeutic targets. Behav Brain Res 195:30–38.

Thiele A, Delicato LS, Roberts MJ, Gieselmann MA (2006) A novel electrode-pipette design for simultaneous recording of extracellular spikes and iontophoretic drug application in awake behaving monkeys. J Neurosci Methods 158:207–211.

Thorpe SJ (1990) Spike arrival times: A highly efficient coding scheme for neural networks.

Tigges J, Tigges M, Cross NA, McBride RL, Letbetter WD, Anschel S (1982) Subcortical structures projecting to visual cortical areas in squirrel monkey. J Comp Neurol 209:29–40.

Törk I (1990) Anatomy of the Serotonergic System. Ann N Y Acad Sci 600:9–34.

Tricklebank M, Daly E eds. (2019) The Serotonin System: History, Neuropharmacology, and Pathology. Elsevier Academic Press.

Trzaskowski B, Latek D, Yuan S, Ghoshdastider U, Debinski A, Filipek S (2012) Action of Molecular Switches in GPCRs - Theoretical and Experimental Studies. Curr Med Chem 19:1090–1109.

Twarog BM, Page IH (1953) Serotonin content of some mammalian tissues and urine and a method for its determination. Am J Physiol 175:157–161.

Üçok A, Alpsan H, Çakır S, Saruhan-Direskeneli G (2007) Association of a serotonin receptor 2A gene polymorphism with cognitive functions in patients with schizophrenia. Am J Med Genet Part B Neuropsychiatr Genet 144B:704–707.

Uller C, Jaeger R, Guidry G, Martin C (2003) Salamanders (Plethodon cinereus) go for more: Rudiments of number in an amphibian. Anim Cogn 6:105–112.

Urbain N, Creamer K, Debonnel G (2006) Electrophysiological diversity of the dorsal raphe cells across the sleep-wake cycle of the rat. J Physiol 573:679–695.

v. Economo C (1929) Der Zellaufbau der Grosshirnrinde und die progressive Cerebration. Ergebnisse der Physiol 29:83–128.

Van der Kooy D, Hattori T (1980) Dorsal raphe cells with collateral projections to the caudate-putamen and substantia nigra: A fluorescent retrograde double labeling study in the rat. Brain Res 186:1–7.

Van Der Kooy D, Kuypers HGJM (1979) Fluorescent retrograde double labeling: Axonal branching in the ascending raphe and nigral projections. Science (80-) 204:873–875.

VanderHorst VGJM, Ulfhake B (2006) The organization of the brainstem and spinal cord of the mouse: Relationships between monoaminergic, cholinergic, and spinal projection systems. J Chem Neuroanat 31:2–36.

Vertes RP, Martin GF (1988) Autoradiographic analysis of ascending projections from the pontine and mesencephalic reticular formation and the median raphe nucleus in the rat. J Comp Neurol 275:511–541.

Vialli M (1966) Histology of the enterochromaffin cell system. In: 5-Hydroxytryptamine and Related Indolealkylamines, pp 1–65. Springer Berlin Heidelberg.

Viguier F, Michot B, Hamon M, Bourgoin S (2013) Multiple roles of serotonin in pain control

mechanisms —Implications of 5-HT7 and other 5-HT receptor types. Eur J Pharmacol 716:8–16.

Vijayraghavan S, Wang M, Birnbaum SG, Williams G V, Arnsten AFT (2007) Inverted-U dopamine D1 receptor actions on prefrontal neurons engaged in working memory. Nat Neurosci 10:376–384.

Villalón CM, Centurión D (2007) Cardiovascular responses produced by 5-hydroxytriptamine:a pharmacological update on the receptors/mechanisms involved and therapeutic implications. Naunyn Schmiedebergs Arch Pharmacol 376:45–63.

Viswanathan P, Nieder A (2013) Neuronal correlates of a visual “sense of number” in primate parietal and prefrontal cortices. Proc Natl Acad Sci U S A 110:11187–11192.

Voigt J-P, Fink H (2015) Serotonin controlling feeding and satiety. Behav Brain Res 277:14–31.

Von Bonin G, Bailey P (1947) The neocortex of Macaca mulatta. (Illinois Monogr. med. Sci., 5, No. 4.). Champaign, IL, US: University of Illinois Press.

Vonk J, Beran MJ (2012) Bears “count” too: Quantity estimation and comparison in black bears, Ursus americanus. Anim Behav 84:231–238.

Wade PR, Tamir H, Kirchgessner AL, Gershon MD (1994) Analysis of the role of 5-HT in the enteric nervous system using anti- idiotopic antibodies to 5-HT receptors. Am J Physiol - Gastrointest Liver Physiol 266.

Walker AE (1940) A cytoarchitectural study of the prefrontal area of the macaque monkey. J Comp Neurol 73:59–86.

Walther DJ, Bader M (2003) A unique central tryptophan hydroxylase isoform. Biochem Pharmacol 66:1673–1680.

Wang T, Zhang X, Bheda P, Revollo JR, Imai SI, Wolberger C (2006) Structure of Nampt/PBEF/visfatin, a mammalian NAD+ biosynthetic enzyme. Nat Struct Mol Biol 13:661–662.

Waselus M, Galvez JP, Valentino RJ, Van Bockstaele EJ (2006) Differential projections of dorsal raphe nucleus neurons to the lateral septum and striatum. J Chem Neuroanat 31:233–242.

Wasson R (1957) Seeking the magic mushroom. Life.

Watakabe A, Komatsu Y, Sadakane O, Shimegi S, Takahata T, Higo N, Tochitani S, Hashikawa T, Naito T, Osaki H, Sakamoto H, Okamoto M, Ishikawa A, Hara SI, Akasaki T, Sato H, Yamamori T (2009) Enriched expression of serotonin 1B and 2A receptor genes in macaque visual cortex and their bidirectional modulatory effects on neuronal responses. Cereb Cortex 19:1915–1928.

Waterhouse BD, Mihailoff GA, Baack JC, Woodward DJ (1986) Topographical distribution of dorsal and median raphe neurons projecting to motor, sensorimotor, and visual cortical areas in the rat. J Comp Neurol 249:460–476.

Welsh JH, Moorhead M (1960) The Quantitative Distribution of 5-Hydroxytryptamine in the Invertebrates, especially in their Nervous Systems. J Neurochem 6:146–169.

Wiklund L, Léager L, Persson M (1981) Monoamine cell distribution in the cat brain stem. A fluorescence histochemical study with quantification of indolaminergic and locus coeruleus cell groups. J Comp Neurol 203:613–647.

Wilkins AJ, Shallice T, Mccarthy R (1987) Frontal Lesions and Sustained Attention.

Williams G V, Rao SG, Goldman-Rakic PS (2002) The physiological role of 5-HT2A receptors in working memory. J Neurosci 22:2843–2854.

Wilson MA, Molliver ME (1991) The organization of serotonergic projections to cerebral cortex in primates: Retrograde transport studies. Neuroscience 44:555–570.

Wingren U, Ahlman H (1988) Endoluminal Secretion Of Serotonin And Histamine Into The Small-Intestine Of Normal And Nematode-Infected Rats. Biog Amin.

Winter JC, Petti DT (1987) The effects of 8-hydroxy-2-(di-n-propylamino)tetralin and other serotonergic agonists on performance in a radial maze: a possible role for 5-HT1A receptors in memory. Pharmacol Biochem Behav 27:625–628.

Woolley DW, Shaw E (1954) A Biochemical and Pharmacological Suggestion about certain Mental Disorders. Proc Natl Acad Sci 40:228–231.

Wurtman RJ, Anton-Tay F (1969) The mammalian pineal as a neuroendocrine transducer. Recent Prog Horm Res 25:493–522.

Zhang Z-W, Arsenault D (2005) Gain modulation by serotonin in pyramidal neurones of the rat prefrontal cortex. J Physiol 566:379–394.

Zhou F-M, Hablitz JJ (1999) Activation of Serotonin Receptors Modulates Synaptic Transmission in Rat Cerebral Cortex. J Neurophysiol 82:2989–2999.

7 Acknowledgements

I most sincerely thank my friend Pooja Viswanathan, who never minded those early morning texts filled with questions about science and life in general. Her advice and help, especially during darker days, were most important to me. I am and will always be beyond grateful.

Thanks to my father, Friedhelm, who did not only support me financially but also has been my gajah in a storm.

Thanks to the rest of my family, especially to all my wonderful aunts.

Thanks to my SF Myrna, to listen and to share.

Thanks to my lab mates (former members included), especially Araceli, Pooja, Felix, Max, Tobi and Ylva, for some fun memories inside and outside science.

Thanks to my supervisor Prof. Dr. Andreas Nieder, for giving me the opportunity to conduct this study.

Thanks to Monkey E and Monkey Y.